Chapter IV

RESULTS AND DISCUSSION

RESULTS AND DISCUSSION

4.1. Corrosion Behavior of Carbon Steel:

This part of the work is directed to examine the electrochemical behavior of carbon steel alloy in seawater by several techniques and to throw more light on the morphology of this alloy.

4.1.1. Open circuit potential measurements:

The open circuit potential (OCP) of carbon steel is found to be – 580 mV (SCE) at the beginning of immersion in seawater as shown in Fig. (4.1). Then, a shift in potential values towards the negative direction is observed, which denotes corrosion stimulation resulting in dissolution of the metal by the aggressive action of NaCl solution [133] . At this stage the anodic reaction dominates the cathodic one ,then an equilibrium potential is attained within about 20 minutes, indicating a steady state of equilibrium for both anodic and cathodic reactions, i.e., $V_{(an.)} = V_{(cath.)}$ where, V represents the rate of process[134].

The open circuit potential of carbon steel alloy was measured, periodically, for 24 months of immersion in seawater. The variation of (OCP) as a function of immersion time is shown in Fig. (4.2). The potential initially decreases from - 580 to - 695 mV (SCE) within the first 6 months of monitoring. This shift towards the negative direction may be obtained as a result of the increase in self polarization of the cathodic areas.On further immersion, the OCP is found to be directed towards more positive values which, may be attributed to the formation of oxide film on carbon steel electrode, this film can increase the resistance of anodic areas and therefore the potential becomes more positive. However, after 9 months exposure time, a shift to the negative direction is observed again which, may be attributed to the breakdown of the passive film and progress of corrosion reaction again.The variation in the potential from cathodic to anodic and vice

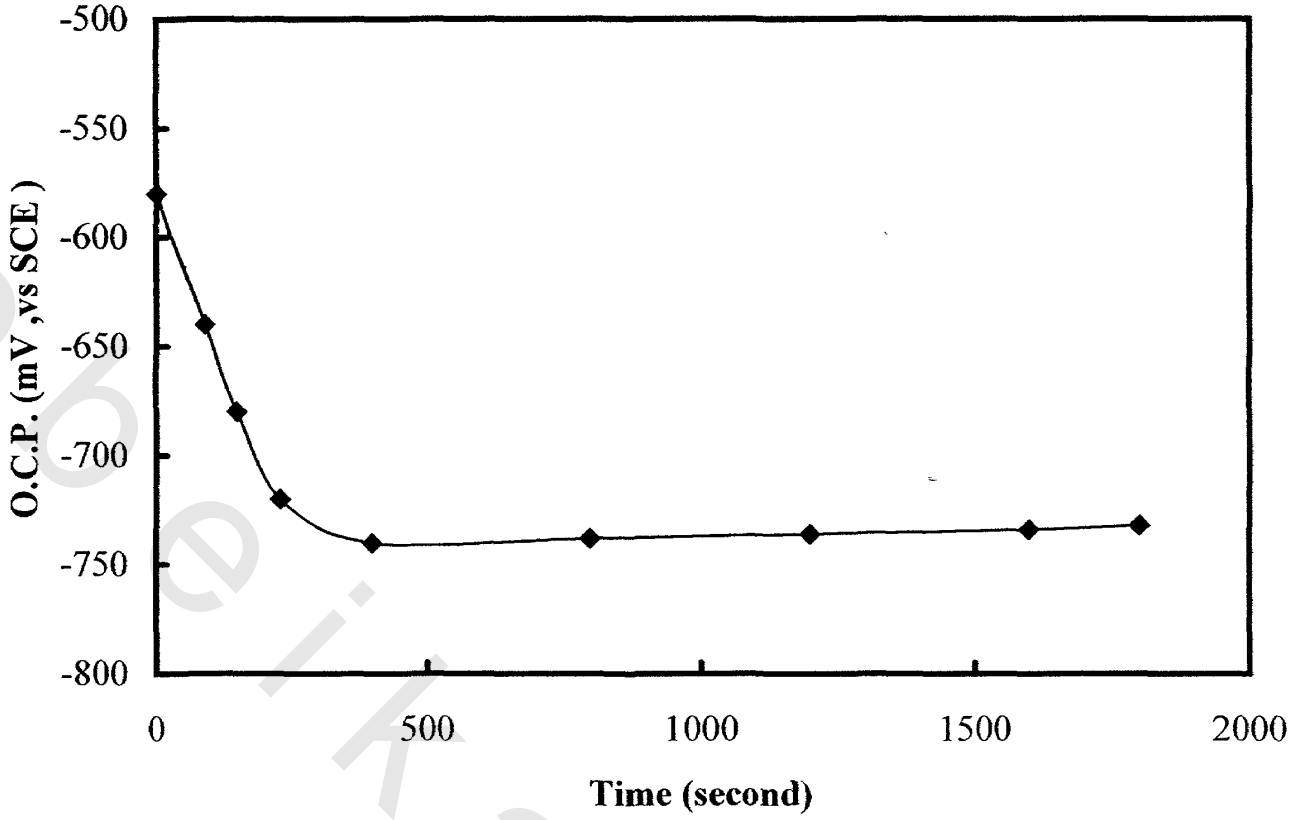

Fig.(4.1) - Open circuit potential of caron steel in sea water at room temperature.

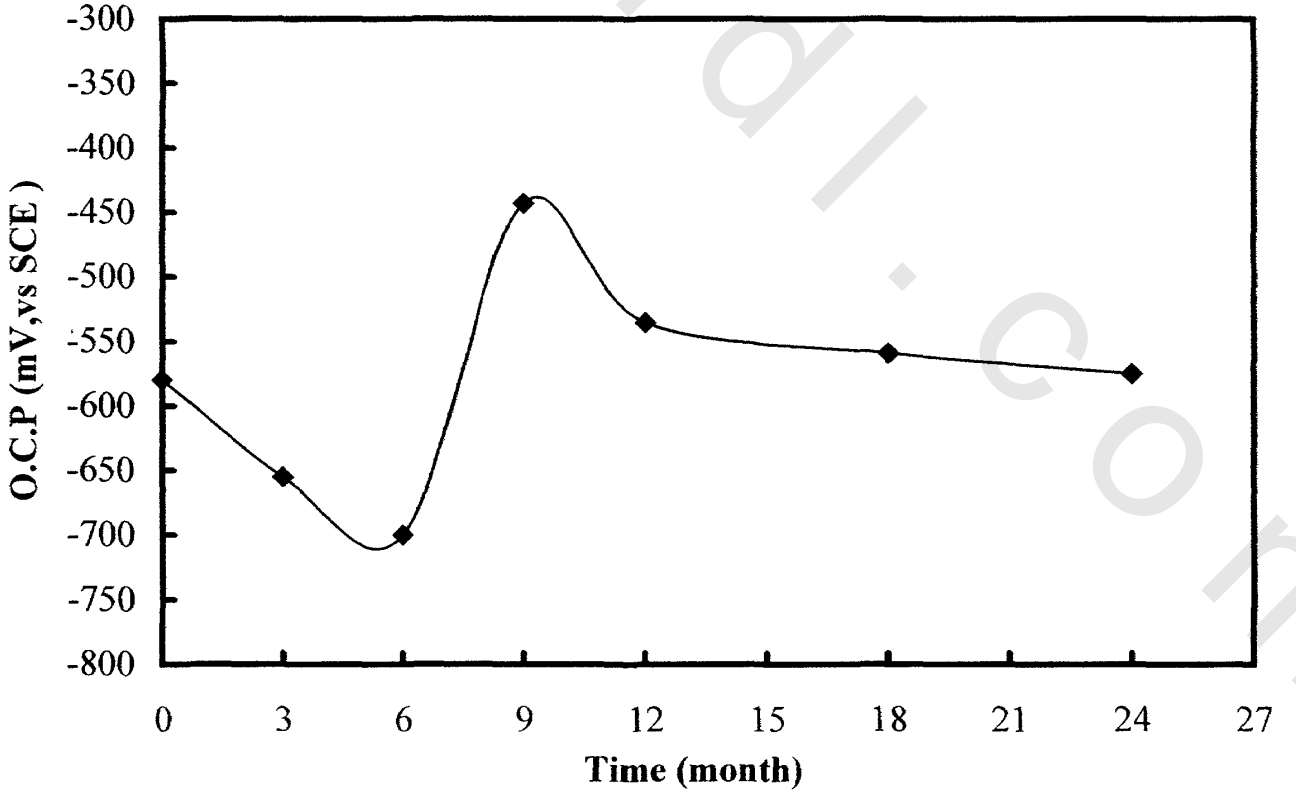

Fig.(4.2) - Open circuit potential of carbon steel in sea water as a function of immersion time.

versa, during duration time, indicates that some corrosion behavior is active at the metal / solution interface [135]. This can be attributed to the fact that marine environment has high concentration of chloride ions, hence, the increase in the corrosion rate and pitting of the specimens are expected [136].

4.1.2. Potentiodynamic measurements :

Typical Potentiodynamic polarization curve for carbon steel electrode in seawater is represented in Fig. (4.3).The values of E_{corr} ,I_{corr} ,β_a, β_c which were obtained from this plot are shown in table (4.1) .These parameters were calculated using PARCalc Tafel analysis routine which uses a nonlinear least-squares approach to fit the data. According to Fig. (4.3), the results show that carbon steel has no active / passive transition when immersed in aerated seawater. Along the cathodic span, the cathodic current density decreases with sweeping the potential to the more positive direction and changing its sign at zero current potential (corrosion potential, $E_{corr,}$). Be yond the corrosion potential, the current flowing along the anodic span are small and increases slowly with the potential with no sign of any active region.

Table (4.1) Data obtained from Tafel plots of carbon steel in seawater .

E_{corr} (mv)	I_{corr} (μA)	β_a (V/ decade)	B_c (V/ decade)
- 563.6	6.759	8.954	- 4837

The relation between E_{corr} and time of electrode immersion is given in Fig. (4.4). The corrosion potential, E_{corr}, is shifted to the negative direction till 6 months, then, a dramatic shift towards the noble direction is observed up to 9 months, followed by a slight decrease in E_{corr} till the end of exposure time (24 months).

The current density values are plotted as a function of time and the results obtained are shown in Fig. (4.5). Tafel constants were determined to obtain the

corrosion current values ,which were used to determine the corrosion rate in milli-inches per year (mpy) according to the following equation [137].

$$\text{Corrosion rate (mpy)} = \frac{0.13\ I_{corr}\ EW}{d} \qquad (4.1)$$

Where, I_{corr} is the corrosion current density in $\mu A\ cm^{-2}$, EW is the equivalent weight in g / eq. wt, d is the density in gm / cm^3 and 0.13 is the metric and time conversion factor. The corrosion rate - time relation is represented in Fig. (4.6). It can be noticed that the three relations represented in Figs. [(4.4) - (4.6)] are composed of three stages, the first stage is characterized by increasing in corrosion with time within the first 6 months, then, it is followed by a noticeable decrease in the rate (second stage) up to 9 months interval. With further immersion, an increase in corrosion is observed till the end of duration time. These results can be explained basing on the following facts, the reduction of water forms the cathodic reaction in the overall corrosion reaction as follows:

$$2\ H_2O + 2e^- = H_2 + 2\ OH^- \qquad (4.2)$$

This gives rise to the formation of iron II species, Fe^{2+}, which changes to iron II hydroxide, $Fe(OH)_2$, and then to magnetite, Fe_3O_4 [138 – 140]. The overall reaction is represented by:

$$3\ Fe + 4\ H_2O = Fe_3O_4 + 4\ H_2 \qquad (4.3)$$

This reaction proceeds in stages [141 – 144]:

$$Fe + H_2O = Fe.\ H_2O\ (ad.) \qquad (4.4)$$

Then, this reaction is followed by one of two reaction steps as follows:

$$Fe.\ H_2O\ (ad.) = Fe.\ OH\ (ad) + H^+ + e^- \qquad (4.5)$$

or

$$Fe.\ H_2O\ (ad) = Fe\ OH^-\ (ad) + H^+ \qquad (4.6)$$

and

$$Fe\,OH^{-}\,(ad) = Fe\,OH\,(ad) + e^{-} \quad (4.7)$$

$$Fe\,OH\,(ad) + OH^{-}\,(aq) = Fe\,(OH)_2 + e^{-} \quad (4.8)$$

$$3\,Fe\,(OH)_2 = F_3O_4 + 2\,H_2O + H_2 \quad (4.9)$$

According to the all above facts, we can say that the first stage in Figs. (4.4 – 4.6) shows that if the working electrode (carbon steel) is immersed in seawater for a long period of time, the metal will be rapidly dissolved and involved in forming the first corrosion product Fe $(OH)_2$ as indicated in equation (4.8), this product is responsible for the increase in corrosion rate. Also, one possible reason for the increase in corrosion with time can be ascribed to the initial formation of pits on the steel surface. As the transition time is achieved, the composition of the corrosion product layer changes from Fe $(OH)_2$ to predominantly Fe_3O_4 protective film as shown in equation (4.9). Then, Fe_3O_4 is partially transformed to $\gamma - Fe_2O_3$ as given in equation (4.10) which corresponds to the formation of stable passivity layer.

$$Fe_3O_4 + H_2O = \gamma - F_2O_3 + 2\,H^{+} + 2\,e^{-} \quad (4.10)$$

Some authors [145,146], assumed that the passive film is consisted of Fe_3O_4 layer facing the metal, and $\gamma - Fe_2O_3$ facing the electrolyte. This film retards the corrosion process as it can limit or arrest further metal dissolution by acting as a physical barrier to the corrosion reaction, [147] resulting in a decrease in corrosion rate (second stage) as shown in Figs. (4.4 – 4.6). Also, the rate of corrosion is controlled by diffusion through the corrosion product layers,i.e, when the thickness of the oxide layer increases the diffusion rate decreases resulting in simultaneous decrease in corrosion rate with time [148]. On further increase in immersion time, a sudden rise of current is observed (third stage) indicating the

end of passive region due to breakdown of passive film and nucleation of pitting attack at a certain critical pitting potential (E_{pit}).

The pitting potential values were obtained by computer analysis of the current-potential curves for carbon steel alloy in seawater at various time intervals ranging from 1 month up to 24 months Fig.(4.7-a). The potential at which the current continuously increased was interpreted to be the pitting potential (E_{pit}). The relation between E_{pit} and time of immersion is shown in Fig. (4.7-b). This curve indicates that E_{pit} shows a dramatic increase within the first 6 months of the exposure time and then it increases slightly till the end of duration time. This process can be attributed to the adsorption of Cl^- ions on the passive layer, as it is reported previously [149, 150]. The halide anions adsorb on both bare iron and passivated surfaces and can displace the adsorbed OH^- and H_2O, hence, these anions are very effective in destroying the passive layer. As natural seawater (our test media) is rich in chlorides, so breakdown of protective layer is expected.

The polarization resistance, R_p, is calculated according to the following equation [137]:

$$R_p = \frac{\beta_a \beta_c}{2.3\, I_{corr} (\beta_a + \beta_c)} \qquad (4.11)$$

Where, I_{corr} is the corrosion current density in $\mu A\ cm^{-2}$ and β_a, β_c are Tafel constants. Fig. (4.8) shows the variations in the polarization resistance, R_p, against time during exposure to corrosion agent. This curve shows a drastic decrease in R_p values within 6 months; this can be attributed to the fact that the polarization resistance is inversely proportional to corrosion rate of the metal [151]. With increasing immersion time an increase in Rp values is observed along the period 6-9 months then followed by a decrease in the polarization resistance as

the majority of the surface becomes active [152]. This behavior indicates that there is a high uptake of NaCl solution, which leads to a production of pits in the passive film resulting in a loss of its barrier property [153].

4.1.3 Weight Loss Measurements:

The variations of the overall integral weight loss of carbon steel, corroded in natural seawater, with the time of immersion are illustrated in Fig. (4.9). The results obtained in this figure show that the relation between weight loss and time of immersion can be divided into three regions. The first region (I) is characterized by a noticeable increase in the weight loss with time, while the second region (II) indicates a sharp decrease in it, then it is followed by a sudden rise again as shown in the third region (III). It can be observed that the transition between the first and second region occurs at about 6 months, while at 9 months the transition from the second to the third one takes place. The behavior in the first region (I) can be attributed to the corrosion of metal, and most of the metal ions resulting from the corrosion reaction are involved in forming Fe $(OH)_2$ as shown previously in equation (4.8). Then, when the first transition time is achieved, the corrosion product Fe $(OH)_2$ is changed to Fe_3O_4 and $\gamma - Fe_2O_3$ layer according to equations (4.9) and (4.10). This protective layer decreases the corrosion process, as judged by the decrease in the weight loss noticed in the second region (II) of Fig. (4.9). As the second transition time is reached (at about 9 months), the protective film is broken and, hence, an increase in the rate of weight loss is observed (region III) indicating a formation of a new hydrous oxide layer. This behavior can be attributed to the presence of chloride ions in the solution. The role of Cl^- ions in inducing the growth of non-protective layer is expected to be related to maintaining finite intergranular porosity. Chloride ions, also, affect the corrosion behavior due to their breakdown action on the passive film [154]. The chloride ions may be associated with the ability of these anions to adsorb on the passive film [155, 156] (at the bottom of cracks and

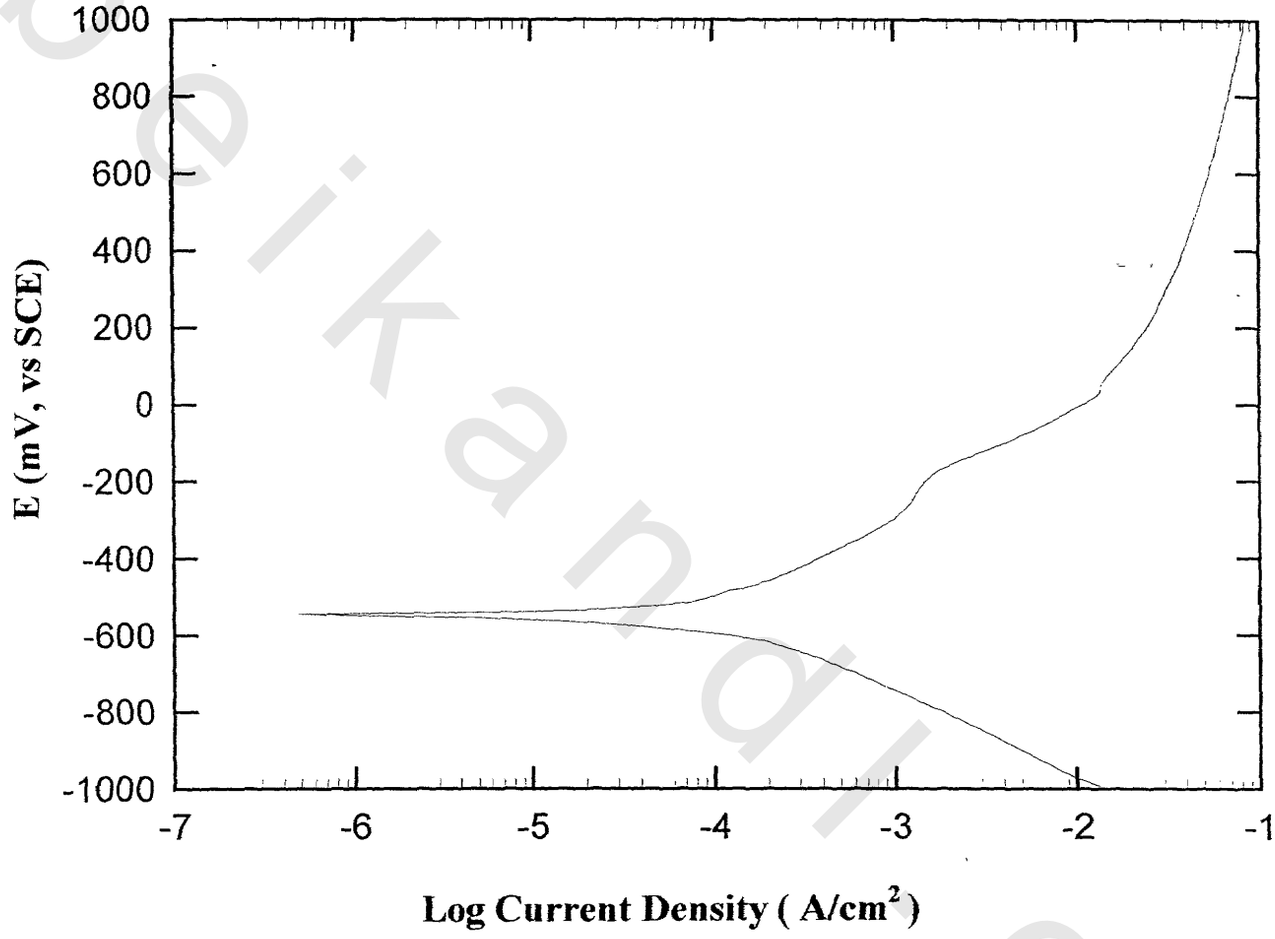

Fig.(4.3) – Potentiodynamic polarization diagram for carbon steel in sea water .

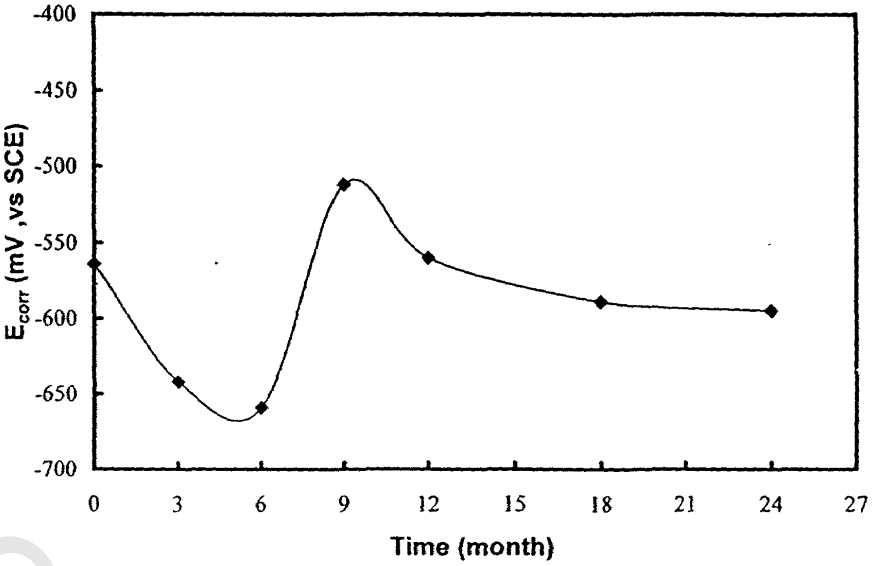

Fig(4.4) - Corrosion potential (E_{corr}) of carbon steel in sea water as a function of immersion time.

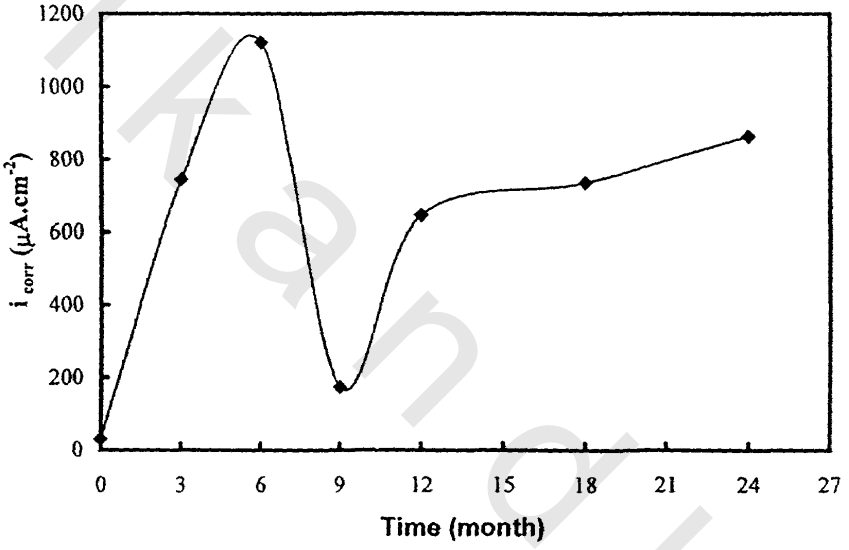

Fig.(4.5) -Corrosion current density of carbon steel in seawater as a function of immersion time.

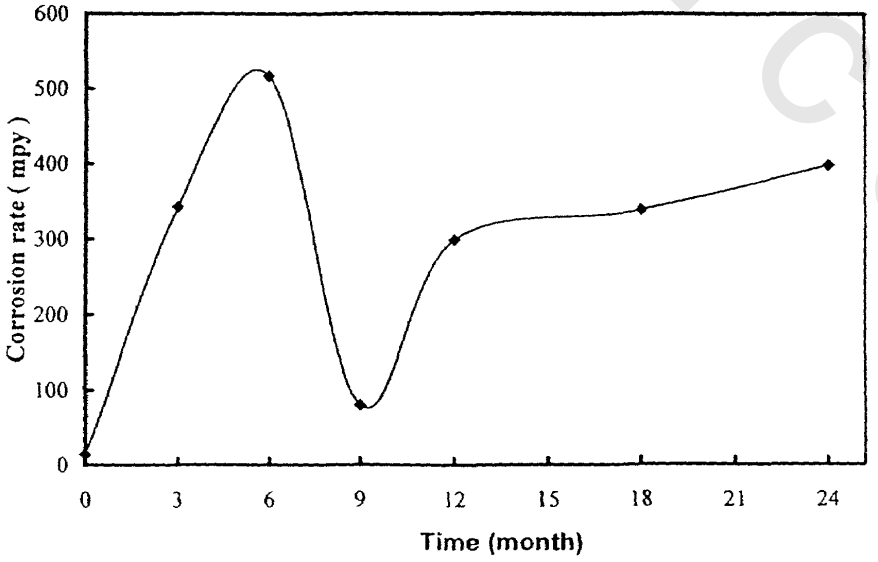

Fig. (4.6) – Corrosion rate of carbon steel in seawater as a function of immersion time .

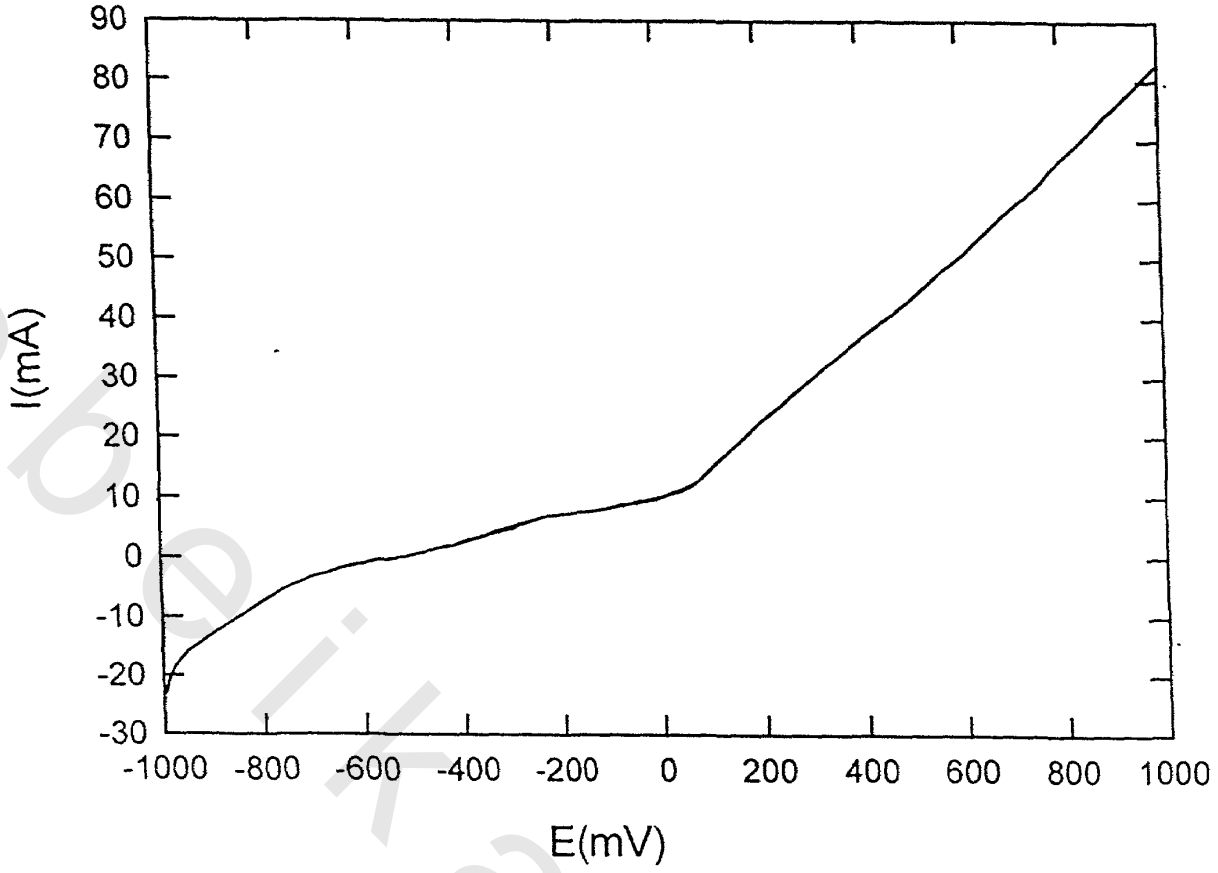

Fig. (4.7-a) - Potential current curve for carbon steel alloy after 24 months of immersion in seawater.

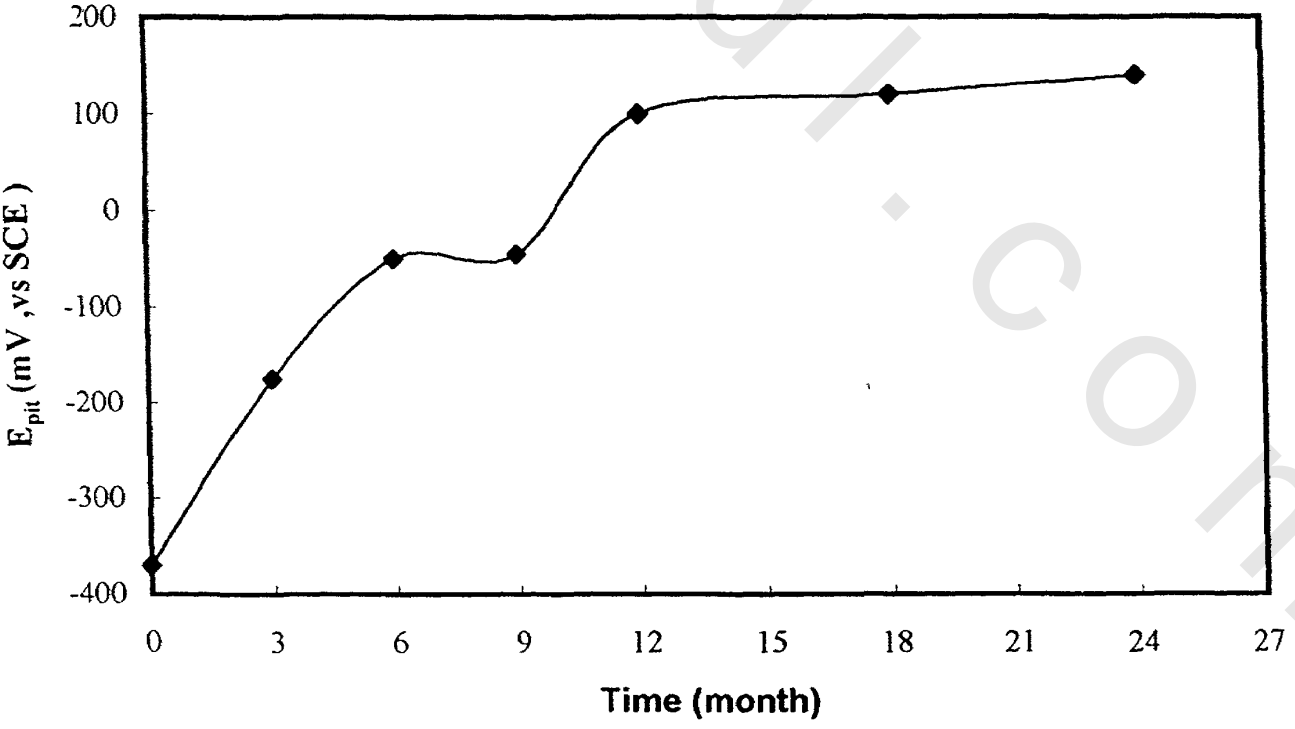

Fig. (4.7 - b) - Pitting potential (Epit) of carbon steel (immersed in seawater) as a function of immersion time.

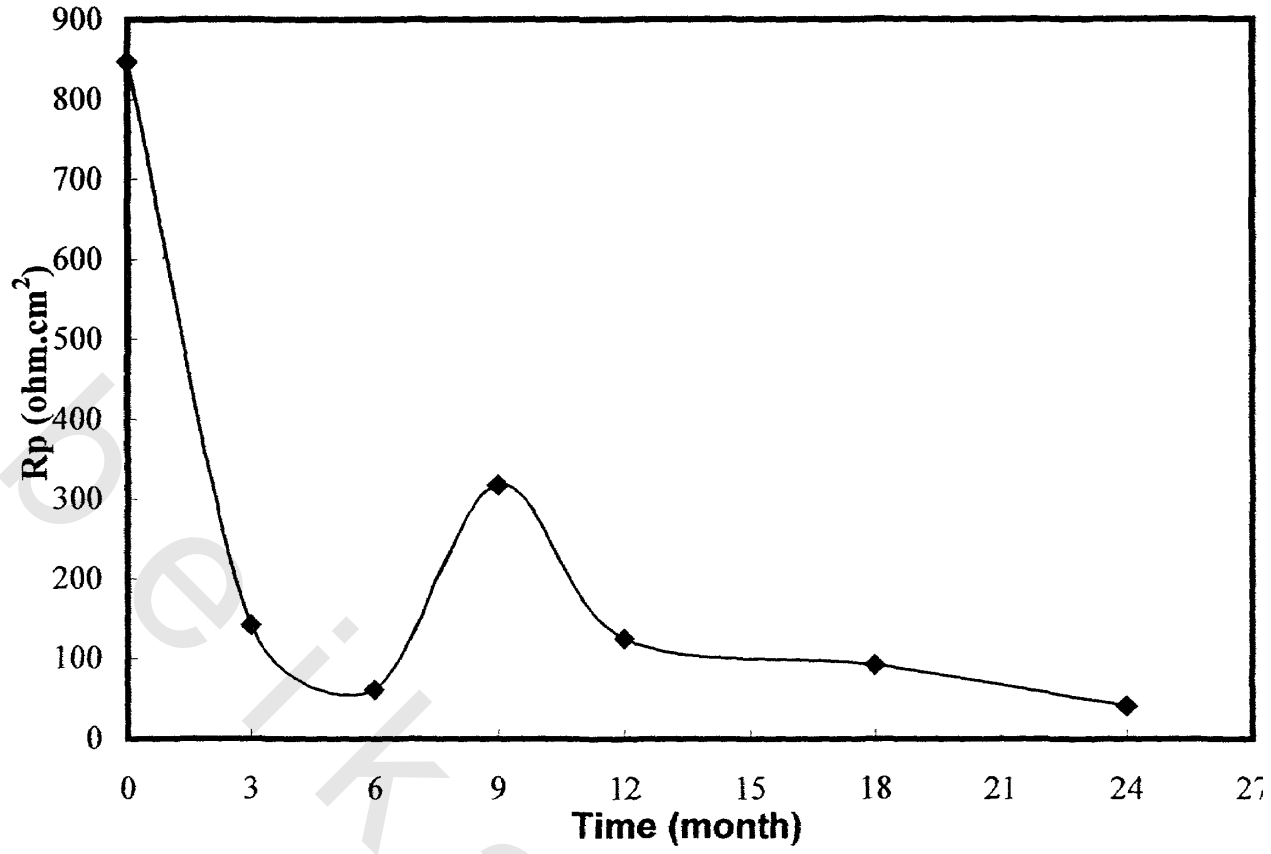

Fig.(4.8) - Polarization resistance of carbon steel in sea water as a function of immersion time.

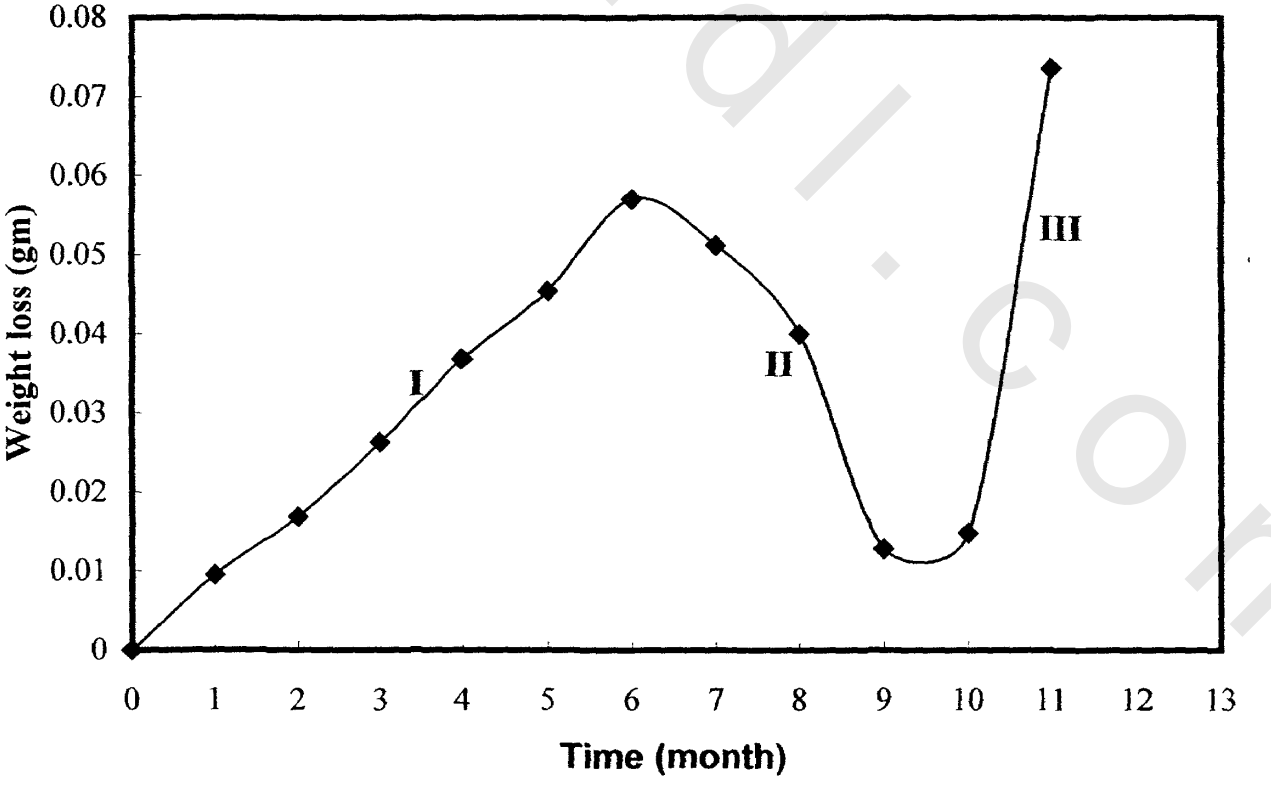

Fig.(4.9) - Weight loss of carbon steel in sea water as a function of immersion time.

pores in the oxide film). Then, the chloride ions pass through the pores and make a contact with iron lattice, forming a complex on the oxide surface [157, 158], as following:

$$Fe^{3+} \text{ (in hydrated } Fe_2O_3 \text{ lattice)} + 2\ Cl^- \text{ (adsorbed on the oxide surface)} + 2\ OH^- = Fe(OH)_2\ Cl_2^- \quad (4.12)$$

These soluble species ($Fe(OH)_2\ Cl_2^-$) diffuse from the reaction site and, as a result, the oxide film is thinned to the point at which Fe^{3+} ions can pass from the metal to the solution interface [159], and hence, further increase in the weight loss is observed [(region III in Fig. 4.9)].

It is apparent that the results obtained from weight loss measurements are in agreement with potentiodynamic data and indicating the same proposed corrosion mechanism for carbon steel alloy.

4.1.4. X- Ray diffraction studies:

A cursory review of literatures [160, 161] shows that X - ray diffraction analysis has contributed to understanding of the corrosion behavior for many metals and alloys.

The X - ray diffraction patterns were recorded in the angular range of 10 - 90° two theta (2° min^{-1}). The patterns were used for identifying iron phases formed in the corrosion products on various carbon steel coupons which were immersed in sea water at atmospheric temperature for different exposure intervals up to 12 months. Each X - ray diffraction pattern has a different look dependent on the immersion time.

Starting with an oxide - free surface, at zero exposure time (i.e., blank steel coupons), the diffraction pattern shows the characteristic peaks of iron phase at values of 2θ of 44.58, 65.01 and 82.23 as shown in Fig. (4.10 – a) and they are found to be matched well with the Joint Committee on Powder Diffraction Standards (JCPDS), card no. (06 – 0696).

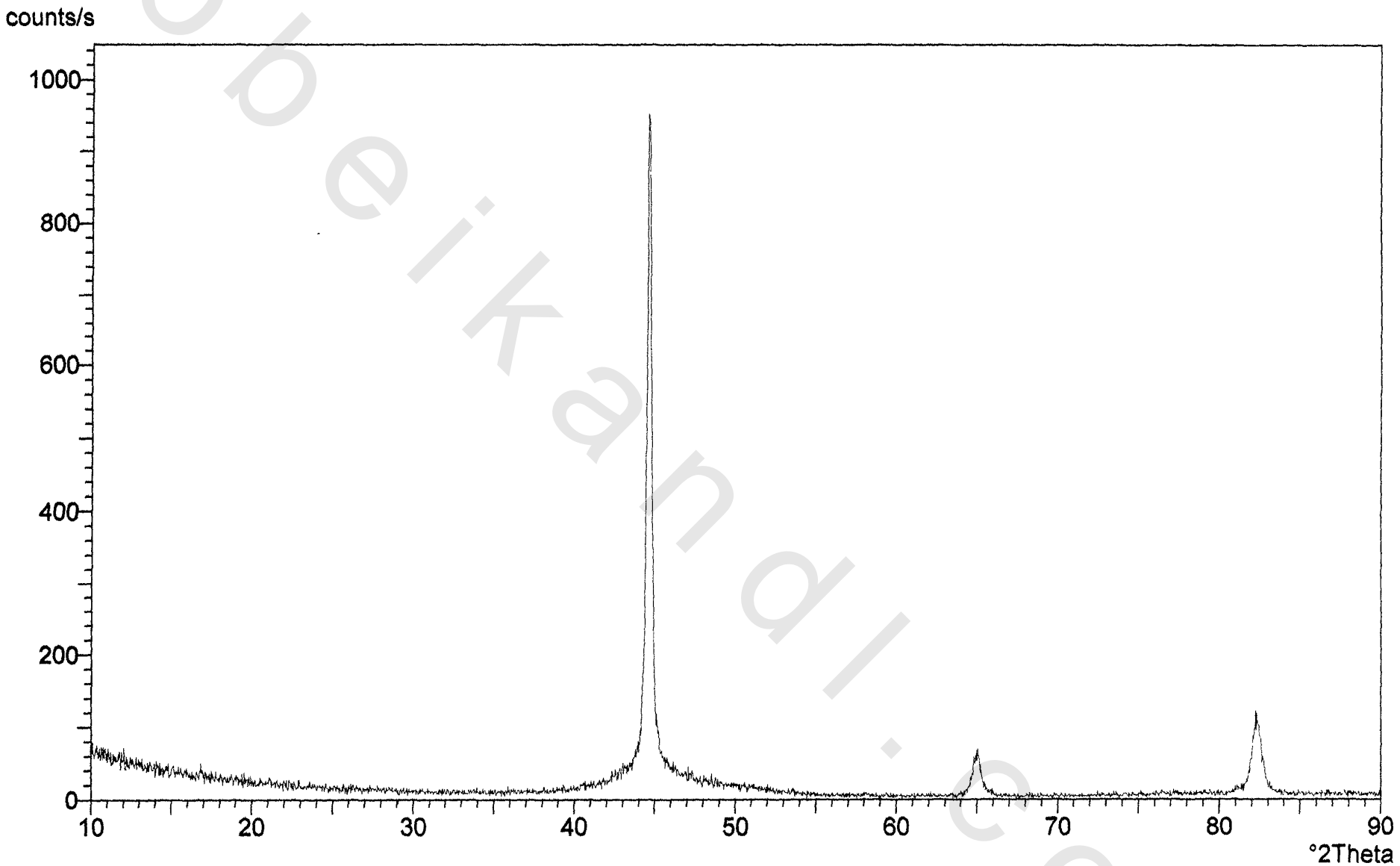

Fig(4.10-a) – X-ray diffraction pattern of carbon steel (blank)

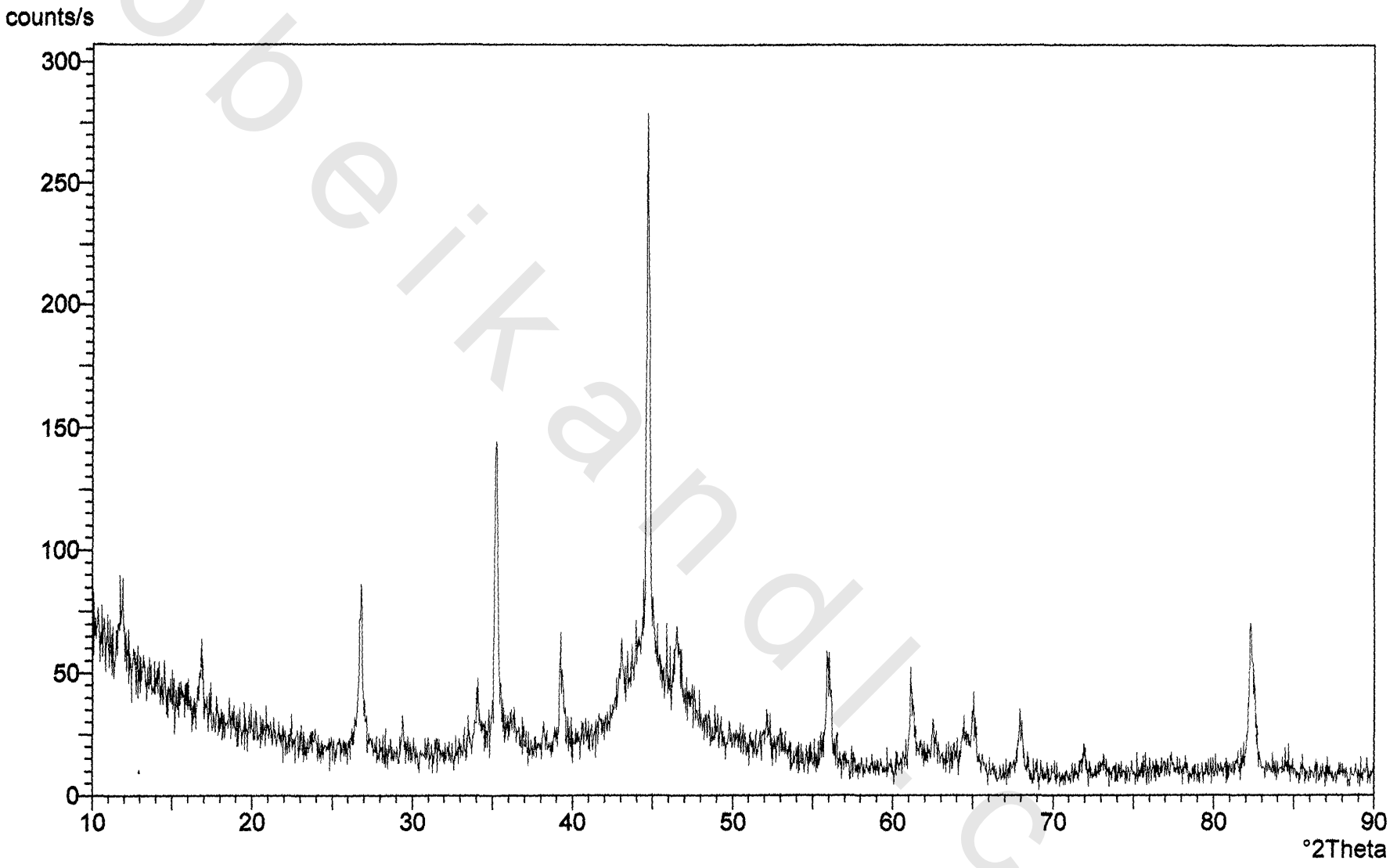

Fig(4.10-b) – X-ray diffraction pattern of carbon steel (immersed in sea water for 3 months)

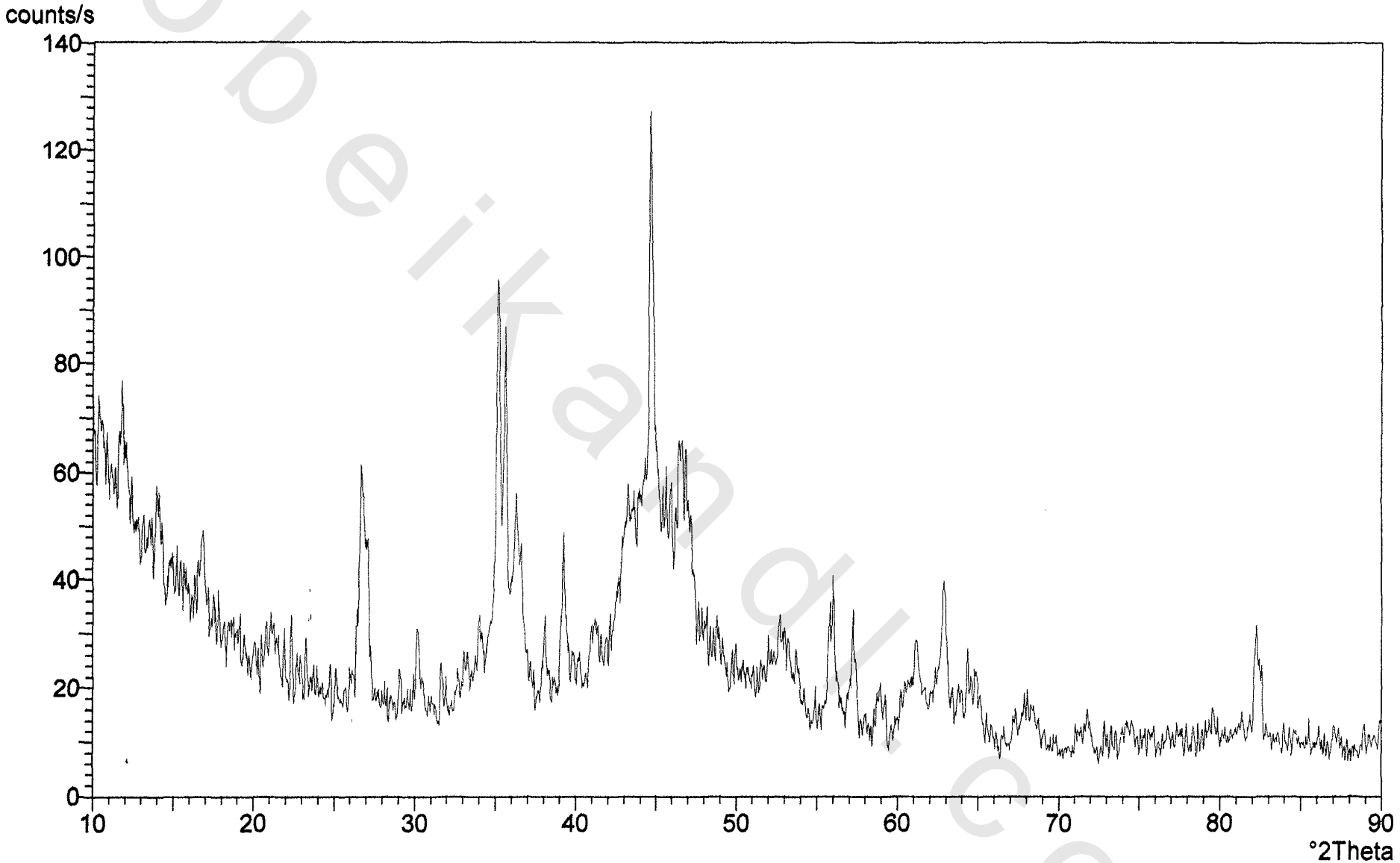

Fig(4.10-c) – X-ray diffraction pattern of carbon steel (immersed in sea water for 6 months)

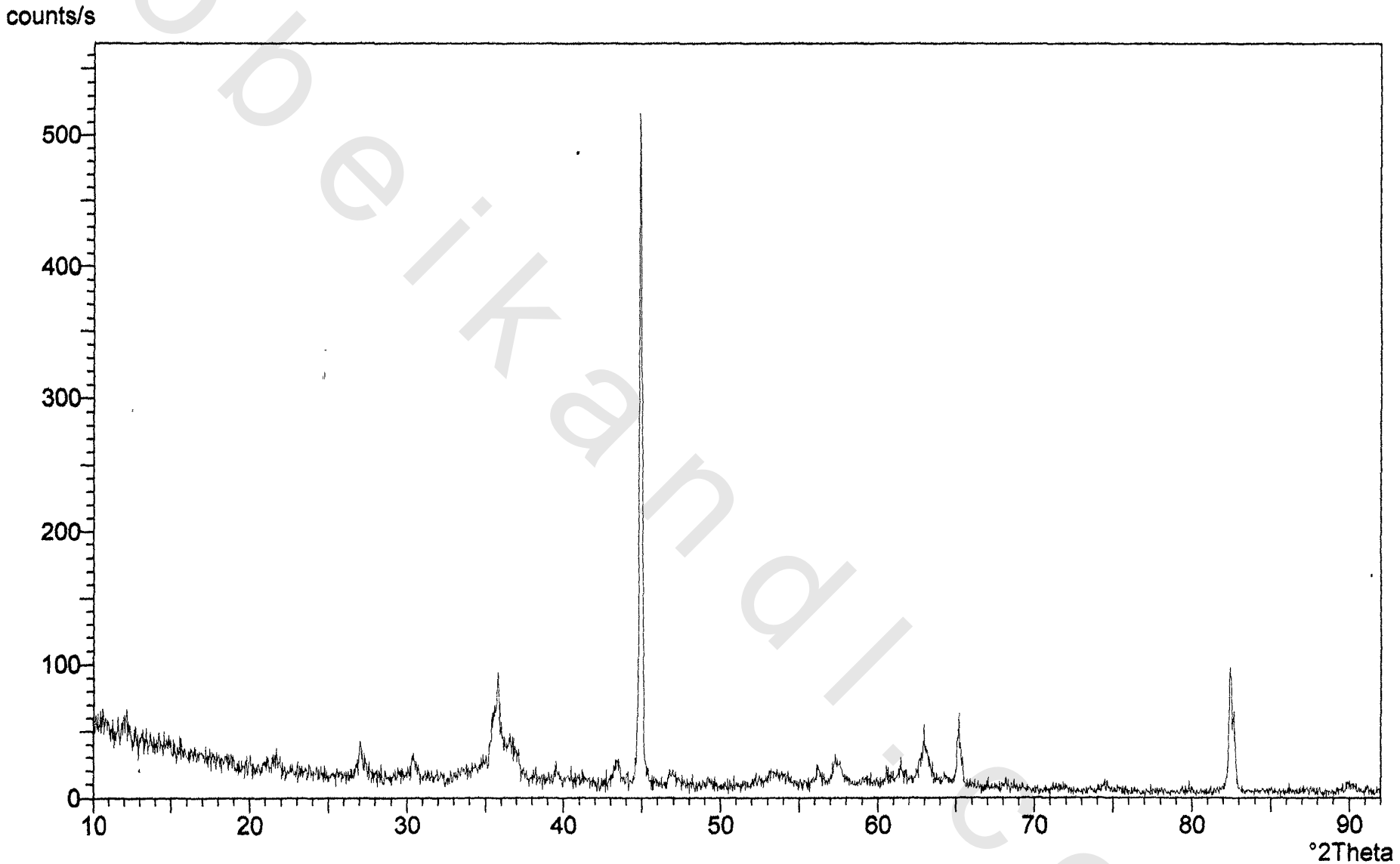

Fig(4.10-d) – X-ray diffraction pattern of carbon steel (immersed in sea water for 9 months)

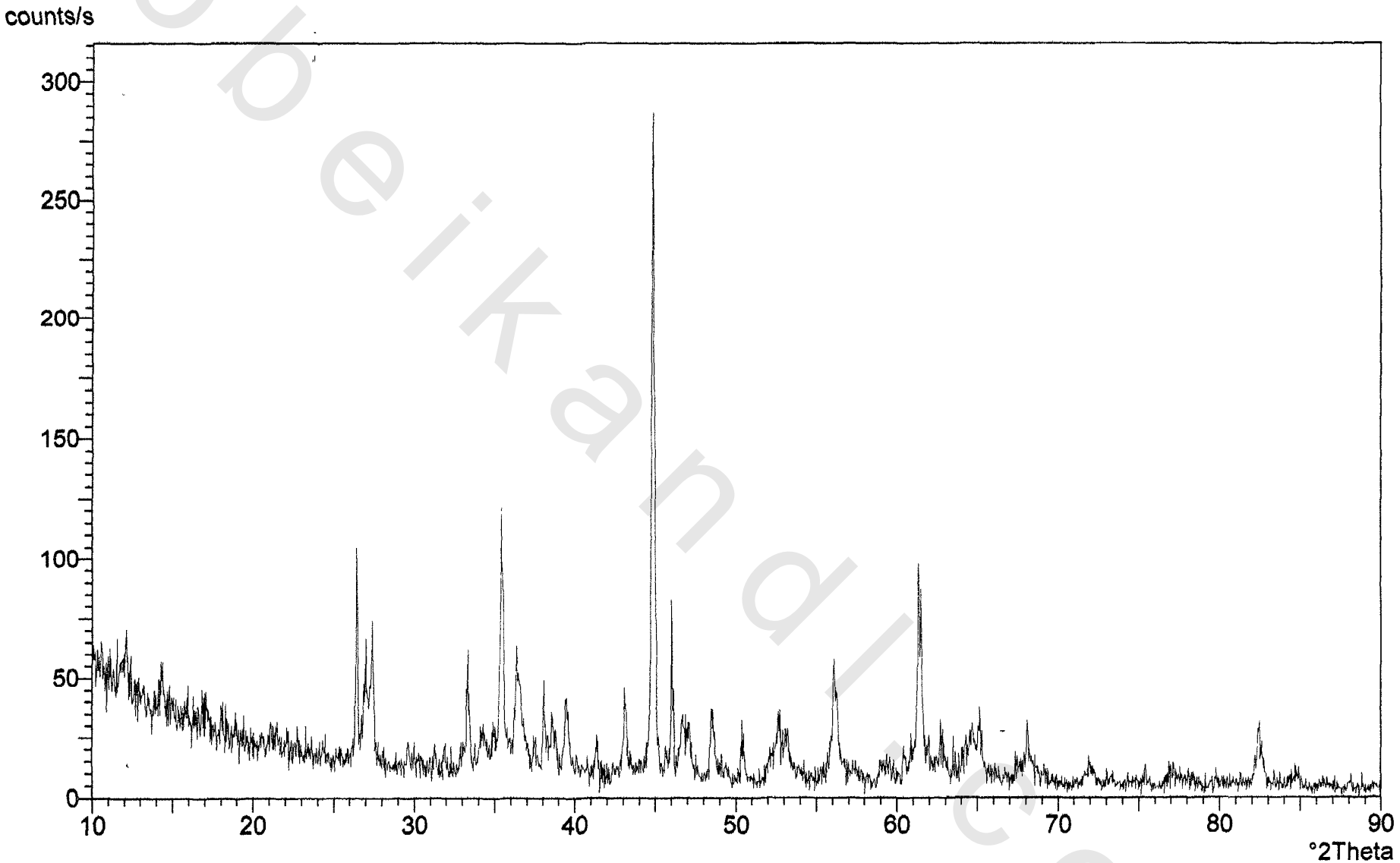

Fig(4.10-e) – X-ray diffraction pattern of carbon steel (immersed in sea water for 12 months)

The diffraction pattern of carbon steel after 3 months of immersion indicates initiation of corrosion by the formation of tetragonal iron oxide hydroxide FeOOH, at 2θ of 26.44, 35.41, 56.08 and 65.13 as shown in Fig. (4.10 – b) card no. (75 – 1594). This oxide layer is not protective against corrosion and it readily cracks allowing the ingress of seawater to the metal surface causing further corrosion [162]. However, the analysis of the corrosion products at 6 months interval as shown in Fig (4.10 – c) indicates the presence of multiphase iron oxide layer where, the most dispersed peaks of the diffraction pattern at values of 2θ : 29.83, 35.64, 57.43 and 62.94 are characteristic of Fe_3O_4 and Fe_2O_3 with cubic and tetragonal crystal structure, respectively cards no. (75 – 0033) and (80 – 2186). The formation of these oxides can be attributed to that on further immersion, a part of the previously formed oxide transforms to protective magnetic oxides of iron composed of Fe_3O_4 and Fe_2O_3 doublet layer [163]. The formation of these oxides results in protection of the metal and decrease in the corrosion rate[164, 165]. The diffraction pattern at 9 months exposure time (Fig. 4.10 – d) shows only tetragonal Fe_2O_3, card no. (80 – 2186), and Fe_3O_4 phases are not detected indicating the beginning of weakness of the protective layer. However, on increasing immersion time, the passivating film of iron oxides ,formed on the surface ,can't prevent the progressive corrosion of steel any more due to breakdown of this film as indicated by diffraction pattern at 12 months (Fig 4.10 – e) where, the only oxide detected is iron oxide hydroxide (FeOOH), card no. (75 – 1594), announcing the beginning of another stage of corrosion.

The results obtained from X-ray examinations are apparently consentaneous with potentiodynamic and weight loss data and give good evidence for the proposed corrosion mechanism of carbon steel alloy in seawater.

4.1.5 Metallography:

A scanning electron microscope (SEM) was used to study the steel surface after removing the corrosion products. A magnification factor of 1000 was used

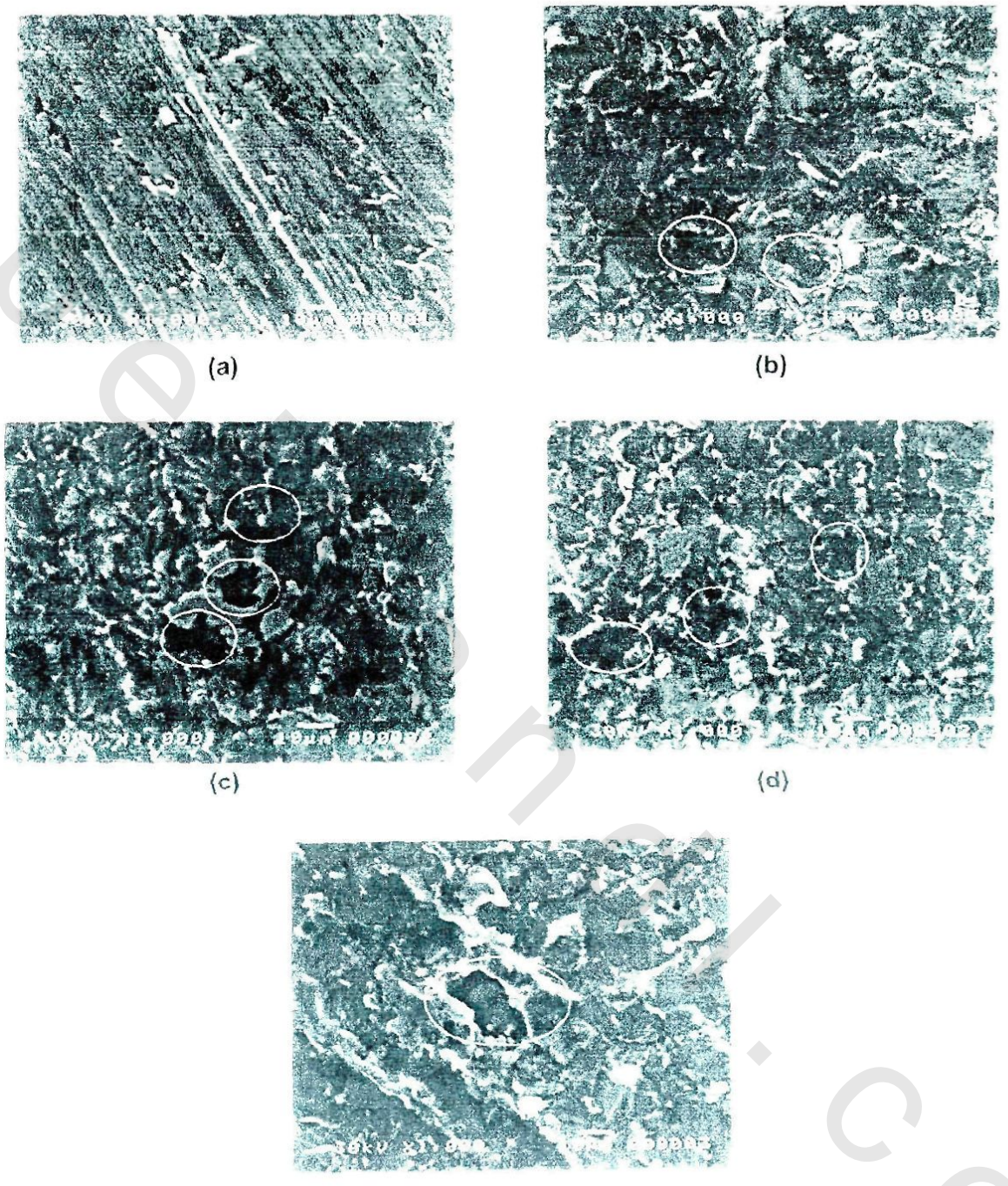

Fig.(4.11)-SEM micrographs of carbon steel surface after ageing by seawater

(a) blank, (b) 3months, (c) 6months,(d) 9months,(e) 12months

(magnification power 1000) .

for the images. Carbon steel samples subjected to 0,3,6,9 and 12 months of immersion in seawater are scanned and the micrographs are shown in Fig. (4.11 a - e), respectively. For comparison, a micrograph of a steel sample at zero exposure time is shown in Fig. (4.11 – a). The micrograph of 3 months exposure specimen [Fig. 4.11-b] shows a little bit change in surface morphology and there is no marked damage but some small pits can be observed. A relatively large number of fairly small and shallow pits are formed after 6 months of immersion as shown in Fig. (4.11 - c). The specimen is observed to undergo extreme pitting and the severity of pitting is enhanced by time.

However, micrograph of 9 months exposure sample does not show a significant change [Fig. 4.11 - d] compared with that of 6 months specimen. With further increase in time (12 months), the pits seem to grow bigger as indicated by Fig (4.11 - e). The number of pits are observed to merge and overlap with one another resulting in a total decrease in the number of pits but with a noticeable increase in area of pits [166].

One possible reason for the increase in the corrosion rate with time can be ascribed to the autocatalytic nature of pitting. In a pit, there is an excess concentration of positive charges due to iron dissolution, resulting in the migration of chloride ions to maintain electro neutrality [167]. Thus, there is a high concentration of $FeCl_2$ in the pit, and as a result of hydrolysis, a high concentration of hydrogen ions too. Both hydrogen and chloride ions stimulate the dissolution of most metals and alloys, hence, the entire process accelerates with time, resulting in an increase in corrosion rate of carbon steel. The following reactions are assumed to take place [166]:

$$Fe = Fe^{2+} + 2\,e^{-} \qquad (4.13)$$

$$Fe^{2+} + 2\,Cl^{-} = Fe\,Cl_2 \qquad (4.14)$$

$$Fe\,Cl_2 + 2\,H_2O = Fe\,(OH)_2 + 2\,HCl \qquad (4.15)$$

The all result from the different methods of investigation of carbon steel corrosion behavior show that, although carbon steel offers a lot of advantages as a material it has one indisputable drawback, which is, its natural tendency to corrode in sea water. Thus it can be concluded that the use of unprotected carbon steel in seawater application is unsafe, and hence, the study of various corrosion protection methods of carbon steel is desirable.

4.2.Physicochemical Properties of EPDM/PE Blends:

4.2.1. Swelling Behavior:

As the solvent is absorbed in the polymer, swelling begins, and its duration depends on the chemical and physical nature of the solvent-polymer pair [168]. Upon swelling polymer properties may change dramatically, therefore the interaction of polymeric materials with different solvents is a problem from both the academic and technological points of view. The mass and dimensions of polymer system may be changed due to the penetration of the solvent into swollen specimen, so swelling process may lead to deformation or destruction of the sample microstructure [169]. When a cross linked polymer is brought in contact with a solvent, the network absorbs a certain amount of liquid depending strongly on the molecular weight of this liquid and the degree of polymer cross linking [170], hence, the swelling process and its kinetics give an idea about the density of cross links in polymer matrix.

a- Degree of swelling

The time dependence of the degree of swelling for various EPDM/PE blends, with different blend ratios and thickness, is shown in Fig. (4.12). The general behavior may be approximated by an exponential growth function for all samples showing positive swelling mechanism of the form:

$$Q = Q_m [1- \exp (-t / \tau)] \qquad (4.16)$$

where, Q is the degree of swelling at time t, Q_m is the degree of equilibrium swelling and τ is a characteristic time which depends on both the polymer matrix and the cross linking density as is observed in Table (4.2).

Table (4.2) -The values of Q_m and τ for EPDM / PE blends with different thickness 1 mm (a), 2 mm (b), 3 mm (c).

(a)

Blend ratio	Q_m	τ (days)
80 / 20	0.003273	20.1977
70 / 30	0.004087	12.74335
60 / 40	0.009536	7.19457

(b)

Blend ratio	Q_m	τ (days)
100 / 0	0.008258	36.1455
90 / 10	0.010562	27.5064
80 / 20	0.012288	27.1533
70 / 30	0.015337	24.6745
60 / 40	0.026791	10.8097

(c)

Blend ratio	Q_m	τ (days)
100 / 0	0.008465	56.3211
90 / 10	0.017250	18.4798
80 / 20	0.022284	14.6067
70 / 30	0.024625	14.4687
60 / 40	0.033018	13.4427

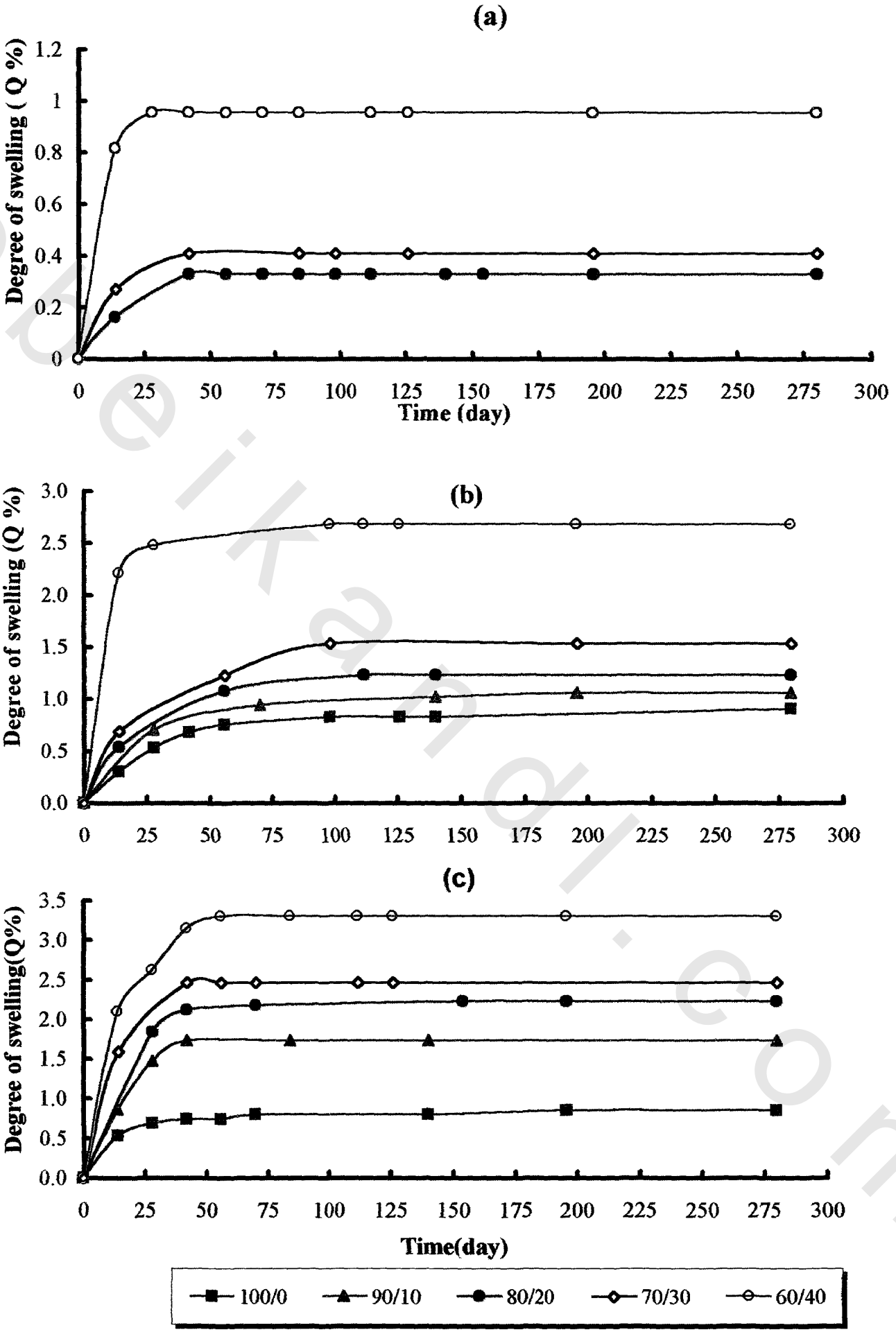

Fig.(4.12) - Dependence of the degree of swelling (Q %) on time for EPDM/PE blends ,(a) 1mm ,(b) 2mm ,(c) 3 mm thickness.

The data shown in table (4.2) indicate that addition of polyethylene (PE) to EPDM is accompanied by a decrease in the values of (τ). Fig. (4.12) shows the dependence of the degree of water uptake by the samples (represented in percent form i.e. Q %) on the blend ratio. It can be noticed that increasing PE content in the blend leads to a slight increase in water uptake. This can be attributed to the fact that the swelling of polymer networks in suitable liquids is found to be large for three dimensional network polymers [171]. Given that polyethylene chains are not flat, but they have a three dimensional shape, where the hydrogen atoms being arranged along an inner zigzag chain of carbon atoms [172],this may explain the increase in the extent of water uptake by the sample upon incorporation of polyethylene into rubber matrix. However, it can be noticed that this negative effect is very weak, and we can simply regard all EPDM / PE blends, even with high PE content, resistant to water uptake but with slightly different degrees.

It can be noticed from Fig (4.12) that the initial rate of water absorption is followed by nearly a horizontal behavior, which indicates early saturation of the samples. This saturation phenomenon can be explained by the fact that the extent of swelling represents a competition between two forces, the first one is the free energy of mixing which, causes the solvent to penetrate and tries to dilute the polymer saturation. The second opposite force is generated when the polymer chains in the cross-linked polymer network begin to elongate, under the swelling action of the solvent, this force is an elastic retroactive force in opposition to deformation. We can say that the swelling reaches steady state when these two forces are balancing [173]. Also this saturation behavior of EPDM / PE blends can be explained regarding the solvent effect. It is well confirmed that, when polymers are exposed to a salt solution the curve leveled off, after an initial high rate of water absorption, and eventually equilibrium is attained. This can be attributed to the fact that the presence of salts in water inhibited the uptake of water by varnishes, and the stronger the salt, the less is the amount of water

absorbed [174] . As the solvent in our swelling tests is natural sea, which is rich in salts, so the equilibrium shown in Fig. (4.12) is in agreement with the previous studies [175]. However, the horizontal part of the curves means that the rubber blend degradation or extraction of its soluble ingredients is very small.

The dependence of the degree of maximum swelling for different blends on temperature was investigated, and the results are shown in Figs.(4.13 – 4.15). It can be noticed that the rising of temperature from 30 to 50° C has a slight effect on the swelling degree of the samples, while samples exposed to 70° C show a noticeable increase in swelling degrees with progress of time, which can be explained by the fact that the rising of temperature leads to an increase in the internal stress caused by the diffused liquid [176]. When this internal stress becomes high compared with the forces between macromolecules, it enhances the swelling and leads to higher degree of swelling at higher temperatures. Also the thermal expansion caused by rising temperature creates, an additional free volume, which is considered as another reasonable explanation for the observed increase of swelling.

(b) Penetration rate and average diffusion coefficient:

It is well known that water uptake and ion penetration of the coating are important factors that determine the corrosion stability of organic coatings. Also, diffusion is one of the major processes, responsible for the transport of water and other species through a coating [177 – 180] ,hence, it was essential to study the penetration rate (P) and average diffusion coefficient ($D_{av.}$) of sea water in EPDM / PE blends. The variation of the increase in weight (due to swelling) with the square root of time, for EPDM / PE blends is shown in Fig. (4.16). The slopes of the straight lines obtained at the early stage of the process ($M_t / t^{1/2}$)

were calculated, then (P) was calculated using the equation: [181]

$$P = \frac{1}{2} \quad \frac{d}{M_e} \quad \left(\frac{M_t}{t^{1/2}}\right) \qquad (4.17)$$

and D_{av} is given by:

$$D_{av} = \frac{\Pi}{4} \quad (P^2) \qquad (4.18)$$

Where d is the sample thickness, M_e is the swelling at equilibrium, and M_t is the swelling after time t.

The calculated values of P and $D_{av.}$ were plotted as a function of PE content in various EPDM / PE blends, and the results are illustrated in Figs. (4.17) and (4.18). The observed low values of P and $D_{av.}$ can be attributed to the reinforcement effect of carbon black i.e the chemical crosslinks between carbon black and macromolecules, which lead to an increase in the crosslinking efficiency of the blends. Also, it can be noticed that incorporation of PE into EPDM rubber matrix has a very slight effect on (P) and hence on ($D_{av.}$), until a critical value of PE is attained, (0.3 weight fraction), a noticeable increase in (P) and ($D_{av.}$) is observed. This behavior can be explained according to the proposed model of electrolyte penetration [182], which suggests that the electrolyte penetration through polymer blend is controlled by the crosslinking density of the polymer network. Thus, it can be said that sulphur vulcanization system is not highly efficient in crosslinking PE [183], hence, the observed decrease in the overall corsslinking degree of EPDM / PE blends upon the increasing PE content. This decrease in crosslinking density results in increasing the values of (P) and ($D_{av.}$).

It is well confirmed that, upon the development of coatings, it is necessary to optimize the permeability of the coating for water and corrosive species, so the above results which show the excellent swelling behavior and low values of

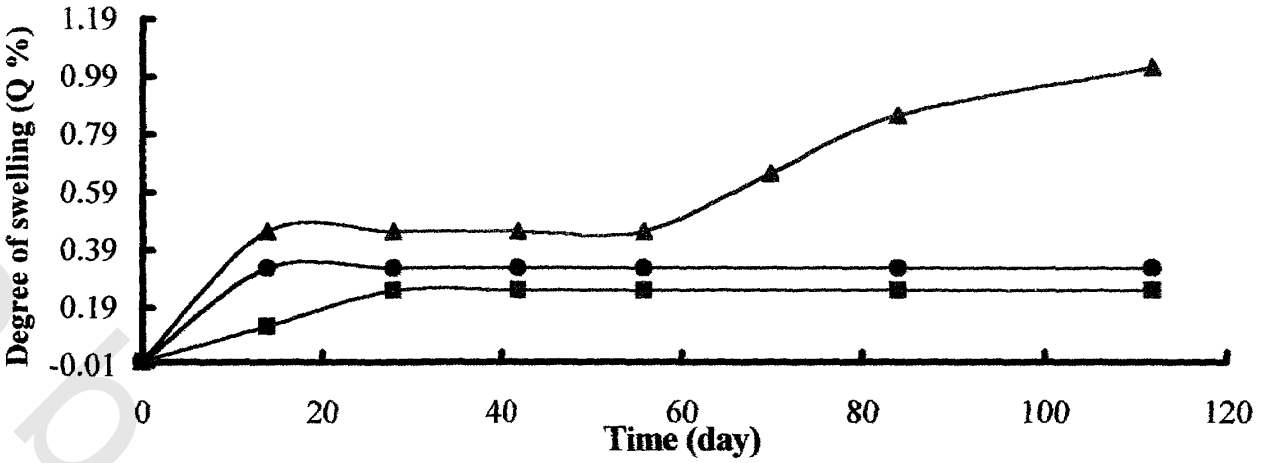

Fig.(4.13) - Variations of swelling degree of EPDM/PE blend (100/0) in sea water at different temperatures

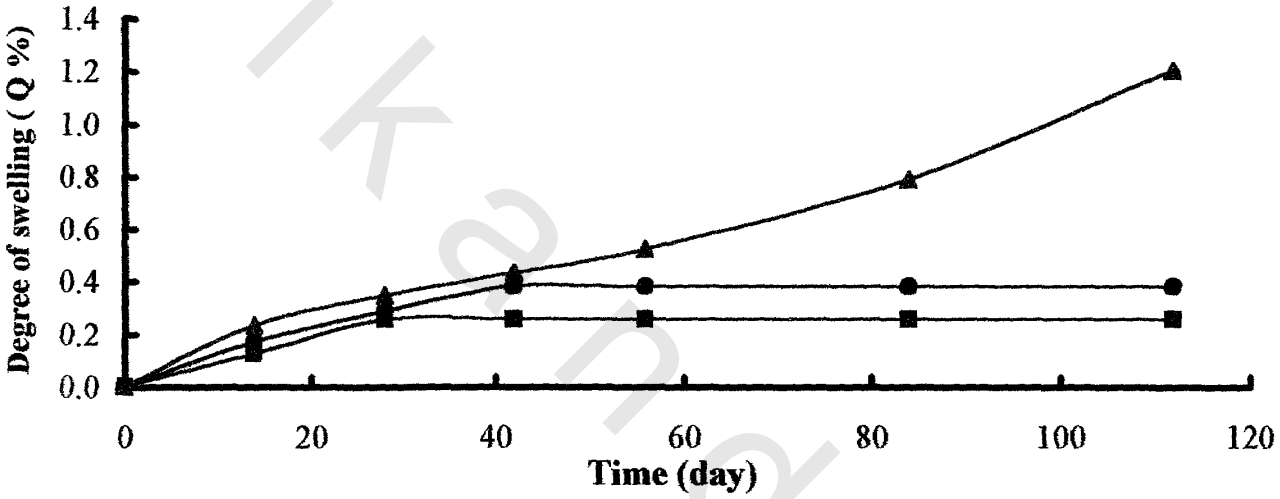

Fig.(4.14) -Variations of swelling degree of EPDM/PE blend (80/20) in sea water at different temperatures

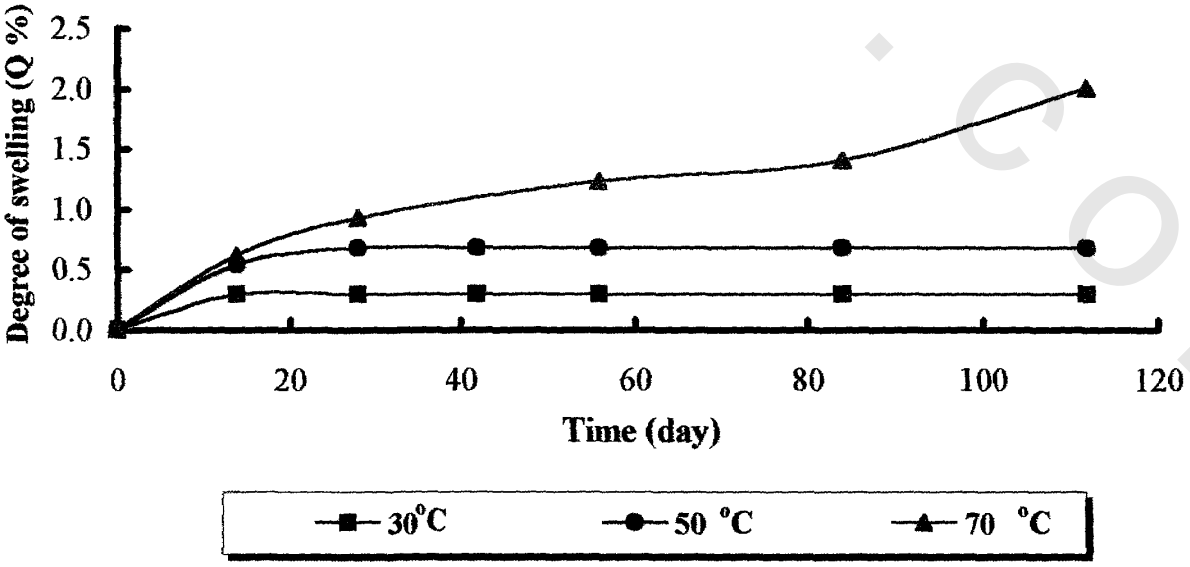

Fig.(4.15) - Variations of swelling degree of EPDM/PE blend (60/40) in sea water at different temperatures .

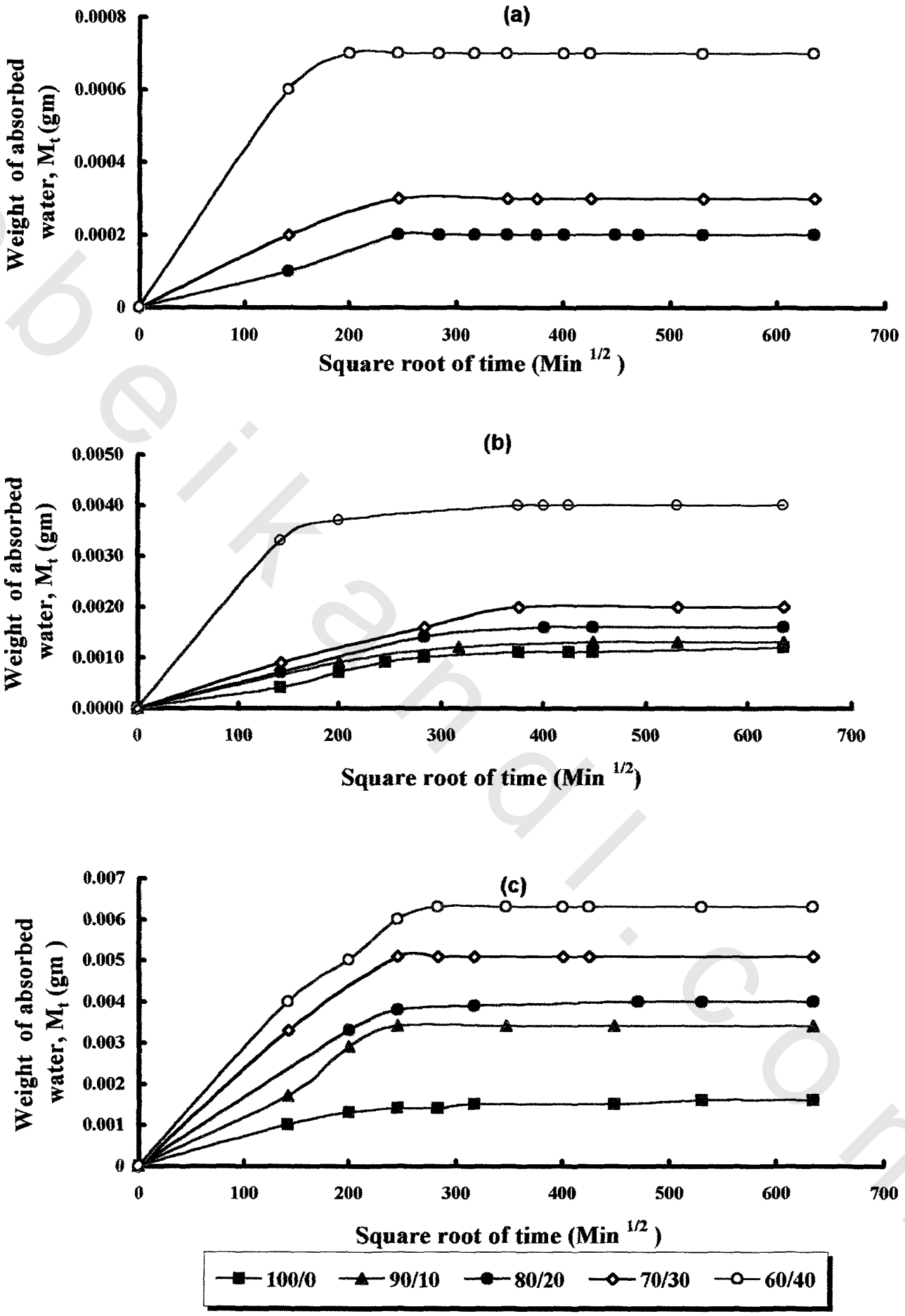

Fig.(4.16) -Weight of abosrbed water (M_t) versus square root of time for EPDM/PE blends with thickness (a) 1mm ,(b) 2mm ,(C) 3mm

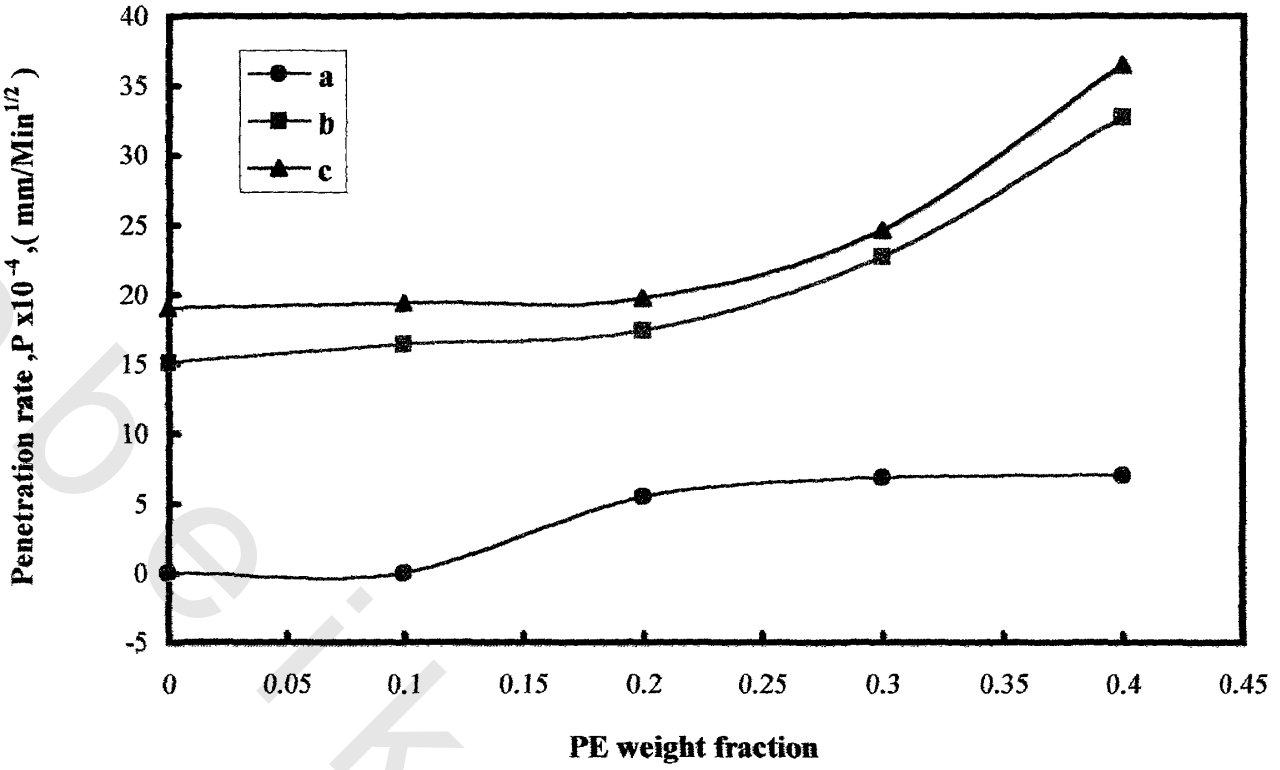

Fig (4.17) - Dependence of penetration rate on PE content of EPDM/PE blends ,with thickness (a) 1mm,(b) 2mm ,(c) 3mm

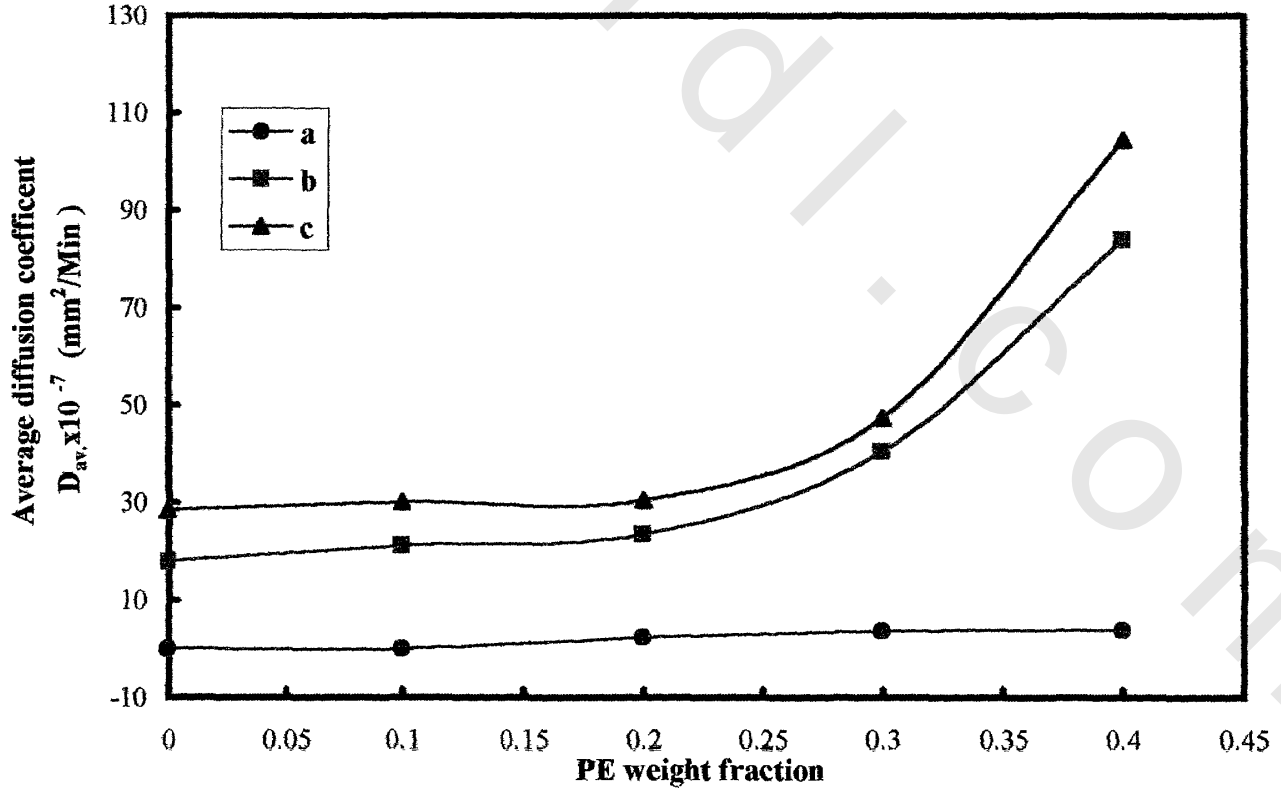

Fig.(4.18) -Dependence of average diffusion coefficient on PE content in EPDM/PE blends ,with thickness (a) 1mm, (b) 2mm, (C)3mm

penetration rate and diffusion coefficient for EPDM / PE blends, indicate that these blends can be considered as promising coatings.

4.2.2 Mechanical properties of EPDM / PE blends:

Mechanical properties are important parameters that characterize polymers. They provide basis for quality control and comparative evaluation of various polymer coatings [184], hence investigation of stress – strain behavior of polymer blends is essential. An important parameter that has been found to be effective in modification of the mechanical properties of the blend is its composition [185] (i.e. the blend ratio), therefore it has been found desirable to present the changes occurring in mechanical properties as a function of blend ratio.

Stress – strain measurements of the samples have been carried out at working temperature (30°C) and the obtained results are shown in Fig. (4.19). Generally, it can be seen that blending EPDM with PE improves mechanical properties of this elastomer as will be discussed later in details.

(a) Tensile strength:

The results illustrated in Fig. (4.20) show the variation of the tensile strength at break (TS) as a function of weight fraction of PE, where two regions can be noticed. Region (I) represents the TS of the matrix of low PE content (0, 0.1 and 0.2 weight fraction) in which the addition of PE to EPDM has no effect on the tensile strength, while region (II) shows that incorporation of PE with greater weight fraction (0.3and 0.4) leads to an increase in TS values of the blend, this increase can be attributed to the predominance of the crystalline phase in the matrix. Also the occurrence of intercrosslinking, either between the macromolecules of each component or between the macromolecules of the amorphous phase of the two components, leads to an increase in the degree of crosslinking, which enables the blend to bear higher stress level and, hence,

shows high tensile strength values. The linearity obtained at region (II), may be taken as an indication for the reasonable compatibility of the two polymers at this stage [186, 187].

It is well known that, tensile strength is important for a material that is going to be under tension. Also functional coatings protect substrates from the ravage of nature, which often provide a hostile environment and can cause wear through rusting or erosion so, a coating with high tensile strength is desirable, therefore EPDM / PE blends can be considered as efficient coatings.

(b) Elongation at break:

The variation of the values of elongation at break (E_b) as a function of weight fraction of PE is presented in Fig. (4.21). It can be noticed that at low concentration of PE the values of E_b undergo a slight decrease, while for high weight fraction of PE (higher than 0.2), a remarked decrease of E_b with noticeable rate is observed. These results can be explained by the fact that elongation is a type of deformation, and as it is well known that, the crystalline polymers resist deformation, it would be expected that the elongation behavior of the blend will be a function of the crystallinity percentage of the plastic component. Thus increasing the weight fraction of PE will increase the crystallinity contribution in the blend hence; it will be accompanied with a decrease in the elongation property of the blend. However it is very interesting to note that polyethylene have a similar tendency with elastomeric materials, even though polyethylene would show plasticity rather than elasticity. Therefore, the approximation may be made that as polyethylene shows essentially energetic elasticity, it can be treated with the same method as those of rubbery materials showing entropic elasticity [188]. However, we can say that although incorporation of PE into EPDM matrix leads to a decrease in elongation at break (E_b), this decrease is not marked and hence EPDM / PE blends still have the desired

elasticity for coatings. It is well known that the coatings must have sufficient flexibility to withstand the hostile environments, and to ensure dependable service and long life [189].

(c) Modulus of elasticity:

Modulus is the ability of a sample of a material to resist deformation [190]. The modulus of elasticity for each EPDM / PE blend was obtained from the initial slope of the stress strain curves, then plotted as a function of polyethylene content in Fig. (4.22), where it becomes clear that three distinct regions are observed. Region (I) doesn't show any change in the modulus of the blend on adding low weight fraction of PE to EPDM matrix while, a gradual increase in modulus can be noticed in region (II) with increasing PE content up to 0.3 weight fraction. Whereas the third region is characterized by a marked increase of modulus upon the addition of higher weight fraction of PE (above 0.3).

Taking in our account that the modulus indicates the stiffness of the material, we can explain these results by the fact that EPDM / PE blend consists of two phases: amorphous and crystalline and the composite behavior of the blend is controlled by the mechanical interaction of the two phases [183]. So, we can consider blends with low concentration of PE as rubber matrix reinforced with partially crystalline LDPE, and as the soft amorphous phase is the dominant phase, this leads to the low modulus values represented in region (I). On the other hand, at high values of PE weight fraction, the blend may be visualized as a matrix of plastic that has been toughened by the amorphous elastomer, i.e., the hard plastic phase is the dominant phase, this explains the high modulus of the blends with high PE concentration observed in regions II and III of Fig. (4.22).

Knowing that coatings must be able to resist permanent indentation, scratching, cutting, and penetration by a hard objects [191], it can be clear that EPDM / PE blends possessing high modulus can act as efficient coatings.

(d) Toughness:

Toughness is a measure of the sample ability to absorb mechanical energy without breaking [192]. Toughness values of EPDM / PE blends (as obtained from the area underneath a stress – strain curve) are plotted against PE weight fraction, where the results obtained are shown in Fig. (4.23). A monotonic decrease in toughness can be observed with increasing PE content in the blend. It is well confirmed that for many common applications polyethylene is a tough polymer due to its elastic behavior [193], this elastic behavior in semicrystalline polymers, such as polyethylene, can be explained with a cluster network model in which these clusters are connected by means of tie molecules and operate as junction points [194]. The elasticity is reflected as a reasonable degree of toughness, hence addition of PE to a tough elastomer (EPDM) show a slight decrease in toughness as indicated in Fig. (4.23). So, we can say that EPDM / PE blends have a reasonable degree of toughness to act as efficient coatings, as it is well known that coatings must properly perform during manufacturing operations and during use, to do this, they must have sufficient toughness to withstand failur when subjected to bending, twisting, expansion and shrinking during temperature changes, and also to mechanical abuse.

(e) Permanent set (PS):

Permanent set is defined as the percentage change in the distance between benchmark before and after rupture.

$$\text{Permanent set (\%)} = \frac{L - L_1}{L} \times 100$$

Where , L = distance between bench marks before rupture .

L_1 = distance between bench marks after rupture .

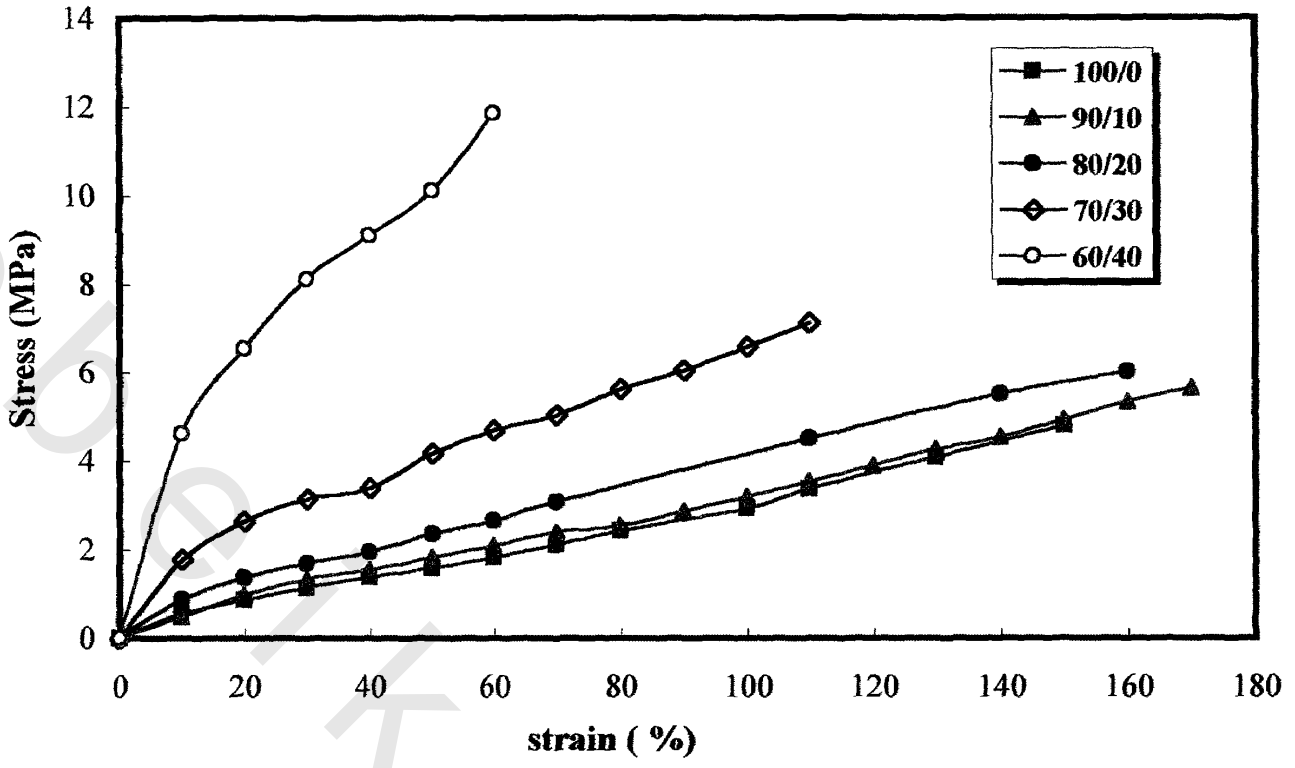

Fig.(4.19) - Stress-strain curves for EPDM/PE blends at 30 °C

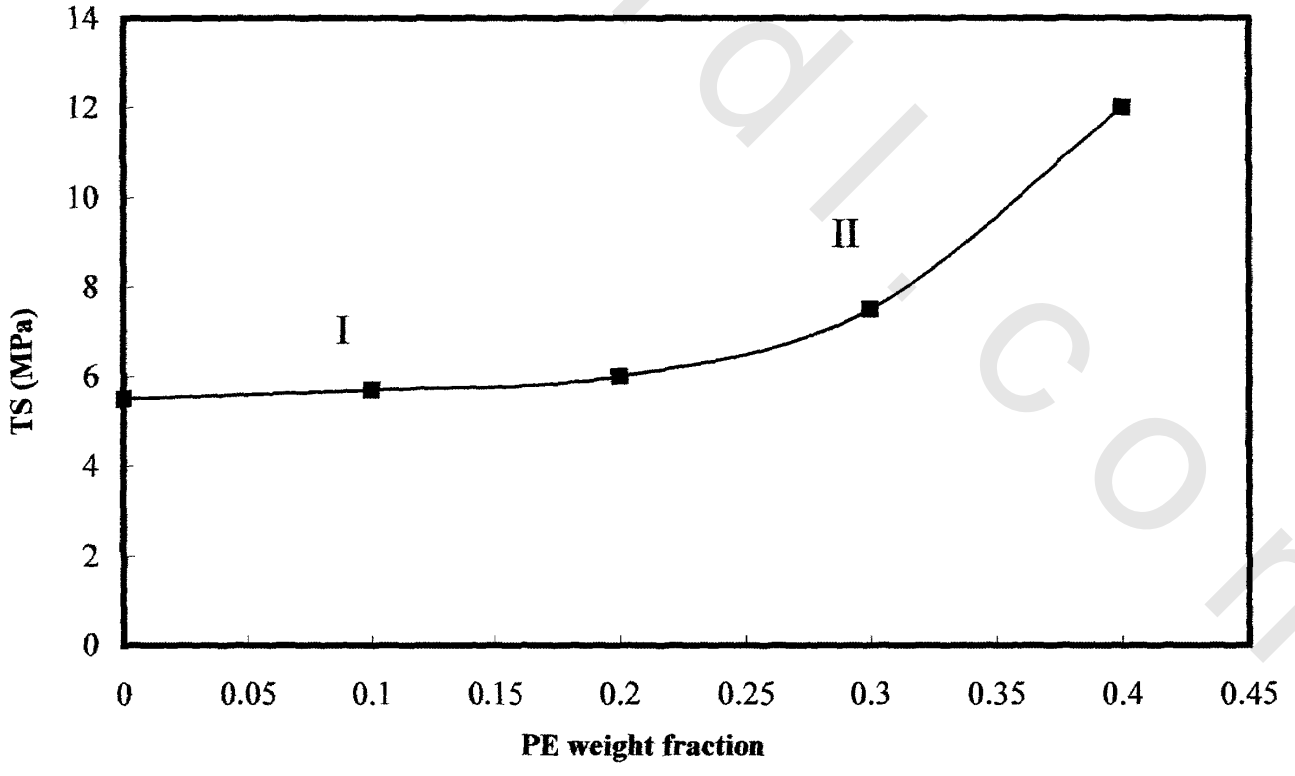

Fig.(4.20) - Tensile strenghth of EPDM/PE blends as a function of PE weight fraction

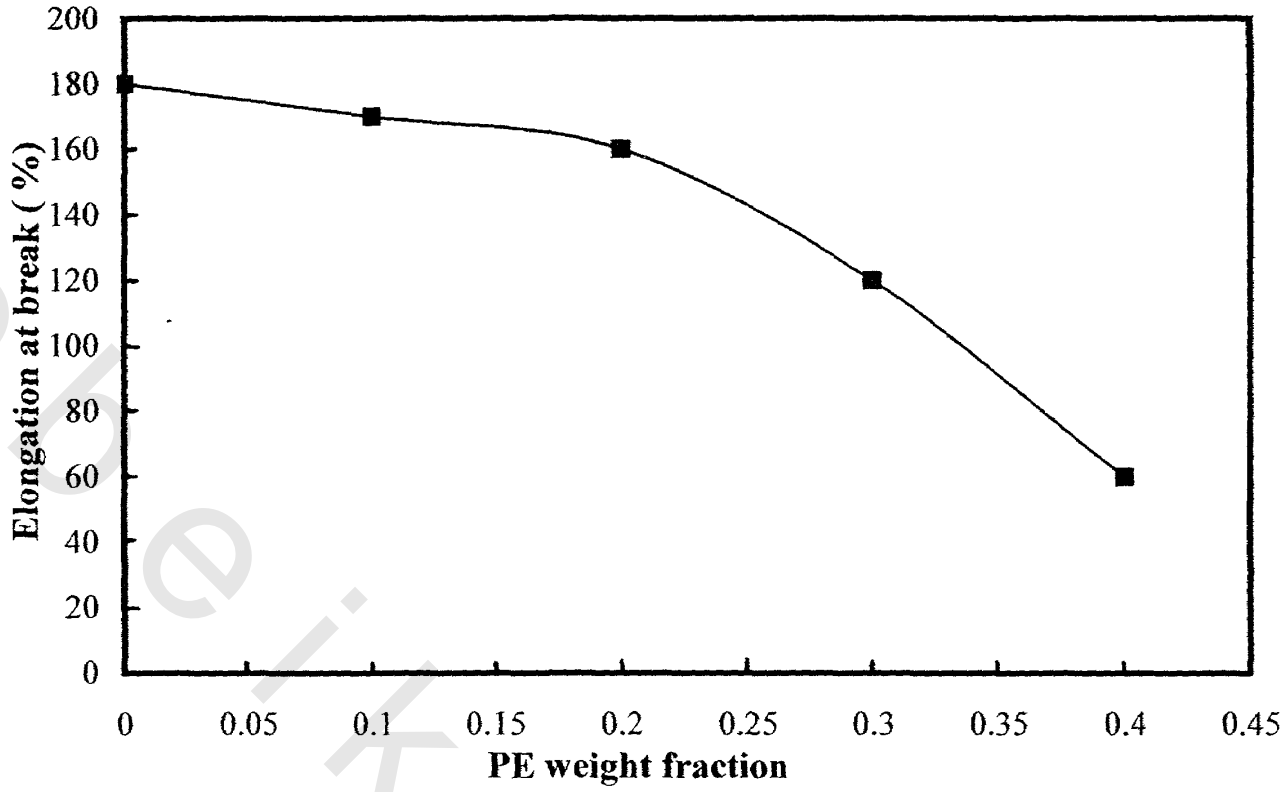

Fig.(4.21) - Variations of elongation at break of EPDM/PE blends as a function of PE weight fraction

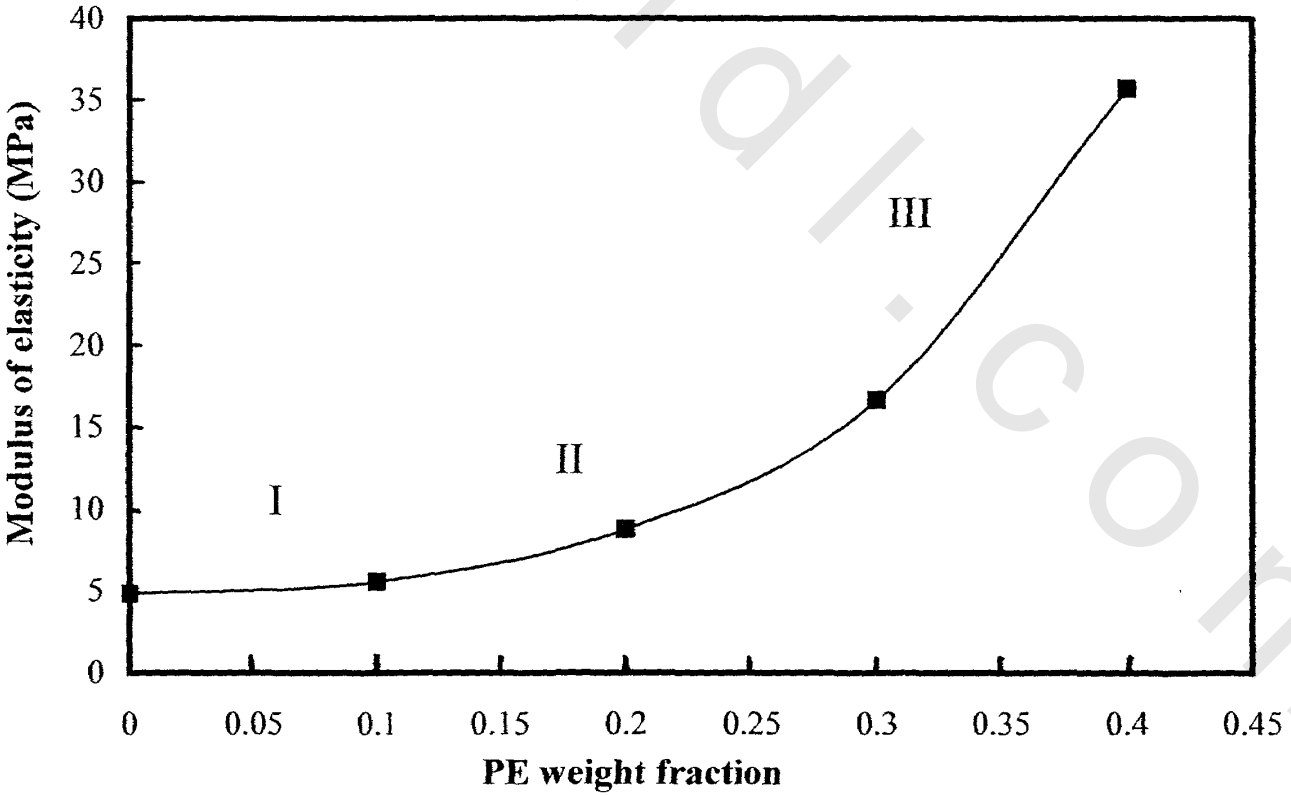

Fig.(4.22) - Modulus of elasticity for EPDM/PE blends as a function of PE weight fraction

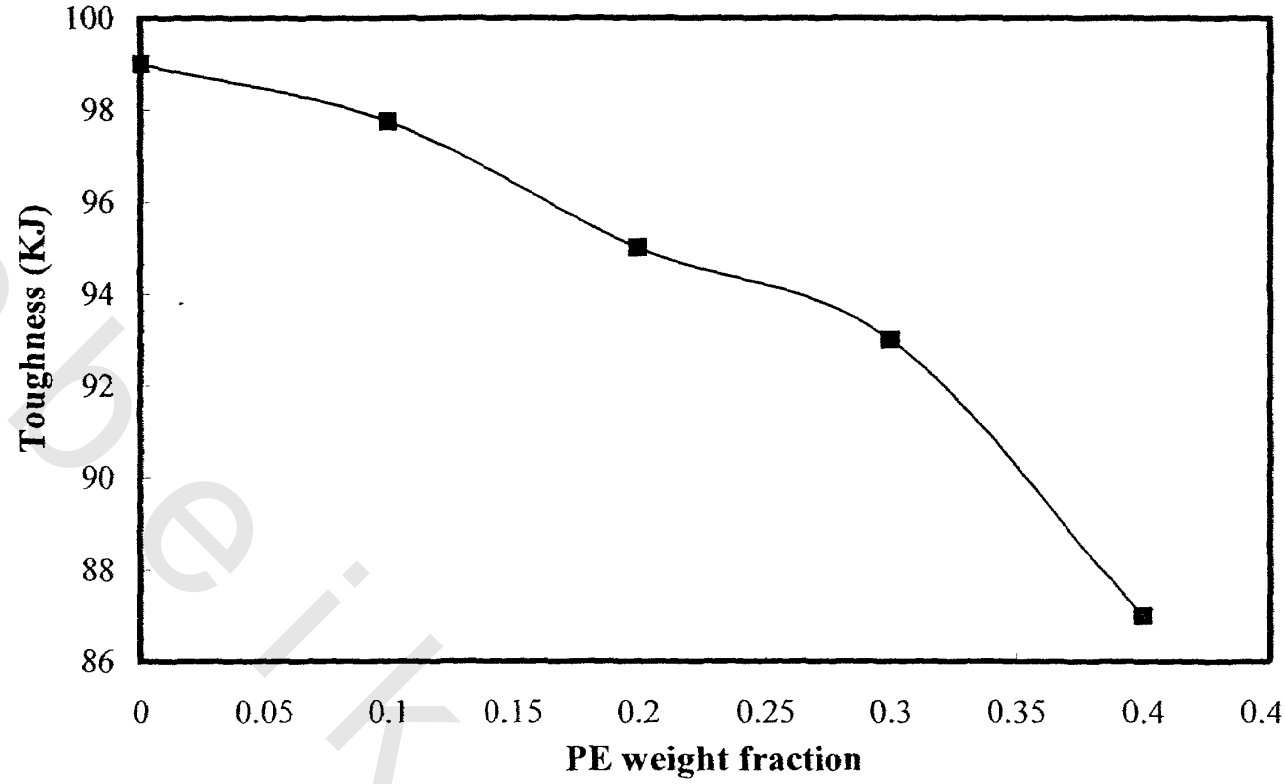

Fig.(4.23) - Variations of toughness of EPDM/PE blends as a function of PE weight fraction

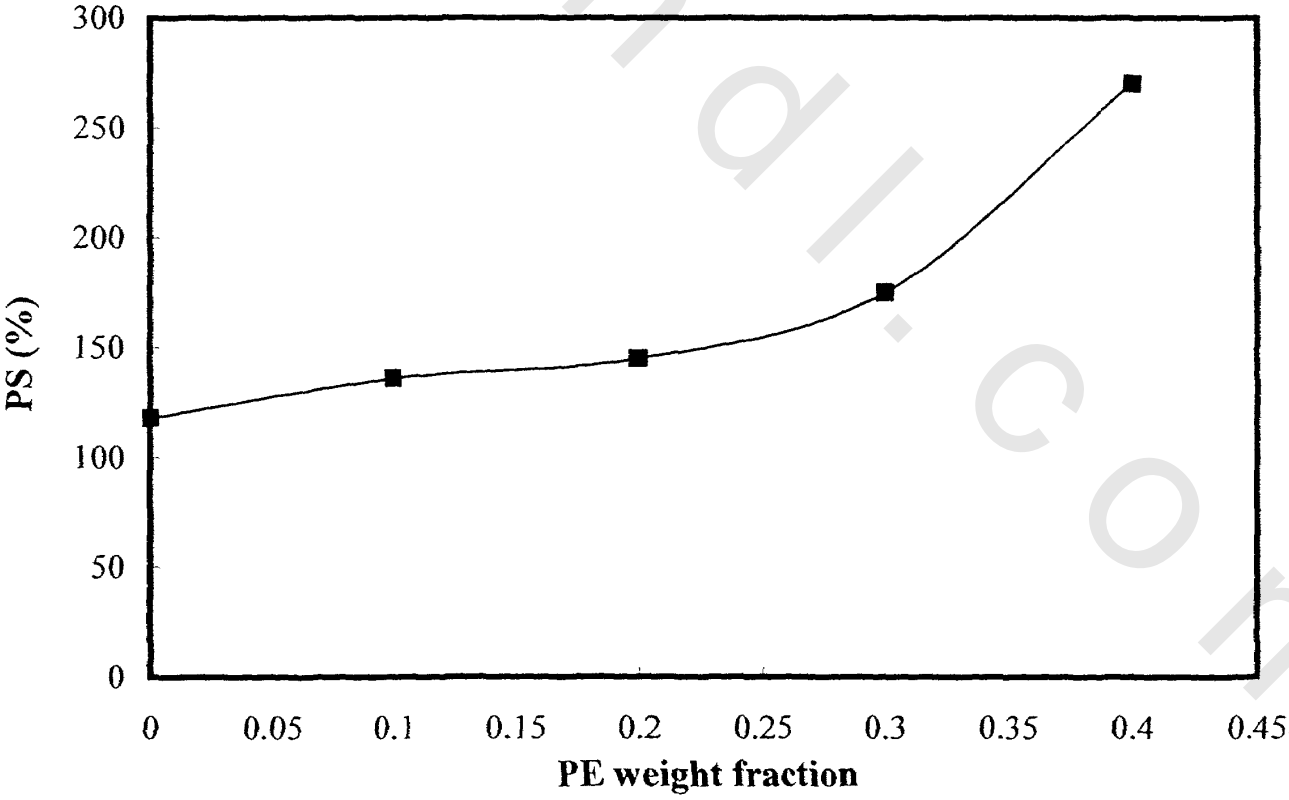

Fig.(4.24) - Permanent set of EPDM/PE blends as a function of PE weight fraction.

Fig. (4.24) gives the variation of the permanent set (PS) values as a function of PE concentration in the blend. It can be observed that PS increases with increasing weight fraction of PE above 0.2. We can explain these results by the fact that; on applying tension to the blend sample, it will be under elastic as will as plastic deformation. So, the contribution of either form of deformation would be expected to be a function of the concentration of the components in the blends. The EPDM phase will contribute mainly the elastic deformation, which is reversible, whereas the crystalline portion of LDPE is going to be the main source of plastic deformation, which is irreversible. This latter form of deformation is caused by distortions in the crystal lattice of LDPE. Knowing that the rupture of the blend sample always occurs after the yield point of PE, i.e., in the plastic deformation region, consequently, the permanent set value of the blend containing higher concentration of PE is expected to be high, and hence, an increase of PS values is observed with increasing PE weight fraction in the blend.

From all the above mentioned data, one may conclude that the addition of PE to EPDM improves the mechanical properties of its vulcanizates [195], as it leads to an increase in tensile strength, modulus of elasticity, and permanent set of corresponding EPDM / PE blend. So, EPDM / PE blends have a very good resistance against mechanical damage and good tolerance to possible mechanical stress.

4.2.3 Electrical conductivity of EPDM / PE blends:

The electrical conductivity of rubber compounds is highly important factor to many rubber products therefore; it has been the subject of considerable interest and experimental study for many years [196]. Electrical conductivity of polymeric materials depends on the presence of free ions, which are not connected chemically with macromolecules [197].

Since macromolecular chains do not participate in the transfer of electric charge so, the conductivity depends on the presence of low molecular weight

impurities that can serve as source of ions. Although the majority of polymers in nature are electrically insulators, they can be rendered conductive either by the creation of conjugated double bond in the backbone chain of the polymer or by adding conductive filler such as metallic powder or carbon black [198]. Moreover the introduction of donor acceptor complex in polymer matrix may play the same role. Carbon black is the widely used filler in rubber due to its reinforcing effect, it gives rise to the formation of rubber vulcanizates with reasonable properties. So the study of electrical properties of rubber matrix loaded with carbon black is very interesting for both technological as well as theoretical points of view.

The d.c. electrical conductivity measurements of the composite were carried out over a wide range of temperature from 25°C up to 140° C. Fig. (4.25) illustrates the temperature dependence of the electrical conductivity of EPDM / PE blends with different blend ratios, loaded with 70 phr FEF black. EPDM/PE blend sample with zero PE content (i.e. 100 / 0) is thermally activated from the room temperature over the studied temperature range. This can be attributed to the amorphous nature of EPDM which allow carbon black particles or aggregates to distribute uniformly, this will lead to increasing the interspacing distances between the conducting centers. Accordingly, the transport occurs by the jumps of carriers from one site to another i.e. conduction occurs via hopping mechanism [198]. On the other hand the blend with highest PE content (i.e. 60 /40) shows negative temperature coefficient of conductivity (NTCC) up to relatively high temperature. This behavior seems to be due to the crystallinity of PE, which leads to the formation of carbon black filaments, that can be considered as conductive paths, giving rise to conduction by tunneling mechanism [199]. The competition between the two conduction mechanisms appears clearly at blends with 0.1, 0.2, and 0.3 PE weight fraction.

Fig. (4.26) shows the dependence of electrical conductivity of EPDM/PE blends on PE weight fraction. It is evident that the incorporation of PE in rubber

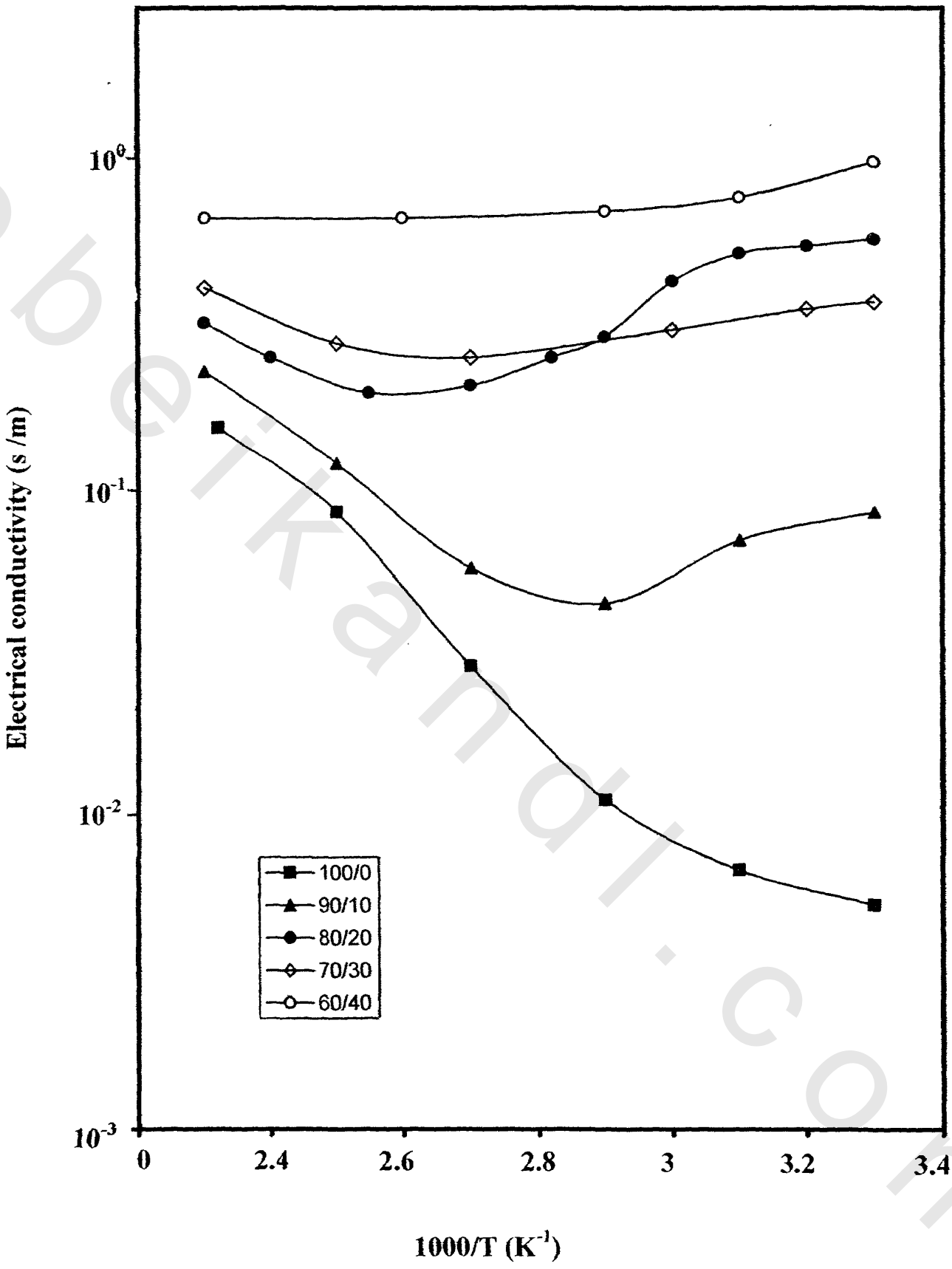

Fig(4.25) -Temperature dependence of electrical conductivity of EPDM/PE blends

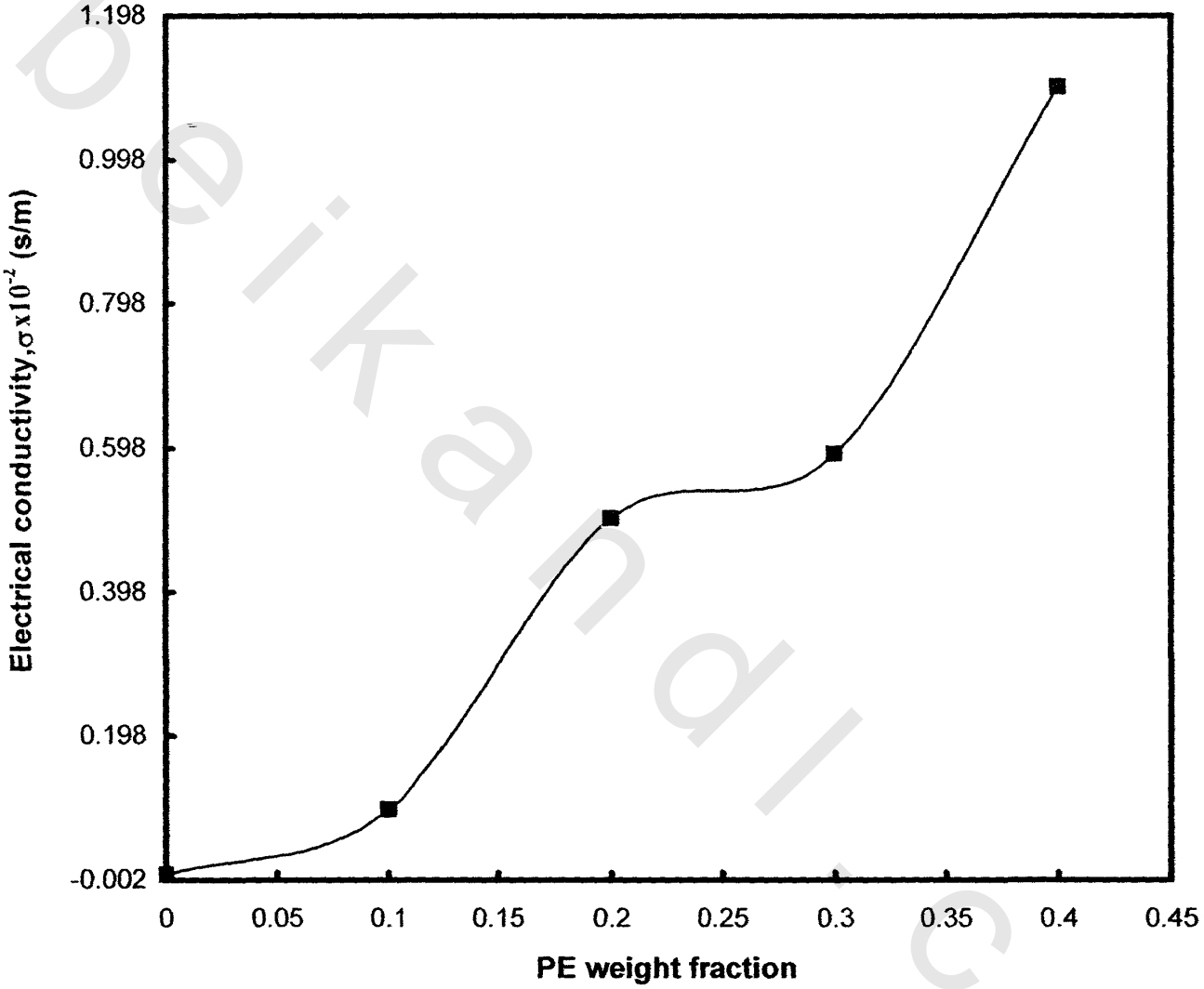

Fig.(4.26) - Electrical conductivity of EPDM/PE blends as a function of PE weight fraction

matrix increases its conductivity, this may be explained by the fact that electrical conductivity is related to crosslinking density of rubber composite. It is well known that, decreasing polymer crosslinking resulted in an increase in mobility of the macromolecular chain and consequently the mobility of the charge carriers increases. Therefore if there is a sufficient segmental motion which, allows the groups to take up energetically favorable spatial positions, charge transference can take place, and hence an increase in the electrical conductivity is observed. [200]

4.2.4 Morphology of EPDM / PE blends:

Surface properties of polymers are important factors for many applications such as adhesion, biomaterials, protective coatings, friction and wear, composites, micro electronics devices, and thin film technology [201], hence studying the morphology of polymers has great importance. Surface analysis techniques such as scanning electron microscopy (SEM) is essential, to determine the physical and chemical properties of polymer blends. The morphology of blend vulcanizates is likely to depend primarily on (i) the blend ratio and (ii) the vulcanization technique (dynamic or static) adopted [202]. It is interesting to examine the morphology of the EPDM / PE blend vulcanizates with different blend ratios trying to understand and interpret the differences in their properties on the light of morphological differences. The micrographs of the EPDM / PE specimens with blend ratios (100 / 0, 90 / 10, 80 / 20, 70 / 30, 60 / 40) are shown in Fig. (4.27 a – e) respectively. It is apparent from micrographs b and c that vulcanized EPDM particles (white specks) are uniformly distributed in the PE matrix (dark background), also, it can be noticed that, tiny hollow globular particles of vulcanized EPDM are clearly appeared, largely interlinked with one another and fairly uniformly dispersed in the PE matrix, thus effectively forming a co - continuous phase morphology. Fine fibrils or strings of PE passing through the EPDM particles help in holding and clustering them together in three

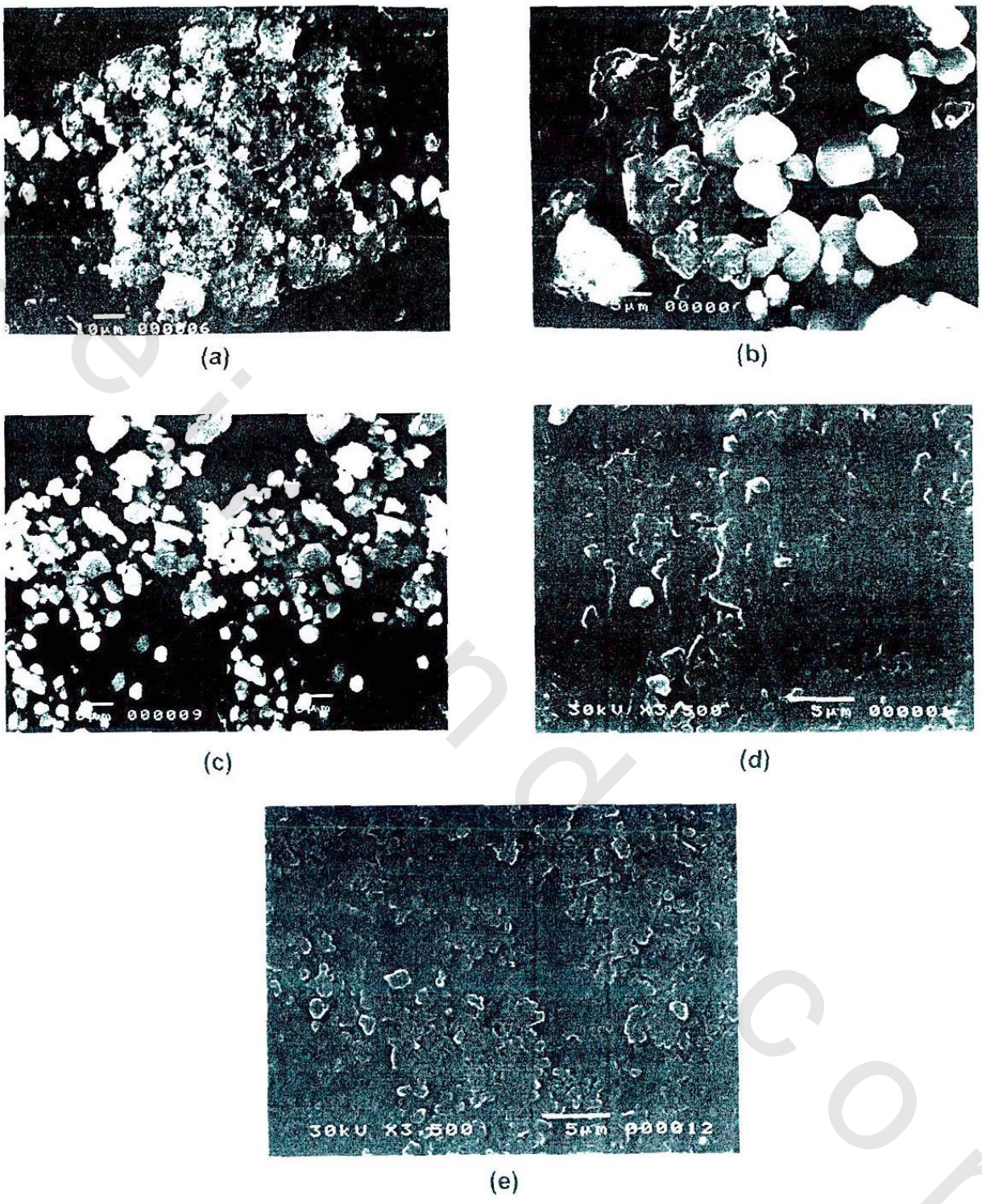

Fig . (4.27) – SEM micrographs of (a) 100/0 , (b) 90/10 , (c) 80/20 , (d)70/30 , (e) 60/40 , EPDM / PE blends (*magnification power 3500*) .

dimensions and enhance the development of a co – continuous phase morphology.

Generally, we can say that both the EPDM / PE blend ratio, and the degree of vulcanization attained will ultimately decide the size and shape of the broken, dispersed vulcanized EPDM particles, their state of distribution in the continuous PE matrix and hence the overall morphology.

4.2.5 Influence of UV exposure on EPDM/ PEblends:

Among the important problems in polymer chemistry is the stabilization against chemical reactions caused by heat, oxygen, moisture, UV radiation, and other environmental factors. When polymers are used out doors they are exposed to solar radiation, the intensity of solar radiation varies with wavelength, and the energy (E) of the light photon of is given by [203]:

$$E = \frac{hc}{\lambda} = h\upsilon \qquad (4.19)$$

Where, h is Planck's constant, υ is the frequency, λ is the wavelength and c is the velocity of light.

Consequently, the small amount of ultra violet (UV) light contains the most energetic photons. If a photon is absorbed by a polymer molecule it raises an electron to an excited state, if the energy level of the excited state is high enough, it can transfer energy to a bond dissociation reaction. The whole process of photon absorption and the subsequent bond breakage can be regarded as photodecomposition, and it causes degradation of the blend hence, the study of effect of UV on polymer blends is of great importance.

4.2.6 FTIR spectroscopy study of blend degradation:

Infraerd spectroscopy plays an important role in assessing degradation, of which, oxidation is one particular form and can sometimes provide valuable

information for determinning degradation mechanisms [204]. EPDM / PE blend samples with thickness 2 mm, in different blend ratios (100 / 0, 90 / 10, 80 / 20, 70 /30, 60 / 40) were exposed to UV radiations, then Fourier Trasform Infrared Spectroscopy (FTIR) was applied on the blends (before and after exposure) to investigate the thermal degradation of different blends and detect the degree of stability against UV radaiation. The obtained results are presented in Figs.(4.28 – 4.32), it is observed that the original spectra change gradually with increasing PE content due to the increase in the crystalline phase beside a consequent decrease in the amorphous phase. The absorption bands at 2850, 2915 cm^{-1} charactrize the symmetric and asymmetric streching CH_2 respectively. The ratio of intensities for these two peaks was selected as identification of EPDM content in the blend [205]. Fig. (4.33) shows a plot of 2850 / 2920 ratio vs EPDM content, it is apparent that the obtained relation is linear one, i.e., the intensity of these bands is dependent on EPDM content. However, It is clear from FTIR spectra shown in Figs. (4.28 – 4.32) that the spectra of the same blend, before and after UV exposure, seem to be almost the same, revealing the high stability of EPDM / PE blends against UV exposure. Oxidation of polymers should result in a range of carbonyl compounds [206], and as it can be noticed that the C = O peaks are not detected in any of the spectra of the exposed blends, so it can be concluded that UV radiation doesn't induce oxidation of the blend, which indicates that EPDM/PE blends are highly resistant towards UV radiation. However, it can be noticed that, the spectra of the exposed blends present some additional absorption bands at 752 – 755 cm^{-1}, characterstic of C = C vibrations [207], which may be resluted from a slight degradation of the blend duo to the action of UV radiation. This degradation may be attributed to breaking of crosslinks between molecules resulting in unsaturated molecular chains. The peak intensity of this new absorbance band is plotted as a function of PE content which is shown in Fig. (4. 34). It is evident from the figure that EPDM / PE blend with

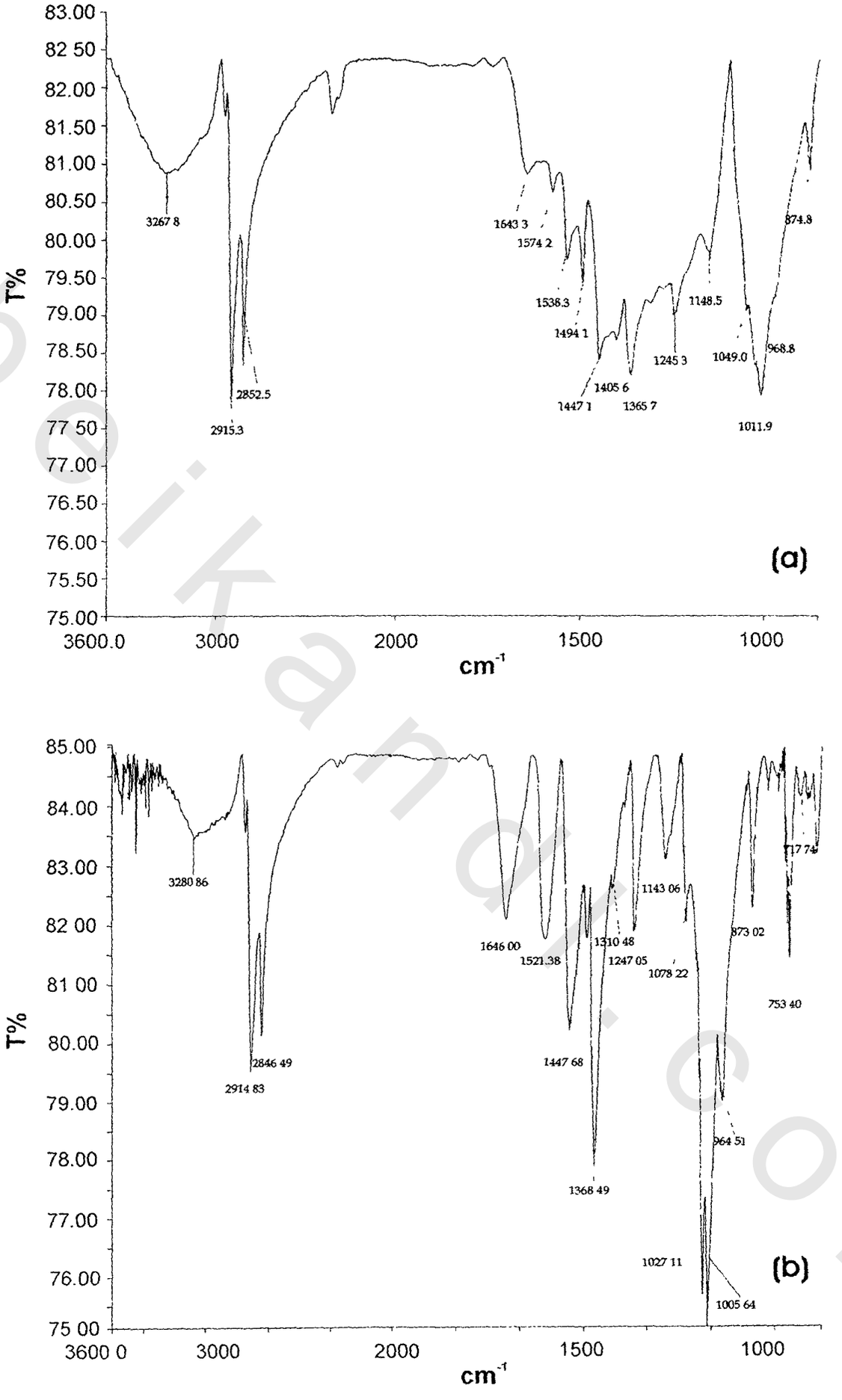

Fig. (4.28) FTIR spectra of EPDM/PE blend (100/0)
(a) before UV exposure (b) after exposure

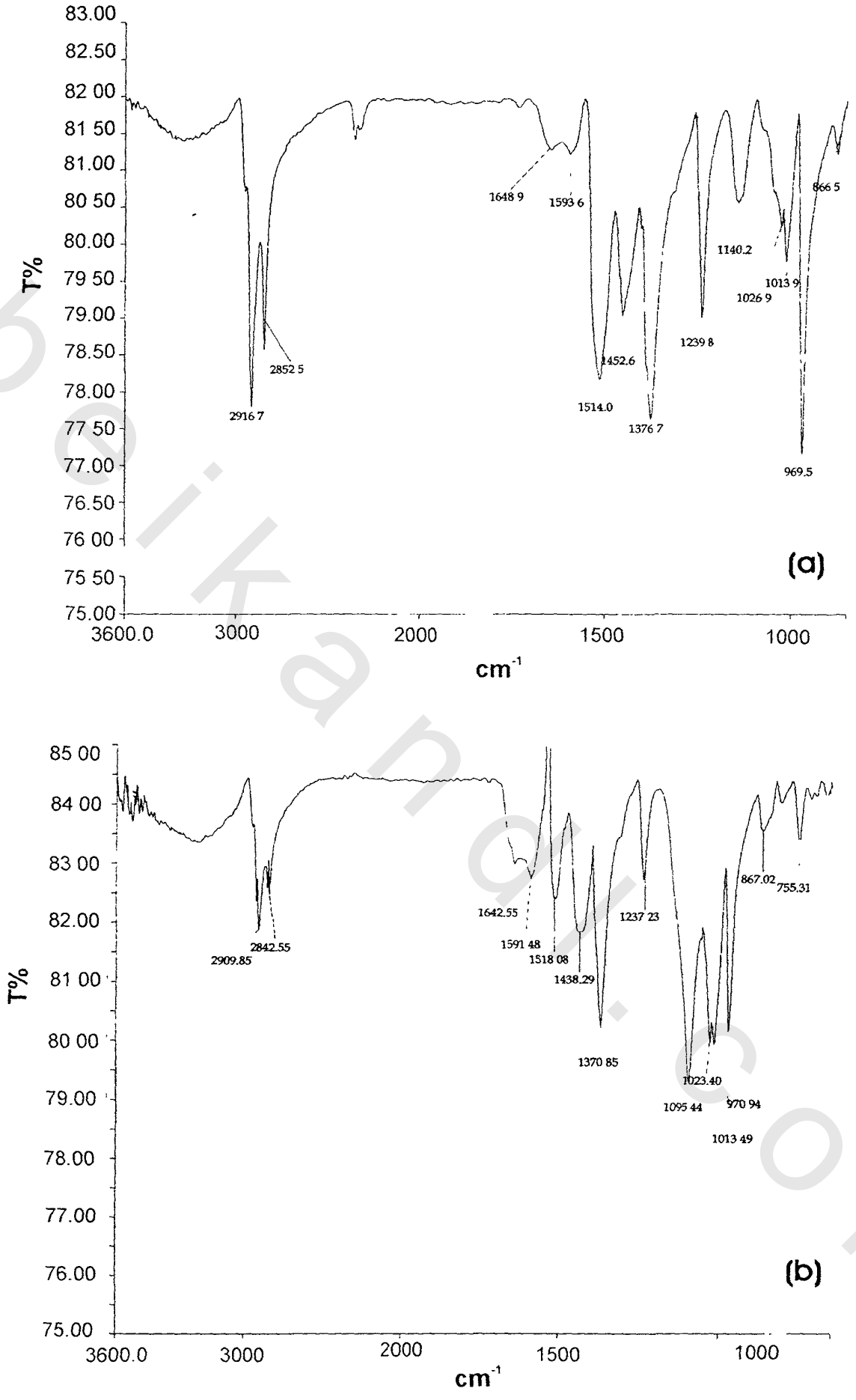

Fig. (4.29) FTIR spectra of EPDM/PE blend (90/10)
(a) before UV exposure (b) after exposure

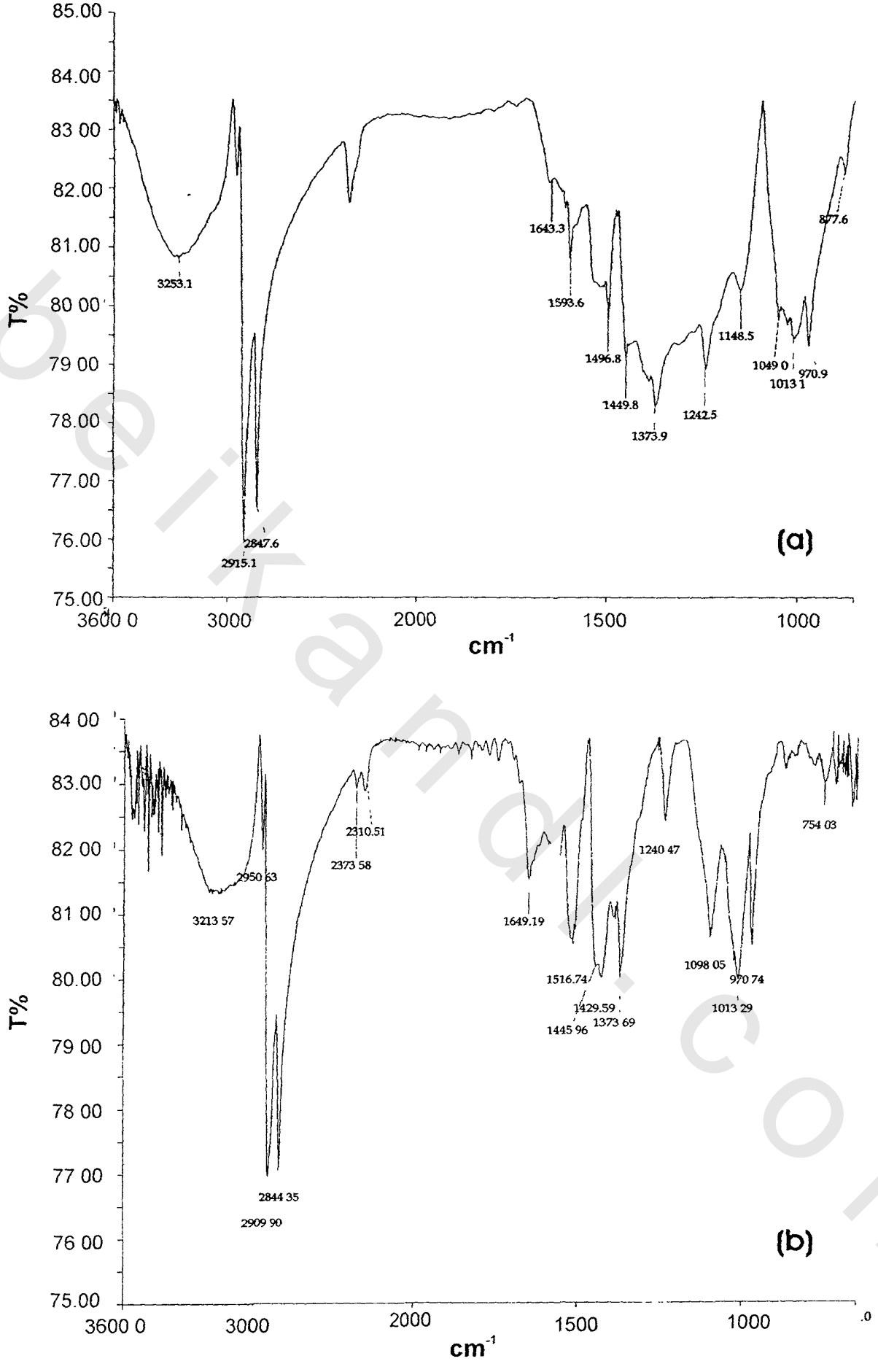

Fig. (4.30) FTIR spectra of EPDM/PE blend (80/20)
(a) before UV exposure (b) after exposure

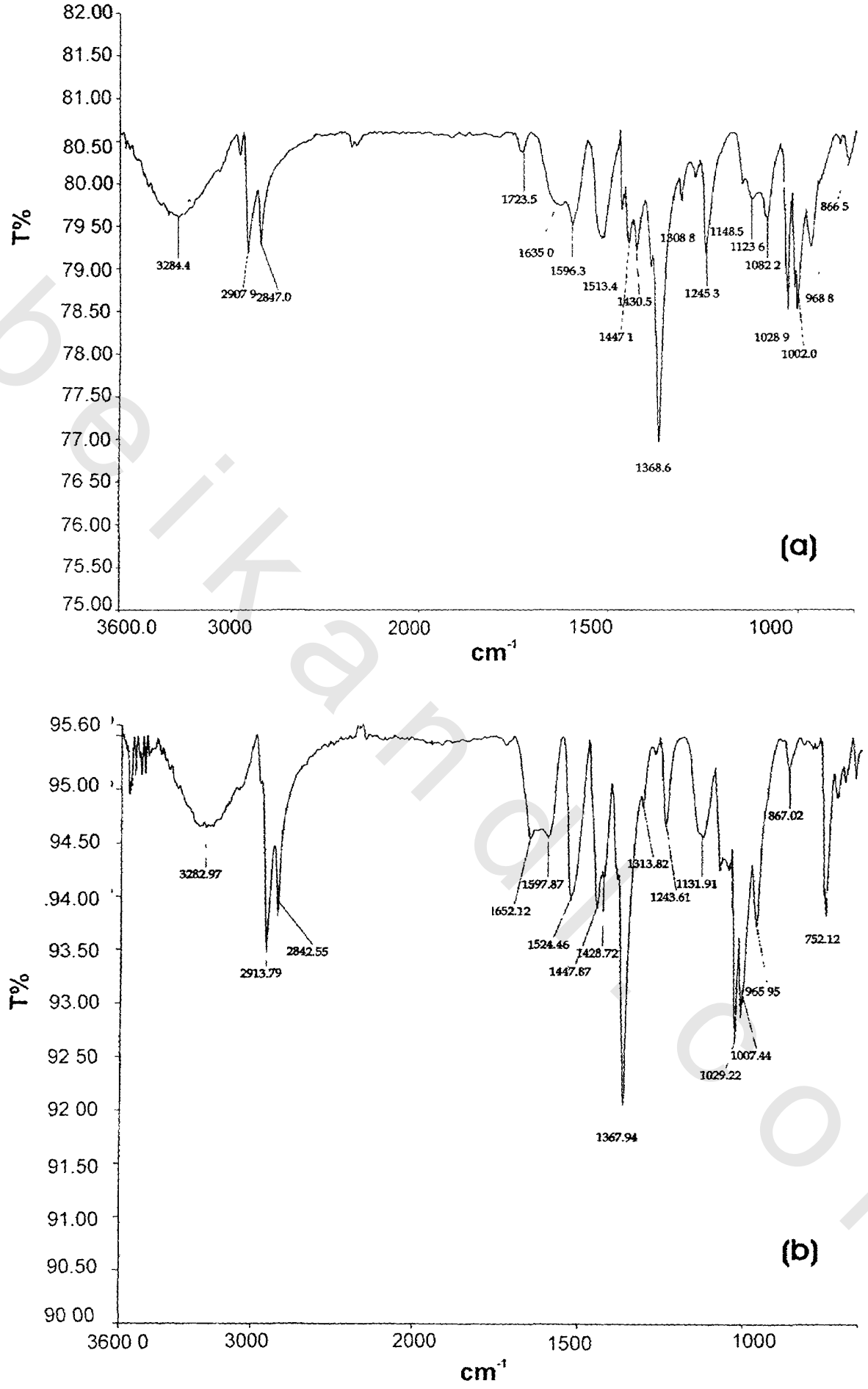

Fig. (4.31) FTIR spectra of EPDM/PE blend (70/30)
(a) before UV exposure (b) after exposure

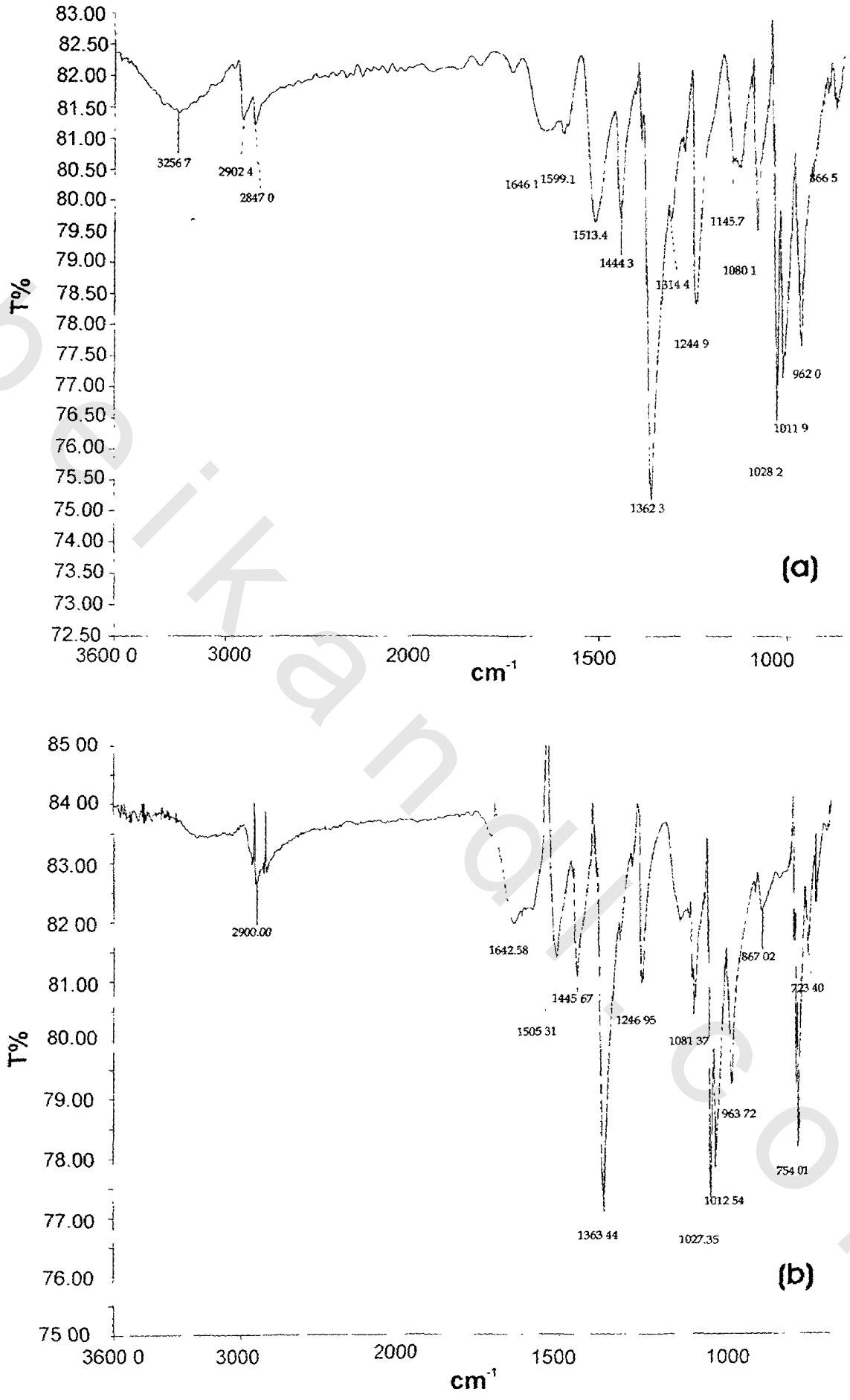

Fig. (4.32) FTIR spectra of EPDM/PE blend (60/40)
(a) before UV exposure (b) after exposure

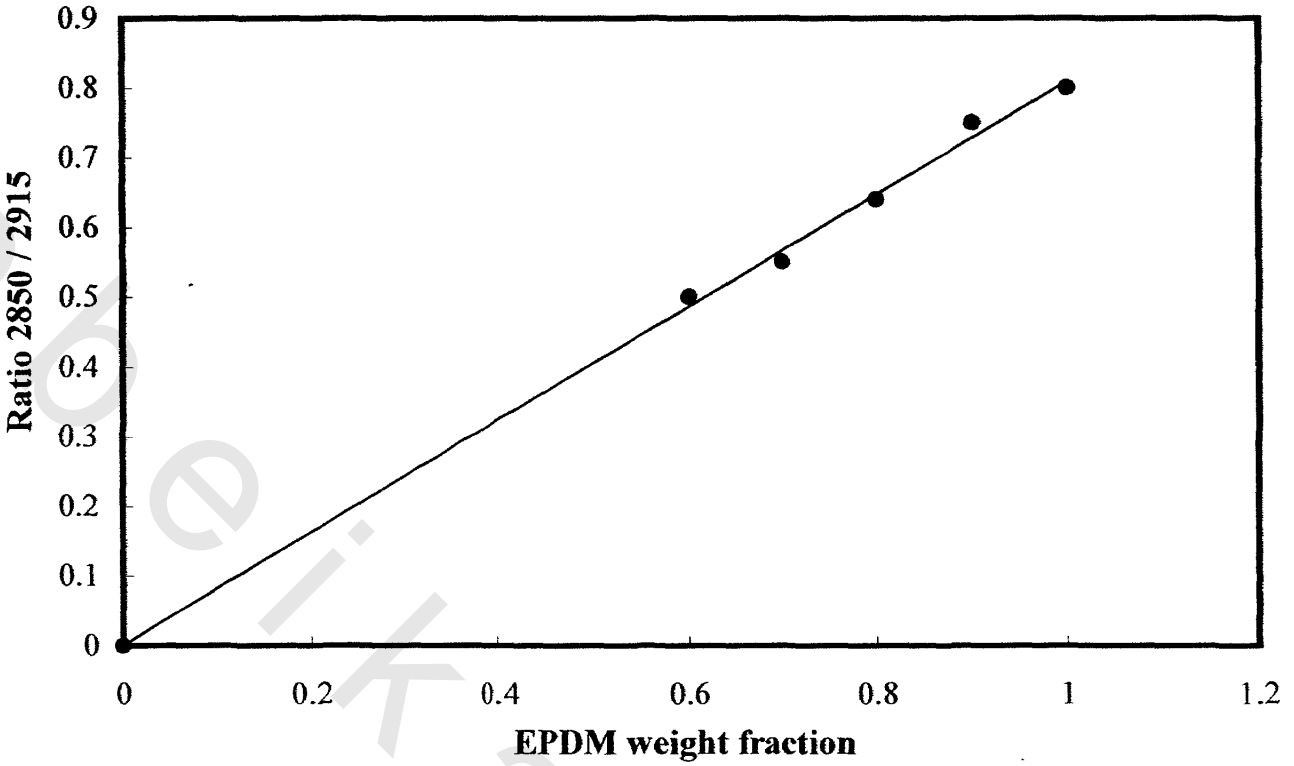

Fig. (4.33) - Calibration curve showing 2850/2915 absorbance ratio vs. EPDM weight fraction

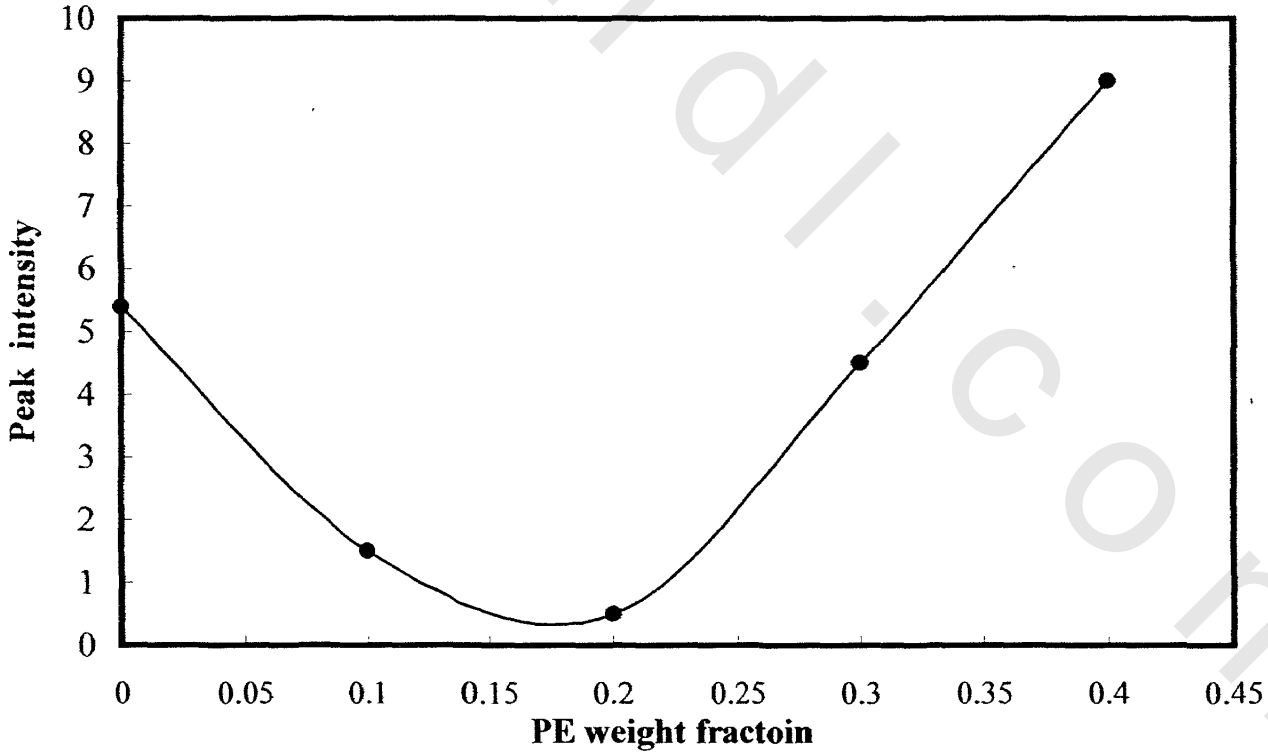

Fig. (4.34) - Calibration curve showing peak intensity of 750 cm^{-1} band as a function of PE weight fraction

ratio 80/20 has the lowest peak intensity indicating the least degradation and hence, it has the highest stability of all the blends. Also it is observed, that addition of PE to EPDM matrix increases the resistance of blend against UV radiation, until a critical value of PE is achieved (80/20) where, above it an inverse behavior is noticed and blend degradation increases, which can be attributed to the decrease in the degree of crosslinking in the blends with high PE content.

4.3. Evaluation of EPDM / PE Blends as Protective Coatings:

The tendency of a coated metal to corrode is a function of three major factors: (1) the nature of the substrate metal, (2) the character of the interfacial region between the coating and the substrate, and (3) the nature of the coating[208]. The measurement of the overall rate of corrosion degradation for a coated metal must be carried out by a simple, repetitive, and non-destructive technique. In this way, mechanistic information and patterns of performance behavior can be built up long before visible signs of failur occur.

4.3.1. Electrochemical test methods:

The coated metal / solution interface involves the seperation of charge (the metal and electrolyte) by a dielectric medium (the coating) also, corrosion of the coated metal involves interconversion of electrons and chemical species at an interface. As this is precisely the definition of electrochemistry, it is not surprising that electrochemical methods have been previously thought to be suited for studying the degradation processes occuring at the coated metal / solution interface [209, 210].

4.3.1.1. Open circuit potential measurements :

The coated metal electrodes, with and without applying adhesive, were left at the open circuit and the (OCP) was monitored in each case.The obtained values were compared to (OCP) of bare carbon steel, and the results are shown in Fig. (4.35). It can be noticed that coating carbon steel with EPDM / PE blend leads to a significant shift of (OCP) to the noble direction of potential. Also,the results show that applying adhesive to the substrate causes surface ennobling, i.e., a shift of potential to more noble range indicating good metal protection.

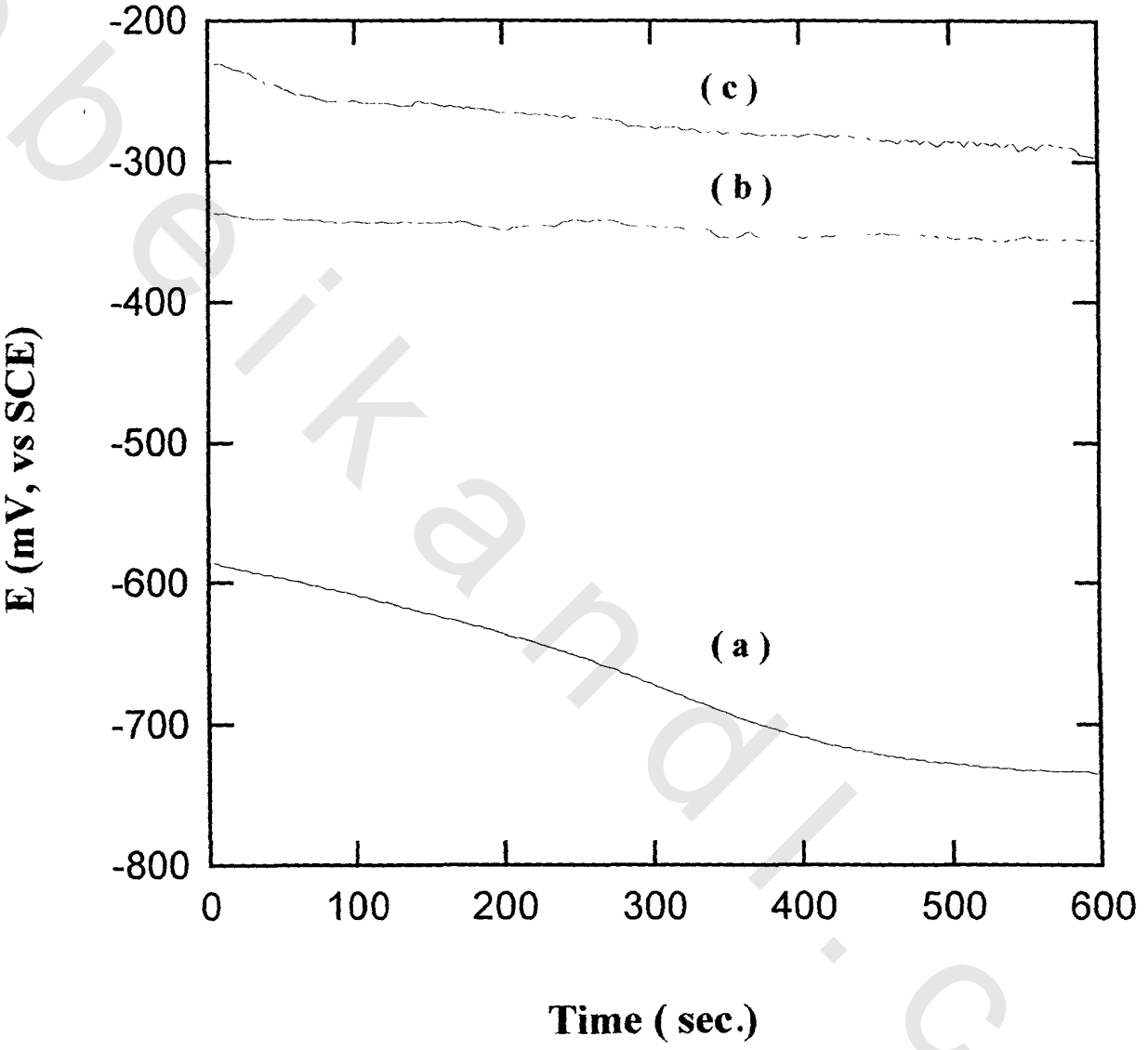

Fig.(4.35) -Open circuit potential of (a) bare carbon steel , (b) coated carbon steel (without applying adhesive) , (c) coated carbon steel (with applying adhesive) .

4.3.1.2. Potentiodynamic measurements:

The corrosion current density is one of the electrical properties for polymer – coated substrates which provides useful information germane to the mechanism of corrosion. The changes in this measured quantity provide significant insights into corrosion mechanism of coated metals [211].

In Fig. (4.36) the potentiodynamic polarization curves for carbon steel with and without EPDM / PE coatings (thickness 2 mm) are compared and one can verify the strong adherece of the coating on the steel surface by the fact that the film is not removed from the surface . Furthermore from these curves one can observe that the protection action of the polymer induces a change in the corrosion potential to more positive values , also the curve corresponding to the coated steel persents a smaller current which implies that the coating indeed provides a physical barrier for blocking the electro- chemical process .

(a) Effect of time:

Potentiodynamic polarization curves were obtained for carbon steel coated by EPDM / PE blends with different blend ratios and different thicknesses. The corrosion current changes ($i_{corr.}$), calculated from Tafel plots, are plotted as a function of immersion time and the results are shown in Fig. (4.37 – 4.42). The data show a striking difference between coated carbon steel and uncoated one(studied previously) . The i_{corr} values corresponding to coated carbon steel are significantly lower than those of bare metal, giving a clear evidence for the protection provided by EPDM / PE coatings, as i_{corr} is assumed to be directly proportional to corrosion rate [212]. Also bare carbon steel, as discussed previously, exhibited a sharp initial increase in current density, indicating an active electrochemical reaction while, coated metal shows a slight initial increase in i_{corr} with the progress of time up to 18 months then followed by a noticeable increase as shown in Figs. (4.37 – 4.42) .

It is well known that the reactants necessary for corrosion to proceed in normal environment are water and oxygen, also the aggressive chloride ions can influence the rate of corrosion. The proposed mechanism for corrosion of coated steel in sea water is that [213], water is first taken up by the coating causing its resistance failure. where, corrosion would be very slight due to iron corroding in the presence of water and oxygen. Chloride ions would be excluded at this stage due to the repulsion resulted from the negative charge on the film.However, corrosion of the steel would continue because the film is permeable to positive ions (iron ions moving outwards at the anode and sodium ions moving inwards at the cathode). Only at a later stage, chloride ions would migrate into the film causing a further decrease in ionic resisteance, and slowly reaching the metal surface and forming soluble corrosion products. In this way, steady breakdown of the coating resistance will occur leading to a progressive increase in corrosion. However, the small values of i_{corr} for EPDM / PE coatings, that has a maximum value of 130 $\mu A.cm^{-2}$ (as shown in Figs. 4.37 – 4.42), indicate that there is no initiation of corrosion for carbon steel revealing that EPDM / PE coatings are good barriers which do not allow corrosive ions to penetrate the substrate. This can be explained by the fact that, organic coatings have a high resistance to ionic conductivity[214]. Also, they offer good barrier properties retarding the diffusion of chemical species promoted by the osmotic pressure through the pores and capillaries of the coating, either from or to the metal surface [215]. These results are in agreement with the data concerned the low penetration rate and small values of average diffusion coefficient of sea water in EPDM/PE blends that obtained previously. However, Figs. (4.37 – 4.42) show that, as the coating is exposed for a prolonged amount of time, it allows the corrosive ions to diffuse with a very small degree which, resulting in the observed increase of i_{corr} values at 24 months. This may be attributed to the fact that the permeability of the coating slowly increases with time due to activation of the micropores located on

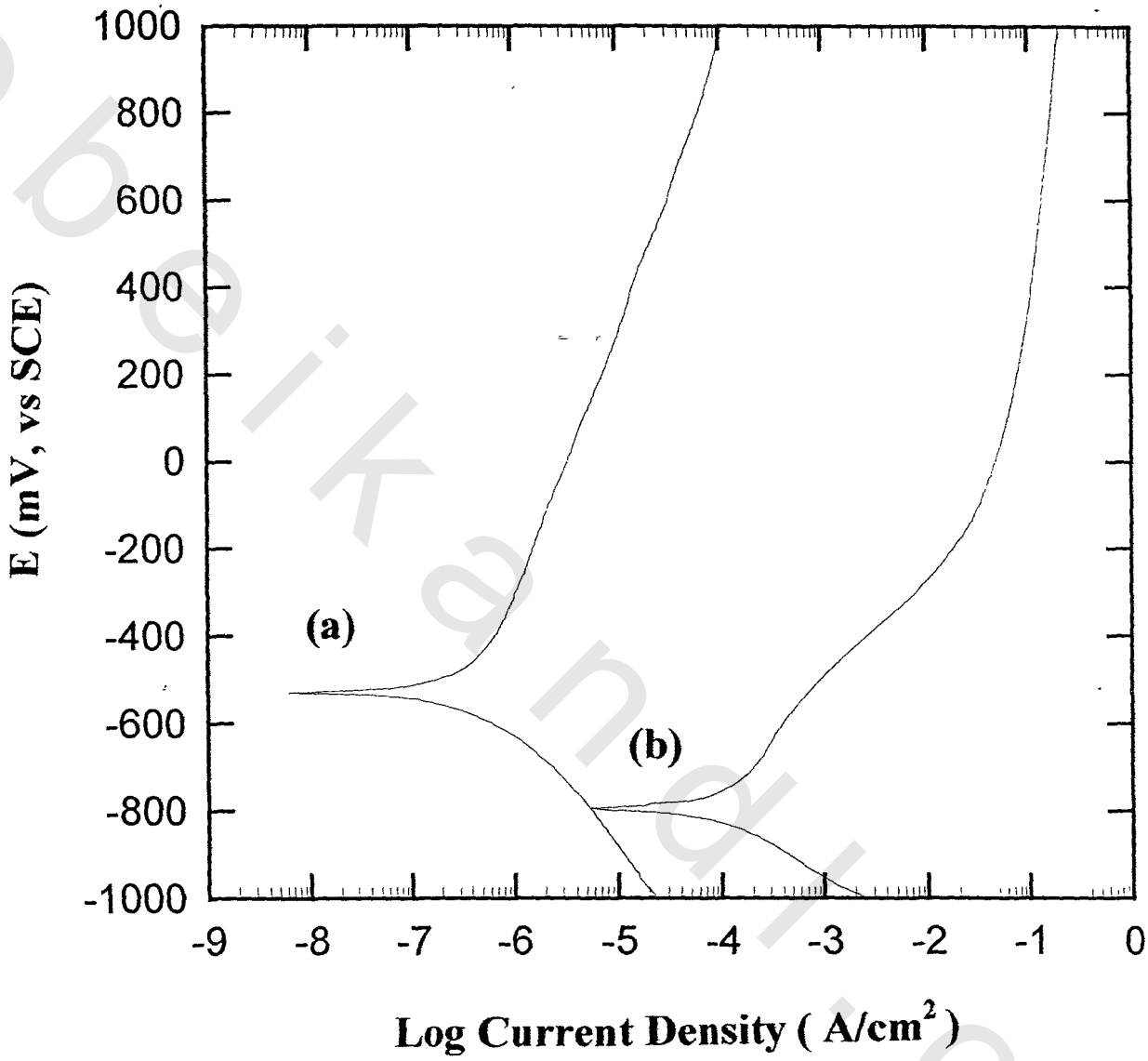

Fig.(4.36) – Potentiodynamic polarization diagram for carbon steel in sea water (a) coated sample , (b) un coated sample

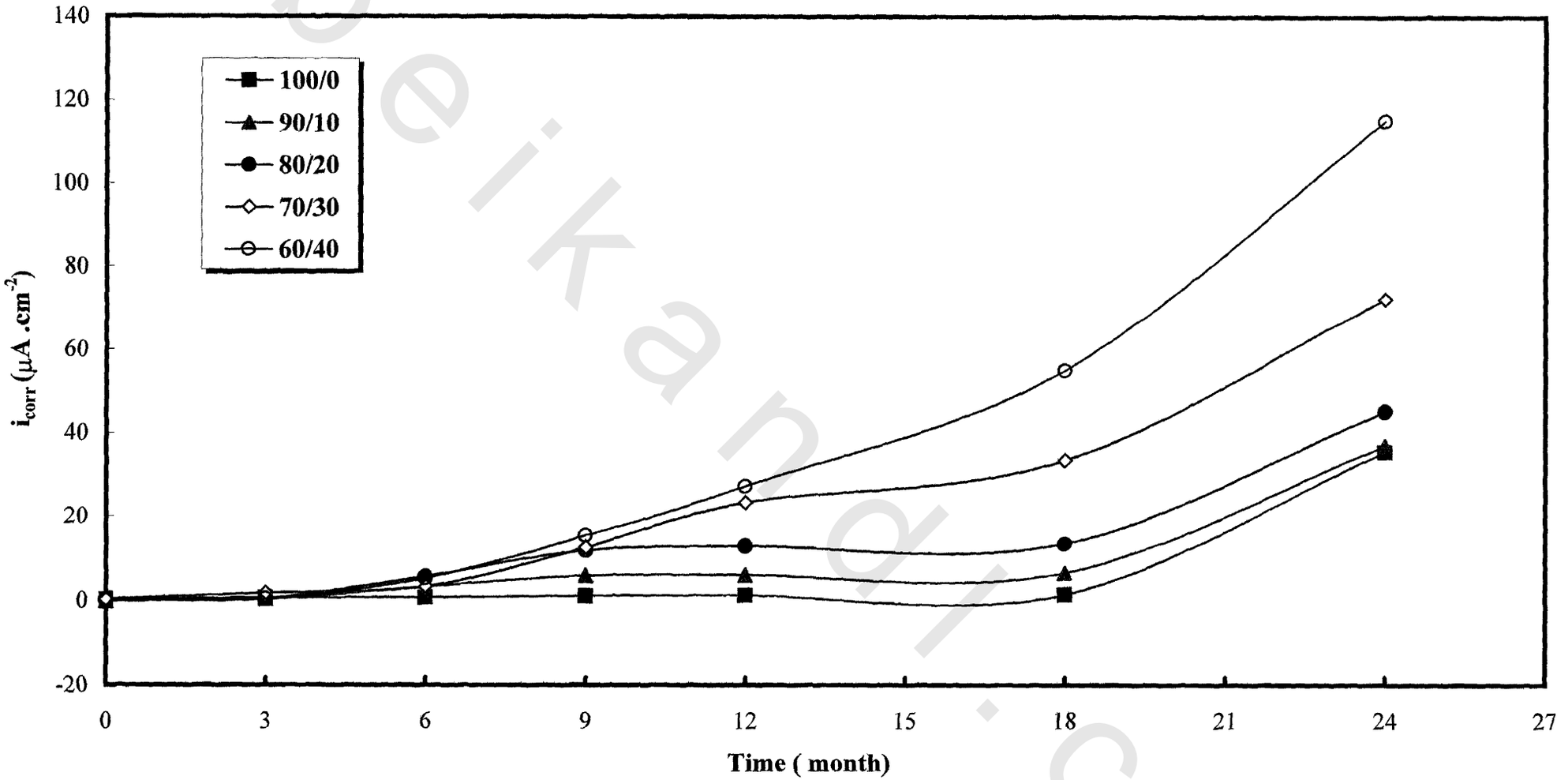

Fig.(4.37) -Variations of corrosion current denisty of EPDM/PE coatings in sea water , (thickness 1mm., without applying adhesive) as a function of immersion time .

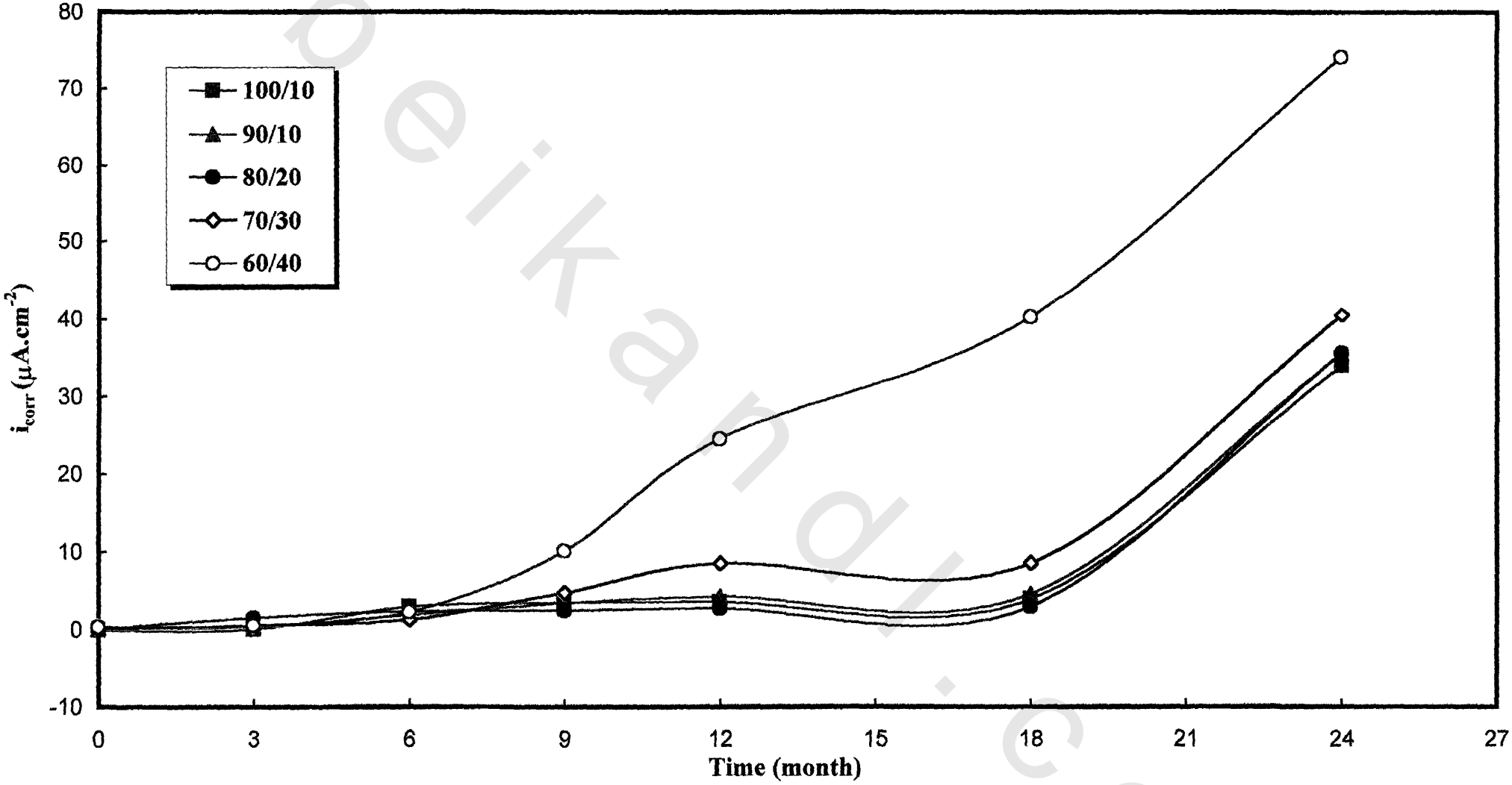

Fig.(4.38) - Variations of corrosion current denisty of EPDM/PE coatings in sea water, (thickness 2 mm , without applying adhesive) as a function of immersion time.

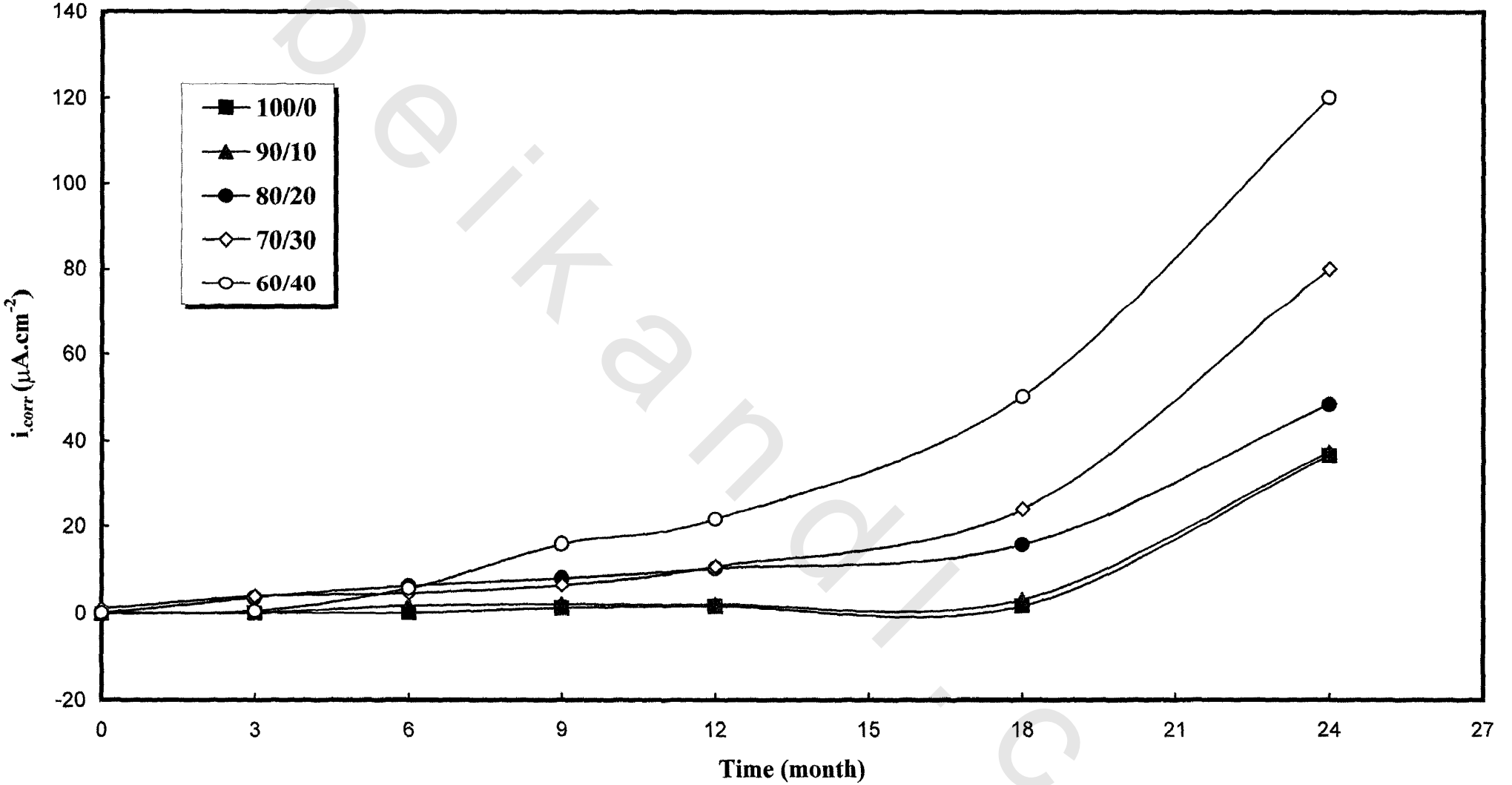

Fig.(4.39) - Variation of corrosion current denisty of EPDM/PE coatings in sea water (thickness 3mm, without applying adhesive) as a function of immersion time.

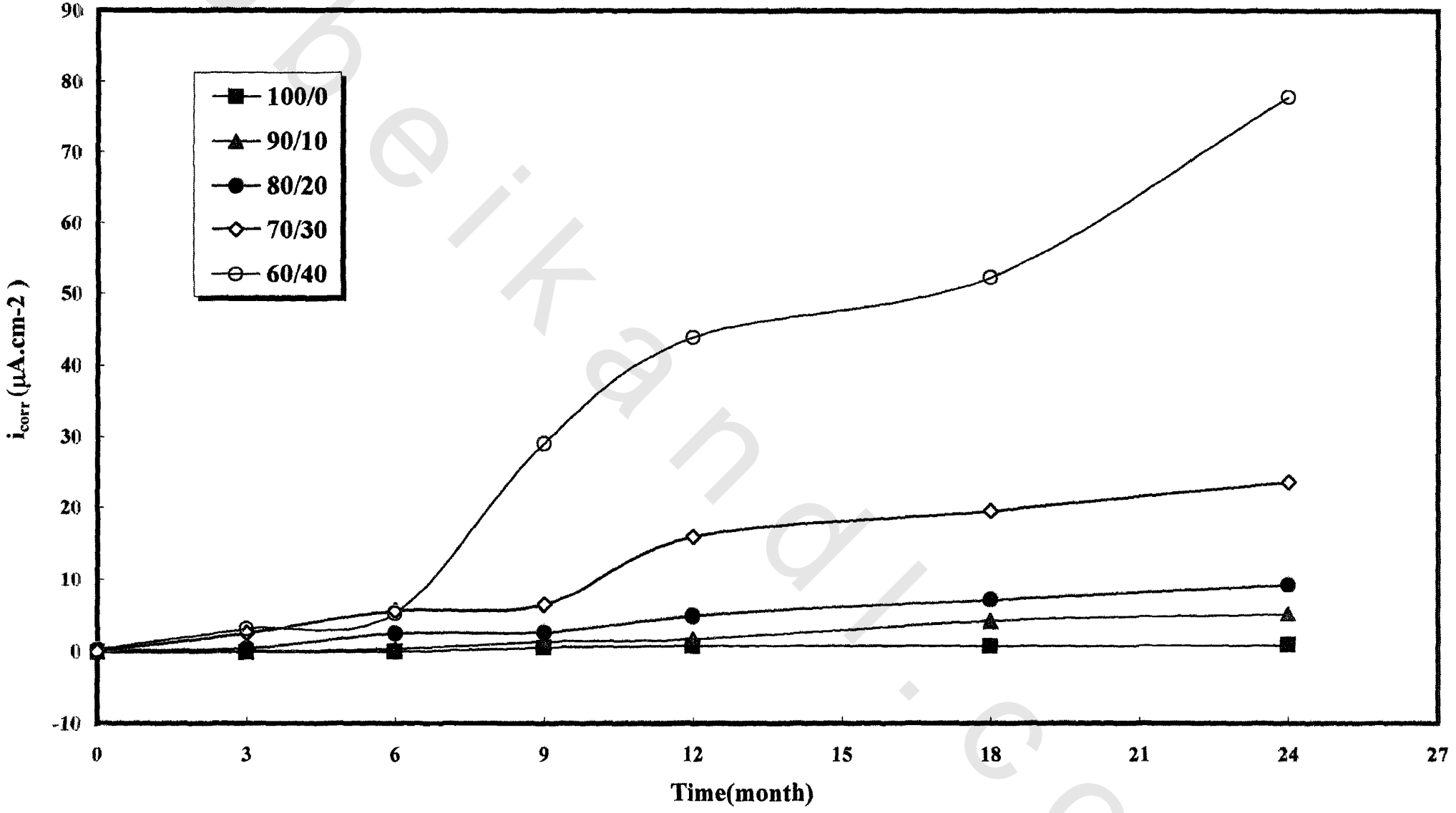

Fig.(4.40) - Variation of corrosion current denisty of EPDM/PE coatings in sea water, (thickness 1mm, with applying adhesive) as a function of immersion time.

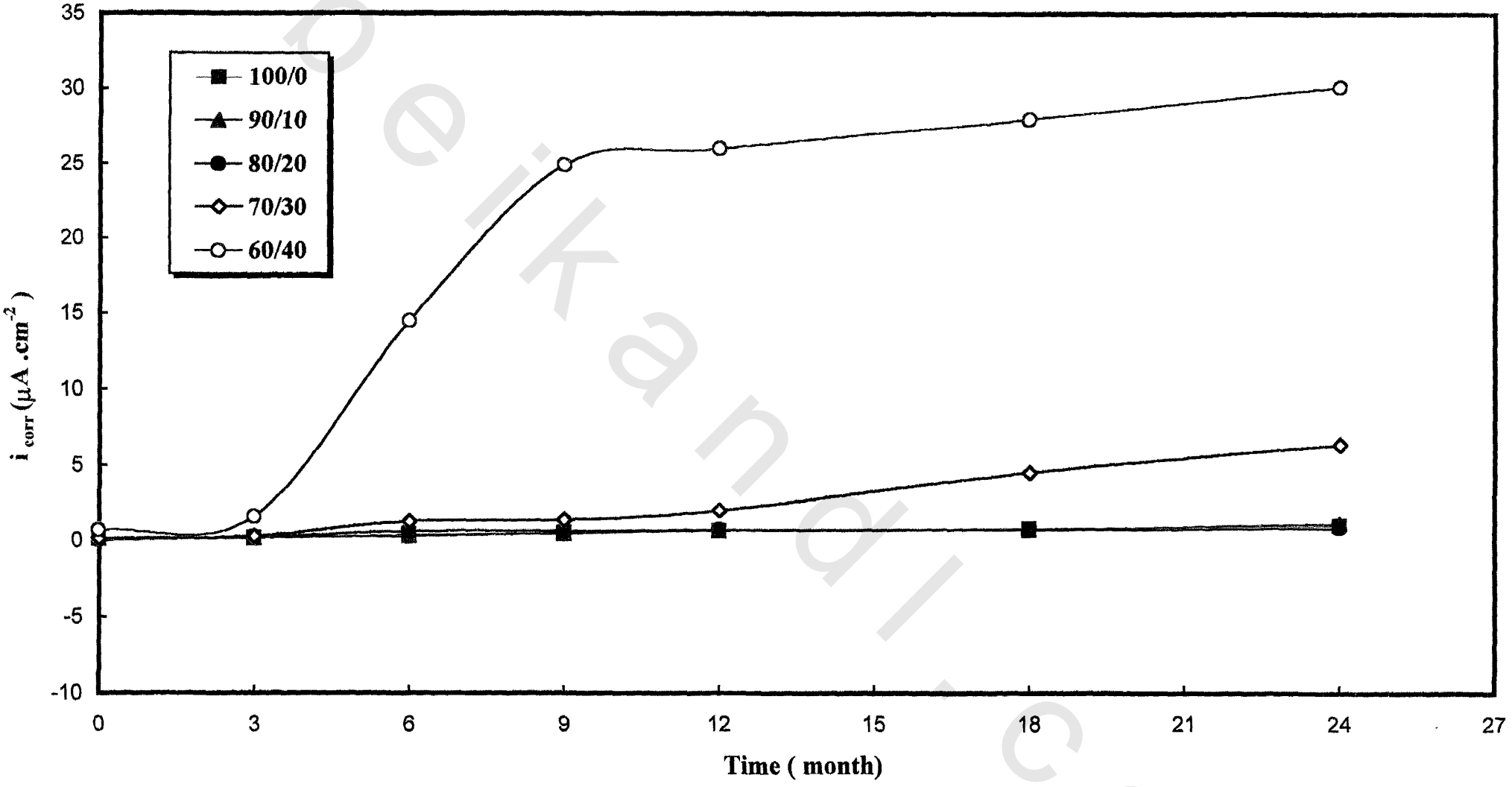

Fig.(4.41) - Variation of corrosion current denisty of EPDM/PE coatings in sea water, (thickness 2 mm, with applying adhesive) as a function of immersion time.

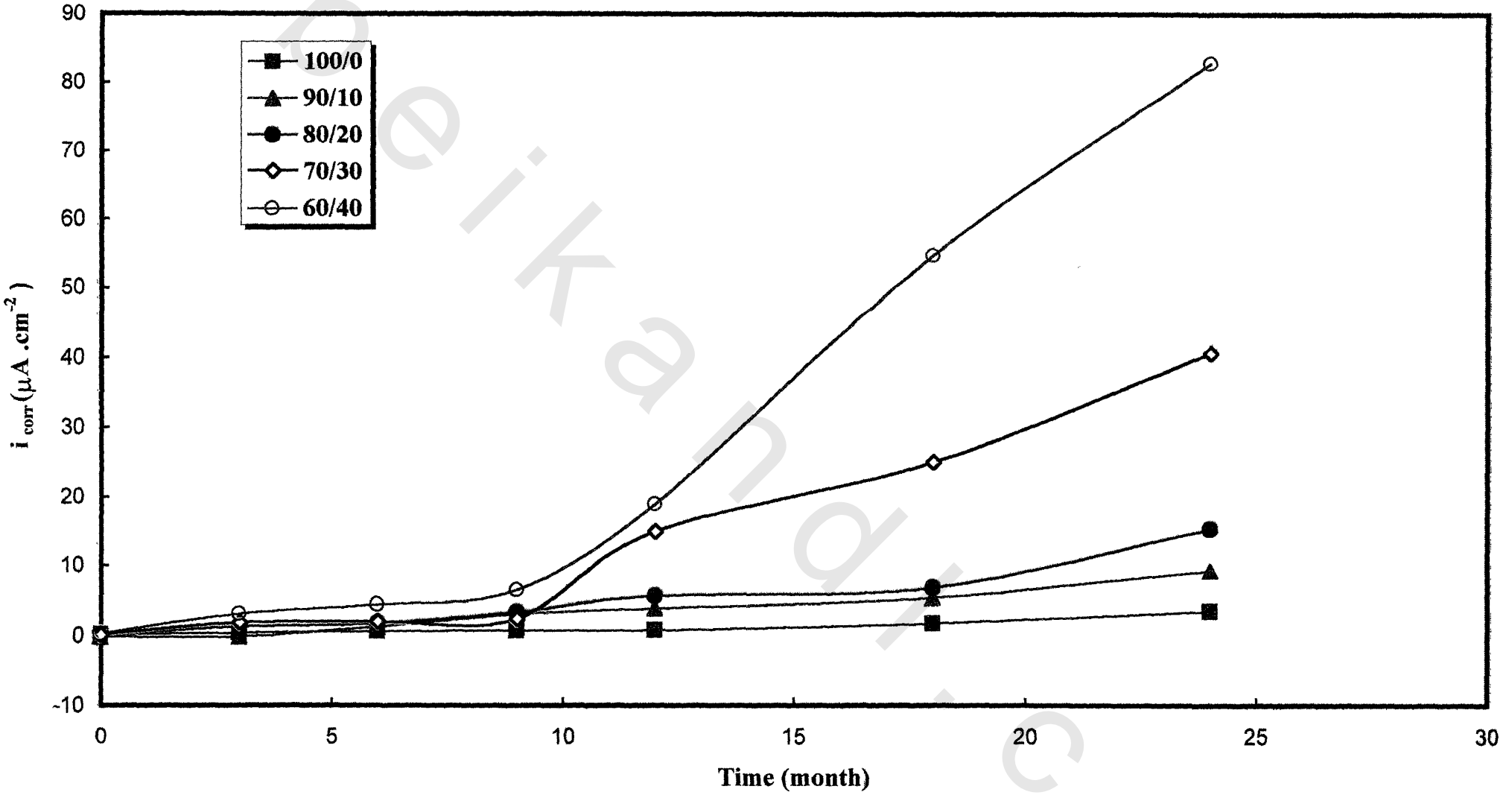

Fig(4.42) - Variations of corrosion current denisty of EPDM/PE coatings in sea water, (thickness 3mm, with applying adhesive) as a function of immersion time.

the surface of the coatings [216]. Generally EPDM / PE blends can be described as effective protective coatings which permits only a slow flux of charge through it. Also ,they have low solubilities and low diffusion coefficients for O_2 and H_2O. This is clearly evidenced from the marked decrease in corrosion current densities in comparison to the un-coated carbon steel.

(b) Effect of blend ratio:

The effect of blend ratio in EPDM / PE blends on the efficiency of corrosion protection is illustrated in Figs. (4.43, 4.44). The obtained results show that the increasing of the PE weight fraction above 0.2 leads to an increase in corroiosn current,this can be attributed to the difference in the degree of crosslinking in EPDM / PE blends. It is well confirmed that a number of crosslinked polymer films have been shown to be heterogeneous in structure, containing small areas, termed by D-type areas, which have a vastly lower ionic resistance than the rest of the film which are called I-type areas [217]. The differences between (D) and (I) type areas have been connected with the differences in crosslinking density within the polymer film. The breakdown of the coated metal has been shown to occur at D-type areas of low resistance where, polymer cross linking density is presumably lower, leading to a decrease in protective properties of the coating[218]. This can be explained by the fact that the electrolyte penetrates into the coating in two ways [219]: water and ions enter into micropores of polymer net in the extrenal portion of the coating then, they penetrate through the macropores, which become deeper over the time. So, when the polymer is highly crosslinked, the micropores will be homogenously distributed through the coating, i.e., the coating has a homogeneous structure, resulting in a decrease in the D- type areas, while in contrary, the drecrease in crosslinking leads to predominance of D-type areas which cause a decrease in the coating efficiency. Another resonable explaination for the unsatifsaied protective properties of EPDM / PE coatings, upon addition of PE above 0.2 weight fraction can be releated to electrical

conductivity of the blends that have been measured previously. It has been found that the electrical conductivity of the blend increases with increasing PE content above 0.2 weight fraction. Electrochemically, the protection by coatings has been described as affording a degree of resistance polarization, due to the high electrical resistance of the film [220]. It is well confirmed that electrical conductivity is inversely proportional to electrical resistance. Also, the mobility of the ions, in the ideal protective coating corrosion, must be equal to zero [221] and , as it is well known that the electrical conductivity is correlated to free ions. According to the above facts , it is expected that EPDM / PE blends possessing high electrical conductivity show less corrosion protection efficiency.

(c) Effect of blend thickness:

In general, EPDM / PE coatings applied in thickness of 2 mm, appear to perform better than those of thickness 1 and 3 mm as shown in Figs.(4.45 – 4.46). The improvement of the protective properties of coatings by increasing the thickness from 1 to 2 mm can be attributed to the higher barrier effect (i.e. lower permeability to aggressive species) of the thicker coatings. It is well confirmed that the thicker the coating, the better the barrier to water and oxygen diffusion through the cathodic areas [222]. Consequently, the O_2 reduction reaction is inhibited and the corrosion of substrate is avoided. Another positive reason for the good protection provided by thicker coatings is presumably due to the longer distance that Cl^- ions have to travel to reach the substrate [223]. However, an inverse behavior is noticed upon increasing the thicknes from 2 to 3mm, as a decrease in protection efficiency is observed. This may be due to occuring of internal stresses within such a thick coating, which enhance defects [224], and leading to a decrease in protective properties of the coating. Generally, it is found that for EPDM / PE coatings a certain threshold thickness is required to eliminate defects, while excessive thickness possibly can lead to an improper cure or excessive internal stresses.

(d) Effect of applying adhesive:

The corrosion protection efficiency of organic coatings depends on a large number of factors, but the adhesion strength at the polymer / metal substrate interface plays a paramount role [225 – 226]. Adhesion is an intrefacial phenomenon which takes place when two surfaces approach each other to form an interface, by the action of physical and chemical forces. In the specific case of organic coatings, two types of adhesion can be identified [227]: physical adhesion, where the coatings penetrate surface pits and crevices, forming a physical bond, and chemical one whereas, interatomic bonds are formed at the interface.

Figs. (4.47 – 4.49) illustrate the values of polarization resistance (R_p) for EPDM / PE coatings with and without applying adhesive (with thickness 1, 2 and 3 mm respectively). Knowing that R_p value is inversely proportional to corrosion rate, it can be obviously noticed that applying adhesive on the substrate provides excellent improvement in the protective properties of EPDM / PE coatings, as indicated by the great difference between R_p values corresponding to the samples with adhesive and those without applying adhesive for all the applied thicknesses as shown in Figs. (4.47 – 4.49). This can be attributed to the fact that an effective adhesion bonding blocks all the electrochemically active sites on the metal surface, as the function of adhesive force is to avoid or at least to delay, the reaching of corrosive species to the metal substrate and prevent them from diffusing along the metal / coating interface. Thus, it can be suggested that the beneficial role of adhesive is the impairment of the formation of an electrolyte layer at the coating / substrate interface, preventing ionic current flow and hence, inhibiting the spread of corrosion over the surface [228]. Though, the preferability of the well attached coatings over the unattached ones, it can be observed from Fig. (4.47 – 4.49) that EPDM / PE coatings with PE weight fraction up to 0.2 could still be regarded as effective barrier coatings, even without applying adhesives.This conclusion is based on the fact that R_p value of 2000 ohm/cm^2

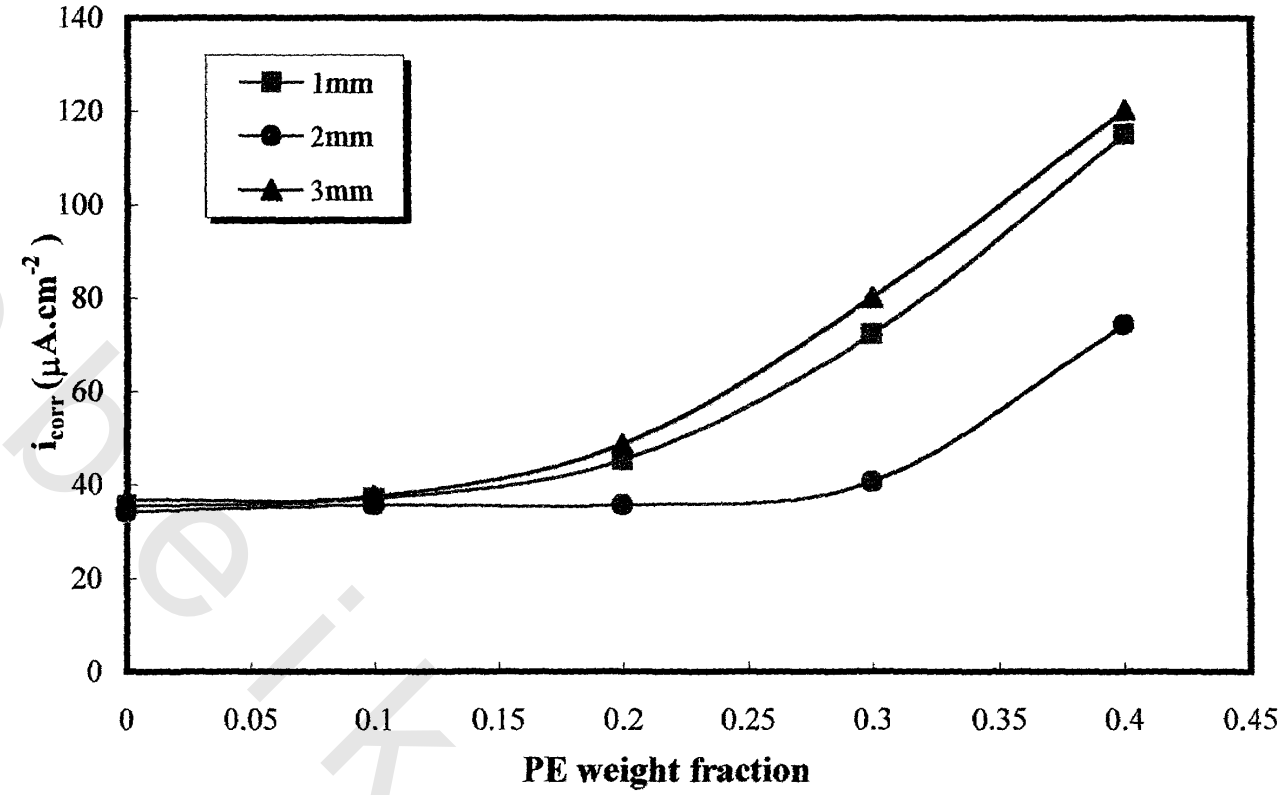

Fig(4.43) - The dependence of corrosion current denisty on EPDM/PE blend ratio (24 months immersion in seawater , without applying adhesive)

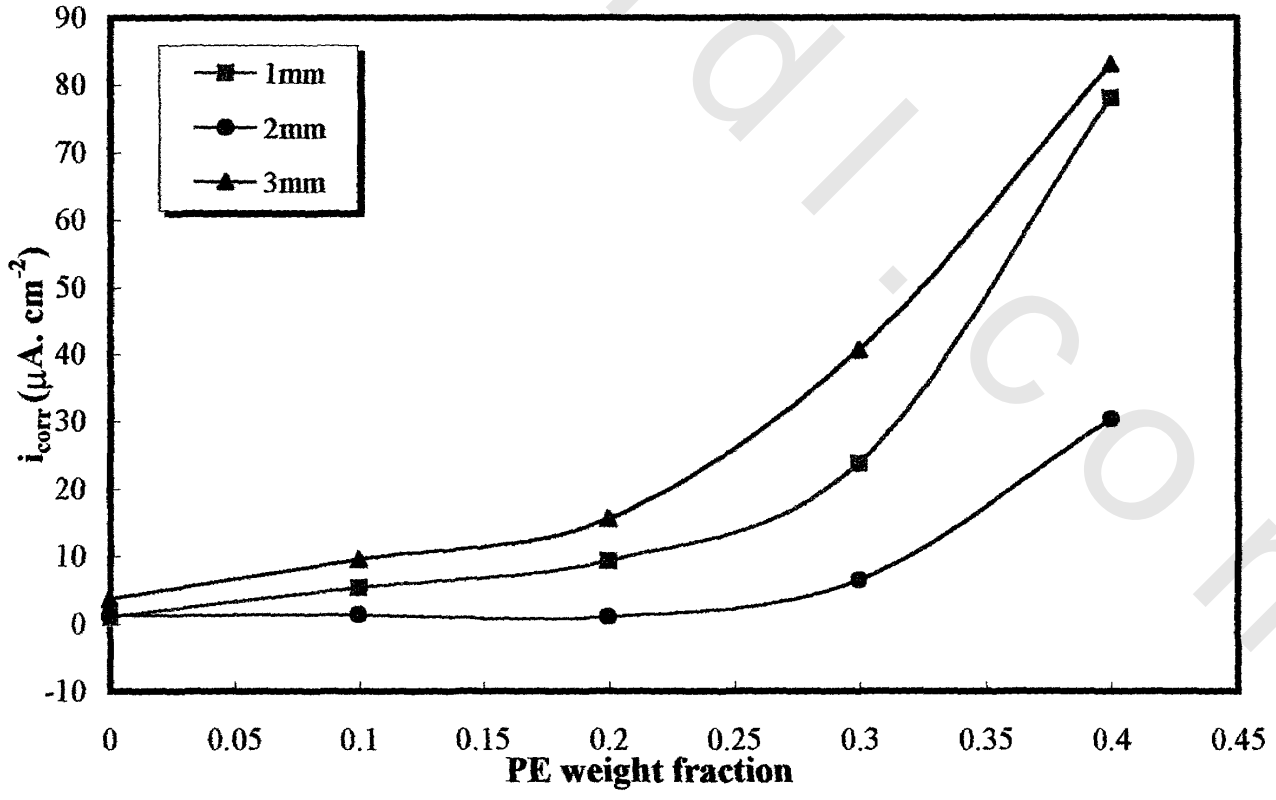

Fig.(4.44) - The dependence of corrosion current denisty on EPDM/PE blend ratio , (24months immersion in sea water , with applying adhsieve)

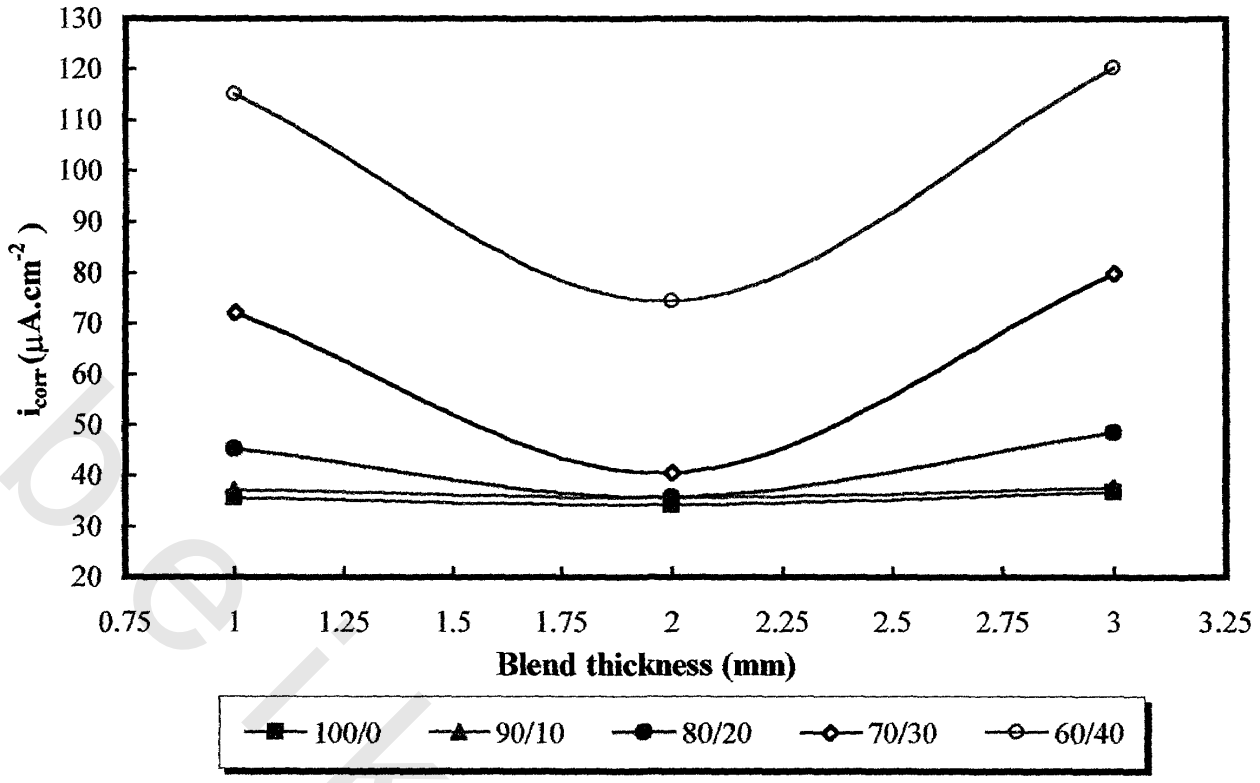

Fig.(4.45) - Corrosion current denisty of EPDM/PE blends as a function of blend thickness (24 months immersion in sea water, without applying adhesive)

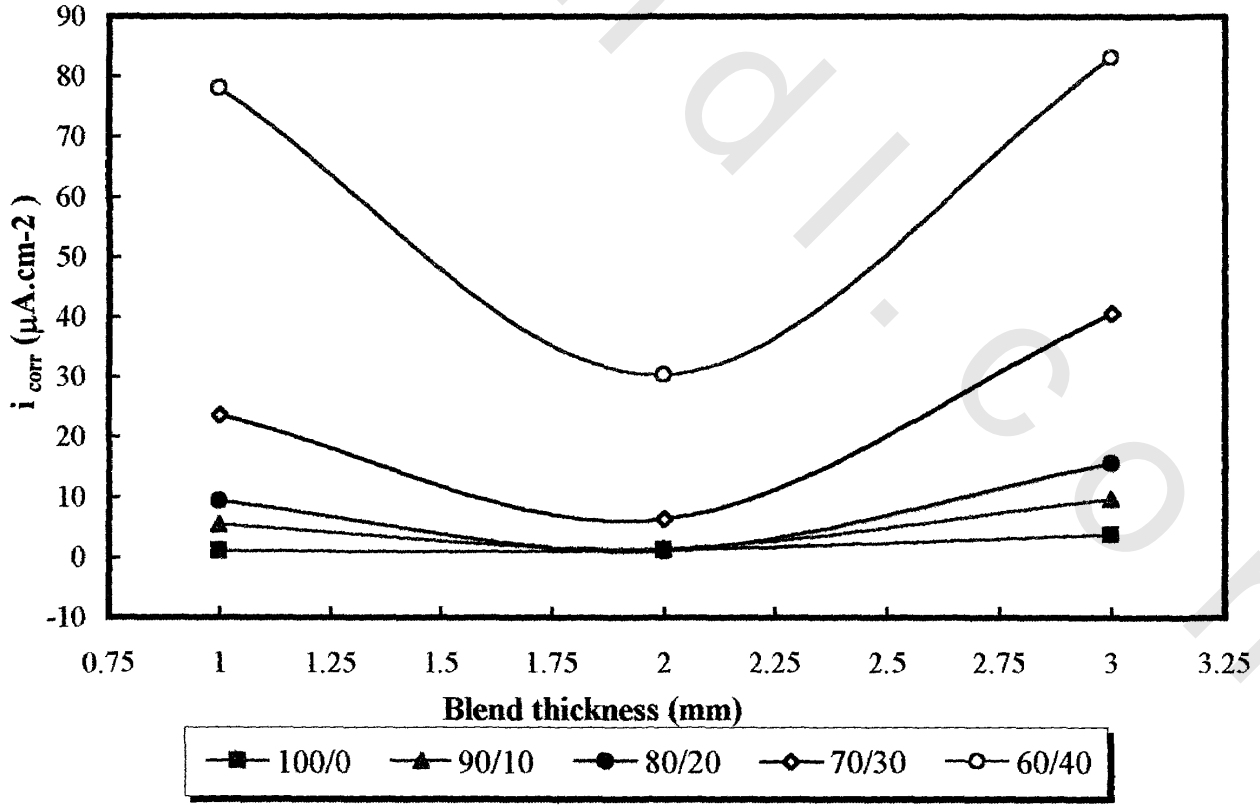

Fig.(4.46) - Corrosion current denisty of EPDM/PE blends as a function of blend thickness (24 months immersion in sea water, with applying adhesive)

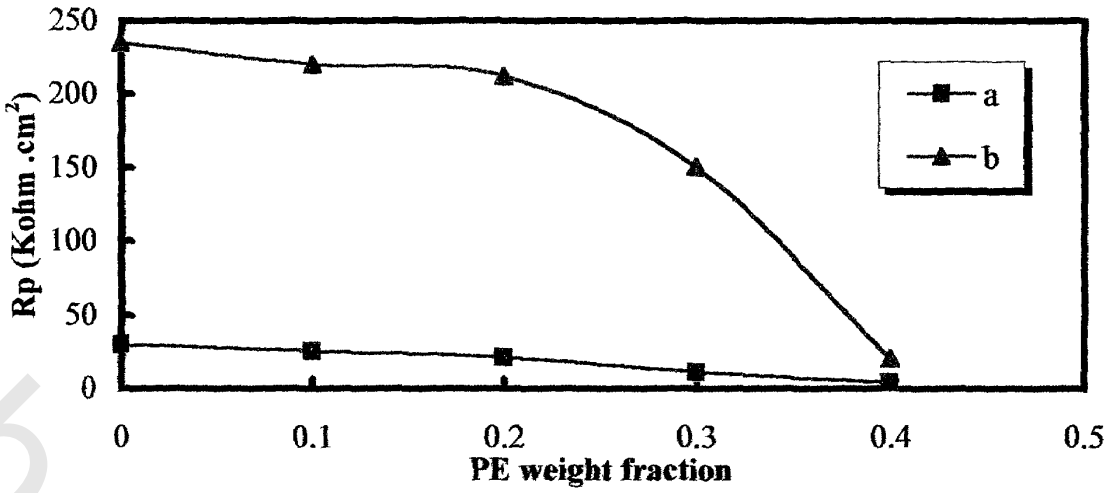

Fig.(4.47) - Effect of applying adhesive on polrization resistance of EPDM / PE blends (thickness 1 mm , 24 months immersion in seawater) (a) without applying adhesive, (b) with applying adhesive.

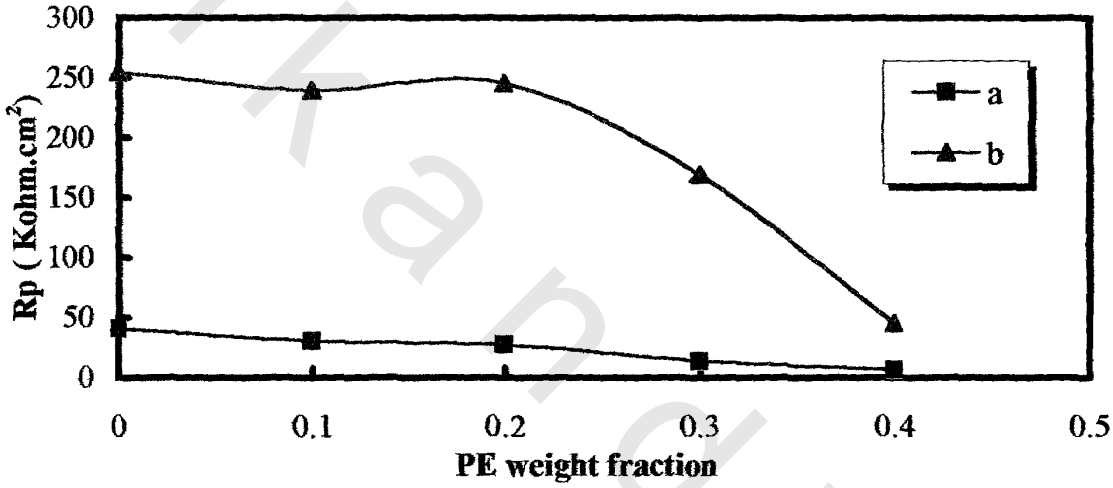

Fig.(4.48) - Effect of applying adhesive on polrization resistance of EPDM/PE blends (thickness 2 mm, 24 months immersion in seawater) (a) without applying adhesive ,(b) with applying adhesive.

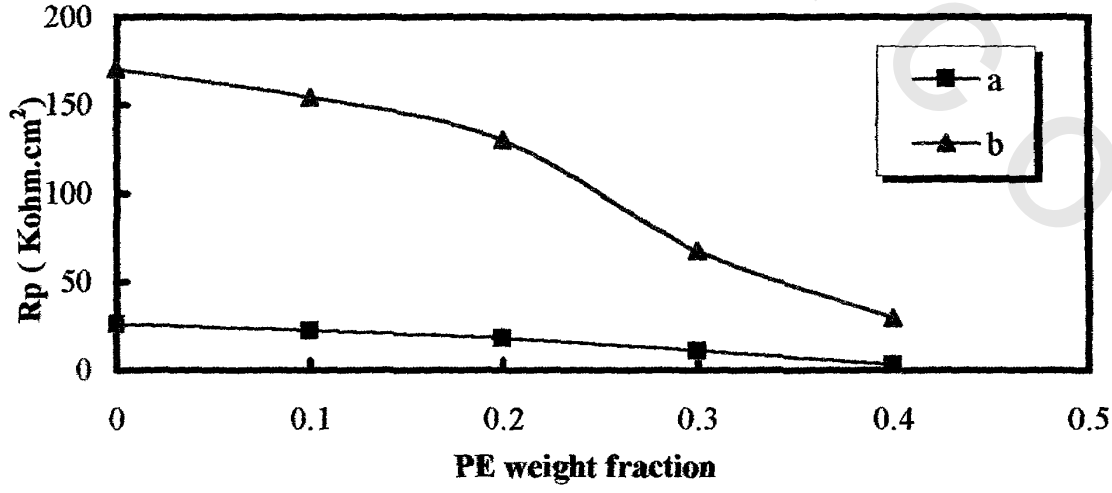

Fig.(4.49) - Effect of applying adhesive on polrization resistance of EPDM/PE blends (thickness 3 mm, 24 months immersion in seawater) (a) without applying adhesive ,(b) with applying adhesive.

is considered to be the boundary between protective and non- protective behavior, [229] and it can be noticed that all R_p values dervied for the corresponding EPDM/PE blends exceed this boundary, even without applying adhesive.

The data obtained from electrochemical measurements indicate that EPDM / PE blend of the ratio 80 / 20 shows the best protective properties, as evidenced from the highest value of R_p and lowest value of $i_{corr.}$ as shown in table (4.3). It can be noticed that there is a shift of corrosion potential with about 280 mV to the noble direction and a decrease with three orders of magnitude in the current. Also a significant increase in R_p is observed.

Table (4.3) - Potentiodynamic polarization data of bare and coated carbon steel (24 months of ageing)

Sample	$i_{corr.}$ (μ A. cm^{-2})	$E_{corr.}$ (mV)	R_p (ohm. Cm^2)
Bare carbon steel	864	- 595	40.62
EPDM/PE coating (80/20) thickness 2 mm	286.5 x 10^{-3}	- 316.5	284.9 x 10^3

After 24 months of immersion, all the coatings were peeled and, there were no visible corrosion products on the substrate indicating the excellent protection efficiency of EPDM / PE coatings

4.3.2. Analytical technique(ICP) :

The mass loss of the metal, that may be resulted from the dissolution of the substrate, is determined from the amount of corrosion products (mainly Fe II, Fe III) which enter the solution through the coating [230]. The solution has been analyzed at various duration time (6, 12, 18 and 24 months) by ICP technique. The obtained values for iron concentration are identical for all the samples at various immersion intervals and it was found to be < 0.0054, which is

the same value obtained from the analysis of blank sea water. Thus it is clear, that there is no increase in iron concentration in immersion media, and hence, there is no metal dissolution which reveals the excellent protection provided by EPDM / PE coatings.

4.3.3 Spectroscopic techniques:

Electrochemical techniques provide only indirect informations on surface structure,thus it is essential to utilise complementary surface techniques to obtain a balanced view of the physical and chemical effects which accompany the corrosion or the formation and breakdown of protective layers [231].

EPDM/PE coating with (80/20) blend ratio and its substrate were analyzed by SEM and X-ray techniques to investigate the corrosion protection efficiency of the blend.

4.3.3.1 SEM investigation:

The coating was peeled after 24 months of immersion in seawater, then the metal surface was analyzed by SEM, and the micrograph is shown in Fig. (4.50). It is found that surface properties don't change, regarding the previously studied SEM image of blank carbon steel, and no pitting is detected along the surface indicating the excellent corrosion protection efficiency of EPDM / PE coating. The (80/20) blend surface is also examined by SEM and the image is shown in Fig. (4.51). No appreciable delamination or cracking is observed, and there is no morphological changes in the blend surface, which indicates that EPDM / PE (80 / 20) can be considered as promising coating.

4.3.3.2 X-ray investigation:

The X-ray diffraction pattern of carbon steel substrate was recorded after peeling the coating, to detect the presence of corrosion products on the surface. It was found that X-ray diffraction pattern of the sample Fig. (4.52) is identical to

Fig. (4.50) SEM micrograph of carbon steel substrate,after removing the coating (magnification power 1000)

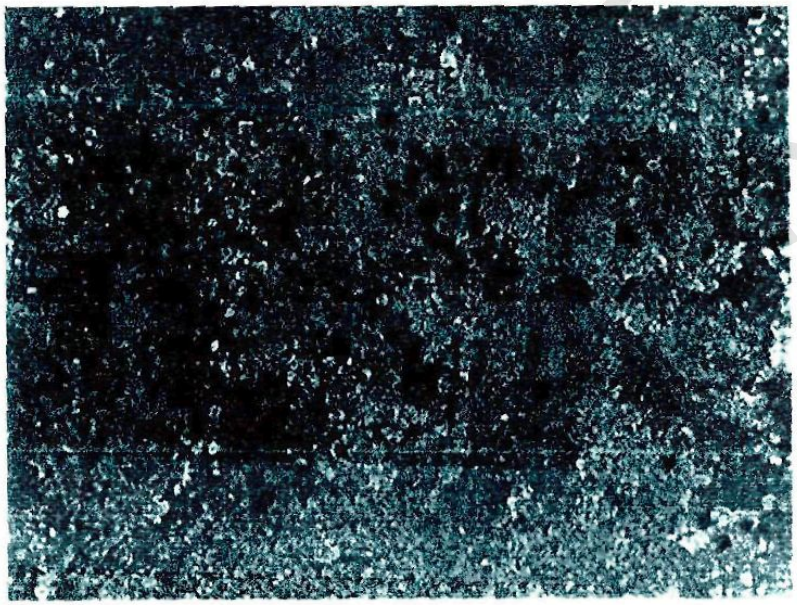

Fig. (4.51) SEM micrograph of EPDM/PE coating (80/20),after 24 months of ageing (magnification power 3500)

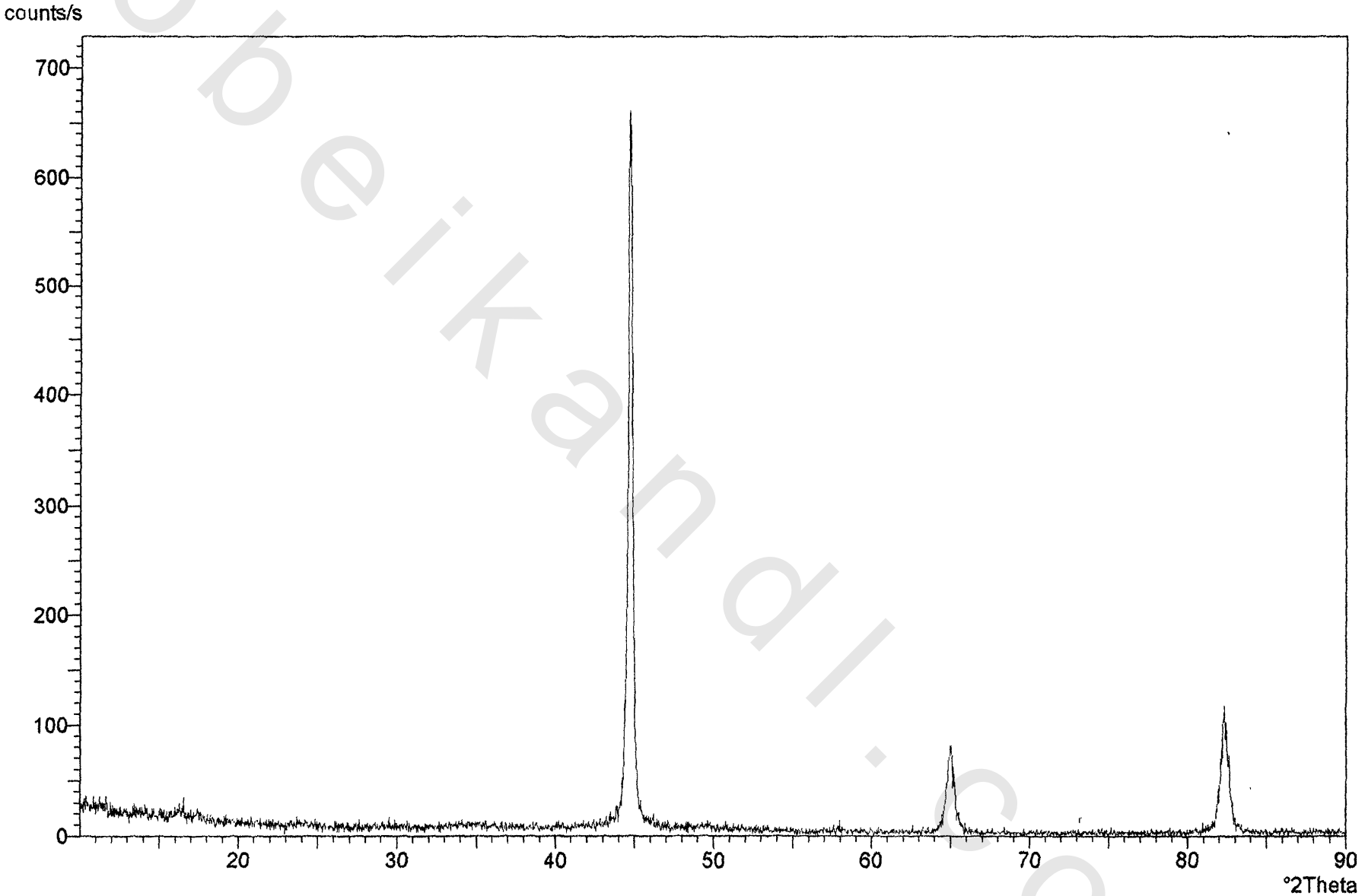

Fig(4.52) – X-ray diffraction pattern of carbon steel substrate after removing the coating (24 months of aging in sea water)

that of blank carbon steel Fig. (4.10 – a). There was no detection of iron oxides phases and the only phase appeared is the iron which, indicates that the surface doesn't undergo corrosion, revealing the good protection provided by EPDM / PE coating (80 / 20) for carbon steel alloy in seawater.

In conclusion, it must be taken in consideration that the mechanism of corrosion protection afforded by the coating is very complex and it is a combination of various contributory factors.